

LIPOSOMES: PRODUCTION AND APPLICATIONS FOR CONTROLLED DRUG  
DELIVERY

by

Gamid Abatchev



A dissertation

submitted in partial fulfillment

of the requirements for the degree of

Doctor of Philosophy in Biomolecular Science

Boise State University

December 2021

© 2021

Gamid Abatchev

ALL RIGHTS RESERVED

BOISE STATE UNIVERSITY GRADUATE COLLEGE

**DEFENSE COMMITTEE AND FINAL READING APPROVALS**

of the dissertation submitted by

Gamid Abatchev

Dissertation Title: Liposomes: Production and Applications for Controlled Drug Delivery

Date of Final Oral Examination: 5 October 2021

The following individuals read and discussed the dissertation submitted by student Gamid Abatchev, and they evaluated the student's presentation and response to questions during the final oral examination. They found that the student passed the final oral examination.

Daniel Fologea, Ph.D. Chair, Supervisory Committee

Julia Thom Oxford, Ph.D. Member, Supervisory Committee

Juliette Tinker, Ph.D. Member, Supervisory Committee

The final reading approval of the dissertation was granted by Daniel Fologea, Ph.D., Chair of the Supervisory Committee. The dissertation was approved by the Graduate College.

## DEDICATION

To my loving family which has taught me to always try my best and be the most I can. Their support, example, and patience has always guided me through the most difficult and confusing times in life. Their sincerity, love, and loyalty make success and achievement all the more meaningful.

## ACKNOWLEDGMENTS

First and foremost, I'd like to thank Daniel Folegea. His endless dedication and commitment as a mentor and teacher are nothing less than admirable. The amount of work and effort he invests in achieving the most for his students and scientific projects is an example to us all. Not only do I see him as an academic mentor, but also as a friend who offers both professional and everyday life advice. To this day, even after seeing him in the lab so much, I still fail to understand how he can achieve so much brilliant work within the time constraints we are given. You are an example to any scientific researcher.

I'd like to thank my committee members: Dr's Julia Oxford and Juliette Tinker for the guidance and counsel they always offered. In addition, I'd also like to thank Dr. Denise Wingett for her advice and support. This gratitude is extended to all the faculty at BMOL who are always very helpful and open to discussion. To Beth Gee, I'd like to express how grateful I am to have had your assistance. Your support and helping hand have guided all of us students through the strangest and most difficult of times. Without you, we'd all be lost.

Of course, all the research and progress in the Folegea lab would not be possible without the efforts and hard work of all the lab members in the Folegea Lab, both graduate and undergraduate. I'd like to especially thank Nisha Shrestha for introducing me to the graduate lifestyle and responsibilities in the lab when I first joined the Folegea lab. A big thank you to Andrew Bogard for helping with the preliminary experimentation pertaining to the Electrodialysis-Driven Depletion technique, along with his willingness

to discuss both life and science. Finally, I'd like to thank Zoe Hutchinson and Caitlin Sall for their help with liposome preparations and assistance with setting up experiments.

Last but not least, I'd like to thank the financial supporters of both myself during my time at BSU and the Fologea lab. An enormous thank you to the BMOL program and Boise State University for funding my research as a graduate student researcher. The research presented in this dissertation was also funded by the National Science Foundation (grant number 1554166) and the Osher Lifelong Learning Institute at Boise State University.

## ABSTRACT

This dissertation recognizes the enormous potential presented by the ever-evolving development of liposomes as drug carriers and seeks to offer further investigation into their useful production and utilization. The first chapter presents the basic principles governing their formation by self-assembly in water solutions, briefly describes the most common production methods, and points out essential past advances that led to their use as drug carriers. Chapter two exemplifies production of liposomes by the traditional methods of extrusion and sonication, detailing passive and active loading, as well as physical characterization by Dynamic Light Scattering, microscopy imaging, and fluorescence spectroscopy. In the next chapter, a novel approach for liposome preparation that relies on removing a lipid-solubilizing detergent from lipid mixtures by electro dialysis is introduced and compared to traditional preparation techniques. This methodology allows accelerated preparation of loaded and purified liposomes, resembling characteristics of ones prepared by traditional methods, in only a few steps. The final experimental chapter is focused on achieving controlled release of liposomal cargo, which is a major roadblock for many current clinical applications. This is realized by irradiation of liposomes containing PhotoClick lipids, as well as pH sensitive liposomes activated by internal pH changes resulting from irradiation of organic halogen solutions. The pairing of X-ray irradiation as a stimulus for releasing chemotherapeutic loaded cargo from liposomes offers possibility for truly concomitant application of radio and chemotherapy, potentially resulting in supra-additive efficacy of treating tumors.

## TABLE OF CONTENTS

DEDICATION.....	iv
ACKNOWLEDGMENTS.....	v
ABSTRACT .....	vii
LIST OF TABLES .....	xi
LIST OF FIGURES .....	xii
LIST OF ABBREVIATIONS.....	xvii
CHAPTER ONE: OVERVIEW OF LIPOSOME DISCOVERY, PRODUCTION, AND THEIR CAPABILITIES AS DRUG CARRIERS.....	1
Formation, Production, and Characterization of Liposomes .....	2
Liposomes as Drug Carriers.....	9
Triggered Release of Payload from Liposomes .....	13
References.....	15
CHAPTER TWO: PREPARATION, LOADING, AND CHARACTERIZATION OF LIPOSOMES MADE BY SONICATION AND EXTRUSION .....	25
Materials and Methods .....	25
Lipids, Loading Molecules, and Buffers.....	25
Liposome Preparation .....	27
Liposome Loading and Dialysis Purification .....	28
Liposome Characterization with Microscopy and Dynamic Light Scattering.....	29
Results and Discussions.....	29

Size and Size Distribution: Liposomes Prepared by Hydration, Sonication, and Extrusion .....	29
Passive and Active Loading of Liposomes.....	35
Cargo Release from Liposomes .....	37
Conclusions .....	41
References .....	43
<b>CHAPTER THREE: RAPID PRODUCTION AND PURIFICATION OF DYE - LOADED LIPOSOMES BY ELECTRODIALYSIS-DRIVEN DEPLETION.....</b>	<b>48</b>
Abstract .....	49
Introduction .....	49
Materials and Methods.....	52
Results and Discussions .....	55
Dye Separation by Electrodialysis .....	55
Simultaneous Liposome Formation, Loading, and Purification by EDD..	57
Production of Long-Circulating Liposomes by Electrodialysis.....	58
Verification of Dye Loading.....	59
Unilamellar or Multilamellar?.....	60
EDD Comparison to Extrusion and Sonication .....	63
Conclusion.....	66
References .....	68
<b>CHAPTER FOUR: CONTROLLED RELEASE FROM PHOTOCCLICK AND PH-SENSITIVE LIPOSOMES .....</b>	<b>76</b>
Introduction .....	76
Materials and Methods.....	81
Lipids, Loading Molecules, and Solutions .....	81

Liposomes Preparation.....	84
Liposome Loading and Purification.....	84
Fluorescence and Spectral Characterization.....	85
UV and X-Ray Irradiation.....	86
Results and Discussions.....	87
Self-Quenching of Calcein and Doxorubicin .....	87
Calcein Release from PhotoClick Liposomes Upon X-ray Exposure .....	91
DOX Release from PhotoClick Liposomes After X-ray Exposure .....	93
CIS Release Upon X-ray Exposure.....	95
Controlled Release From pH-Sensitive Liposomes.....	98
Conclusions.....	102
References.....	105
CHAPTER FIVE: CONCLUSIONS AND PERSPECTIVES .....	113
Outlooks and Perspectives .....	116
References.....	118

## LIST OF TABLES

Table 1.	Physical characterization of liposomes by DLS analysis. Average hydrodynamic diameter and polydispersity index (PDI) of liposomes composed of either a regular or PEGylated formulation using hydration, sonication, or extrusion. *Liposomes were denoted by a two-letter code with the first letter representing preparation method (hydration = H, sonication = S, extrusion = E) and a second letter denoting lipid formulation (regular = R, PEGylated = P).....	31
----------	---	----

## LIST OF FIGURES

- Figure 1. Typical structure of a phospholipid and phospholipid structures formed upon hydration. (A) Phosphatidylcholine, a frequently used phospholipid in liposome preparation. Adapted from van Hoogvest, P. Review – An update on the use of oral phospholipid excipients [14]. Available under Creative Commons License. (B) Lipid structures typically formed upon hydration of dehydrated lipid films. This includes lipid monolayers, lipid bilayers, micelles, unilamellar and multilamellar liposomes, as well as aggregates of these structures. .... 3
- Figure 2. Free energy diagram of liposome (vesicle) formation. Absolute relative minima of free energy seen with phospholipid aggregates, as compared to the local minima seen in formation of multilamellar vesicles (MLV), then large unilamellar vesicles (LUV), and finally small unilamellar vesicles (SUV). Figure originally from Lasic 1988 - The Mechanism of Vesicle Formation [16]. Used with permission from the publisher. .... 4
- Figure 3. Example of an extrusion setup. The metallic block holds an extrusion assembly, which houses the polycarbonate membrane through which the polydisperse and multilamellar liposomes are extruded. Extruding action aides in creating a monodisperse and unilamellar sample of liposomes. Images acquired from the Avanti Polar Lipids website [<https://avantilipids.com/divisions/equipment-products>]. .... 5
- Figure 4. Diagram of basic ethanol injecting setup. A solution of lipids with ethanol is rapidly diluted by an aqueous buffer to result in liposomes in buffer with diluted ethanol. .... 6
- Figure 5. Principal methods of liposome loading with hydrophilic cargo. Left side showing passive loading as formation of the liposome leads to encapsulation of drug molecules at the concentration present in the surrounding buffer. Right side showing active loading driven by electrochemical gradient (generated by pH difference in this example) which drives drug entrance into preformed liposome and ionization of drug molecule, preventing it from exiting the liposome. .... 9
- Figure 6. The versatile use and modification of liposomes as drug carriers. Apart from drug loading in the core or membrane, liposomes are highly customizable. Surface modifications are frequently made to better reach

	and interact with their intended target (i.e, by using antibodies) as drug carriers or to avoid the immune system (PEG). Figure originally from Beltran-Gracia et al., 2019 - Nanomedicine review: clinical developments in liposomal applications [45]. Available under Creative Commons License. ....	10
Figure 7.	The Enhanced Permeability and Retention (EPR) effect presented by small, PEGylated liposomes. The fenestrated endothelial lining of blood vessels developed by tumors allow entrance of small liposomes into the tumor tissue. Upon entrance, liposomes fail to escape because of the ineffective lymphatic drainage in tumors. Figure originally from Børresen et al., 2017 - Liposome-encapsulated chemotherapy: Current Evidence for its Use in Companion Animals [50]. Used with permission from the publisher.....	12
Figure 8.	Structural details of phospholipids and cholesterol used for preparation of liposomes. Naturally derived asolectin is a combination of equal parts lecithin [phosphatidylcholine], cephalin, and phosphatidylinositol, with small amounts of other phospholipids and polar lipids (“R” indicates possible variable structure in fatty acid tail). Synthetic lipids 1,2-distearoyl-sn-glycero-3-phosphocholine (DSPC) and 1,2-distearoyl-sn-glycero-3-phosphoethanolamine-N-[methoxy(polyethyleneglycol)-2000] (DSPE-PEG) and cholesterol were also utilized for liposome production. ....	26
Figure 9.	Chemical and optical properties of dye and drug molecules passively and actively loaded into sonication and extrusion prepared liposomes. Fluorescent dyes calcein (CAL) (ex/em) 495/520 nm, and rhodamine 6G (R6G) (ex/em) 528/550 nm were passively loaded. Fluorescent dye acridine orange (AO) (ex/em) 485/530 nm was both passively and actively loaded. Anthracycline chemotherapeutic doxorubicin (DOX) (ex/em) 470/560 nm was actively loaded. ....	27
Figure 10.	Light microscopy images of liposomes. P formulated liposomes prepared by hydration (A) and extrusion through 400 nm polycarbonate membranes (B). Edits were made to remove foreign particles in the foreground from view. Scale bars are 50 µM.....	32
Figure 11.	Size distribution of liposomes prepared by sonication and extrusion. Graphical size representation on a logarithmic scale of EP liposomes made by extrusion with a 400 nm polycarbonate membrane (A) and SP liposomes prepared with 15 minutes of probe sonication.....	33
Figure 12.	PEGylated liposomes. Liposome with protruding polyethylene glycol moieties from the phospholipid bilayer membrane. Figure taken from	

Labruere et al., Anti-Methicillin-Resistant *Staphylococcus aureus*  
Nanoantibiotics [23]. Available under Creative Commons License. .... 35

- Figure 13. Fluorescence microscopy of PEGylated liposomes passively loaded with drug simulating fluorescent dyes. CAL loaded (A) and R6G loaded (B) liposomes prepared with extrusion. Scale bar is 30  $\mu$ M. .... 36
- Figure 14. Self-Quenching curves of used drug and dyes. Graphs show how fluorescence increases with concentration up until a peak fluorescence, at which point increasing molecular concentration results in a diminished fluorescence concentration for CAL (A), R6G (B), AO (C), and DOX (D). .... 39
- Figure 15. Analysis of dye and drug loading into liposomes. Non-ionic detergent induced CAL (A) and actively loaded AO (B and C) and DOX (D) release from regular liposome formulations (red) and PEGylated formulations (blue) induced by addition of Triton X-100. .... 40
- Figure 16. Experimental setup for liposome production by electrodialysis-driven depletion (EDD) and fluorescence monitoring. The custom setup includes the electrodialysis tank (ElectroPrep Electrolysis System), an Ultra-Fast Dialyzer chamber, and a microfluidic setup to recirculate the solutions through a constant volume fluorometer cuvette for real-time fluorescence measurements. This specific setup describes migration and quantification of an anionic dye transferred from the dialysis chamber to the left reservoir. The solutions in the two reservoirs were continuously stirred with magnetic bars. The diagram is not to scale. .... 54
- Figure 17. Electrodialysis leads to rapid depletion of charged dyes from solutions. Acridine orange (AO) (a) migrates faster than rhodamine 6G (R6G) (b) but both are depleted from the dialysis chamber and transferred into the reservoirs in less than 40 min. .... 57
- Figure 18. Microscopy imaging of fluorescent liposomes produced and purified by EDD. The liposomes are composed of asolectin and cholesterol and are loaded with AO (left panel) and R6G (right panel). The scale bar is 10  $\mu$ m. .... 58
- Figure 19. Microscopy image of PEGylated liposomes loaded with AO, prepared, and purified by EDD. The scale bar is 10  $\mu$ m. .... 59
- Figure 20. AO release from PEGylated liposomes produced, loaded, and purified by EDD. (a) AO fluorescence indicates self-quenching at bulk concentrations over 10  $\mu$ M. (b) The sustained release of AO from liposomes solubilized by addition of Triton X-100 indicates successful loading. .... 60

Figure 21.	Lysenin-induced permeabilization of sphingomyelin-based liposomes. The sustained release of AO (~80 % in less than one hour, relative to 100% release achieved by Triton X-100 addition) suggests that the target membranes are unilamellar. The dashed line shows the 100% release achieved by Triton X-100 addition. ....62
Figure 22.	Dynamic light scattering characterization of liposomes produced by extrusion (a), probe sonication (b), and EDD (c). Each plot shows the mean intensity percent $\pm$ SD (n = 3) determined as a function of diameter. ....65
Figure 23.	PhotoClick reaction of diazirine. The diazirine moiety on PhotoClick sphingomyelin, one of the UV sensitive components used in our liposomes, releases nitrogen and results in reactive carbene formation upon UV exposure. Carbene readily covalently bonds, allowing for crosslinking in the membranes, and leading to permeabilization. Similar chemical process occurs in PhotoClick cholesterol, the other UV sensitive component used.....78
Figure 24.	Lipid components used in the production of liposomes used for investigations on controlled release. Cholesterol (Chol) and 1,2-distearoyl-sn-glycero-3-phosphocholine (DSPC) were used for both UV/X-ray and pH sensitive liposomes. PhotoClick sphingosine (P-SM), PhotoClick cholesterol (P-Chol), and sphingomyelin (SM) were used specifically for UV/X-ray sensitive liposomes (DSPE-PEG was used in one variation of PhotoClick composed liposomes with DOX loading. Phosphatidylethanolamine (PE), oleic acid (OA), and 1,2-distearoyl-sn-glycero-3-phosphoethanolamine-N-[methoxy(polyethyleneglycol)-2000] (DSPE-PEG) were used specifically for pH sensitive liposomes. UV/X-ray sensitive components are outlined in dashed blue line; the dotted red line outlines the components used for preparation of pH sensitive liposomes.83
Figure 25.	Optically absorbing complex formation of Cisplatin. Reaction with o-phenylenediamine (OPDA) and dimethylformamide (DMF) results in increased absorbance at 704 nm.....86
Figure 26.	Self-quenching of CAL and DOX, followed by detergent induced release measurements from loaded liposomes. We established maximum fluorescence concentration for CAL of about 20 $\mu$ M (A) and DOX of about 100 $\mu$ M (B) characterizing their concentration dependent quenching behaviors. Maximum release of CAL (C) and DOX (D) was induced by Triton-X 100 addition, showing loaded and purified liposomes in dye/drug free buffer.....88
Figure 27.	UV induced release of CAL from liposomes. 100 $\mu$ L of CAL loaded PhotoClick liposomes exposed to UV light resulted in ~70% release.

Comparatively, liposomes lacking PhotoClick components showed negligible release (~1%) over the time span measurements were taken. 100% release was achieved by treating PhotoClick liposomes with Triton X-100..... 91

Figure 28. Normalized release percent of CAL from PhotoClick liposomes in X-ray. Comparatively, liposomes lacking PhotoClick components showed negligible release over the time span measurements were taken. 100% release was achieved by treating Photoclick liposomes with Triton X-100. .... 93

Figure 29. X-ray induced release of DOX from PhotoClick liposomes. Relative release percent intensity of non-irradiated PhotoClick liposomes loaded with DOX (X), irradiated PhotoClick liposomes loaded with DOX (Y), and PhotoClick liposomes loaded with DOX and treated with Triton X-100 (Z) (100% release).  $p < 0.01$  between Y and X ( $n = 3$ )..... 95

Figure 30. A standard curve for CIS is established by measuring the absorbance of the colorimetric product at 704 nm ( $n = 3$ ). ..... 96

Figure 31. CIS release upon X-ray exposure of PhotoClick liposomes. PhotoClick liposomes loaded with CIS at rest (A), irradiated control liposomes loaded with CIS (B), irradiated PhotoClick liposomes loaded with CIS (C), and PhotoClick liposomes loaded with CIS and treated with Triton X-100 (D) (100% release).  $p < 0.01$  between C and A as well as C and B ( $n = 3$ ).... 97

Figure 32. CAL release from pH sensitive liposomes. External pH was reduced from 7.2 to 6.44 by addition of dilute HCL. Percent release is normalized to an identical liposome sample treated with Triton X-100..... 100

Figure 33. Relative release of CAL fluorescence intensity of pH sensitive CAL and BH loaded liposomes. pH sensitive liposomes at rest (1), non-pH sensitive control liposomes loaded with CAL and irradiated with X-ray (2), pH sensitive CAL and BH loaded liposomes irradiated with X-ray (3), pH sensitive CAL and BH loaded liposomes treated with Triton X-100 (4).  $p < 0.01$  between 3 and 1 as well as 3 and 2 ( $n = 3$ )..... 101

## LIST OF ABBREVIATIONS

AO	Acridine Orange
Aso	Asolectin
BH	Bromal Hydrate
CA	Cholic Acid
CAL	Calcein
Chol	Cholesterol
CIS	Cisplatin
DLS	Dynamic Light Scattering
DMF	Dimethylformamide
DOX	Doxorubicin
DSPC	1,2-distearoyl-sn-glycero-3-phosphocholine
DSPE-PEG	1,2-distearoyl-sn-glycero-3-phosphoethanolamine-N- [methoxy(polyethyleneglycol)-2000]
E	Extrusion
EDD	Electrodialysis-Driven Depletion
Em	Emission
EPR	Enhanced Permeability and Retention
Ex	Excitation
H	Hydration
HCL	Hydrochloric Acid

HEPES	4-(2-hydroxyethyl)-1-piperazineethanesulfonic acid
IR	Infrared
KCl	Potassium Chloride
LED	Light-emitting Diode
LUV	Large Unilamellar Vesicle
MLV	Multilamellar Vesicle
MPS	Mononuclear Phagocyte System
NaCl	Sodium Chloride
OA	Oleic Acid
OPDA	O-phenylenediamine
P	PEGylated Formulation (8.2:3.8:2.6 1,2-distearoyl-sn-glycero-3-phosphocholine to Cholesterol to 1,2-distearoyl-sn-glycero-3-phosphoethanolamine-N-[methoxy(polyethyleneglycol)-2000] mass ratio)
PBS	Phosphate-buffered Saline
P-Chol	PhotoClick Cholesterol
PDI	Polydispersity Index
PE	Phosphatidylethanolamine
PEG	Polyethylene Glycol
P-SM	PhotoClick Sphingosine
R	Regular Formulation (10:4 Asolectin to Cholesterol mass ratio)
R6G	Rhodamine 6G
RES	Reticuloendothelial System
RPM	Rotations Per Minute

S	Sonication
SM	Sphingomyelin
SUV	Small Unilamellar Vesicle
UV	Ultraviolet
VIS	Visible



## CHAPTER ONE: OVERVIEW OF LIPOSOME DISCOVERY, PRODUCTION, AND THEIR CAPABILITIES AS DRUG CARRIERS

Based on the two Greek words lipos and soma, meaning “fat” and “body”, liposomes have unprecedently advanced biomedical and scientific research. Usually ranging from approximately 20 nanometers to several microns in diameter, liposomes most notably consist of at least one lipid bilayer resulting from the favorable orientation and self-assembly of the hydrophobic lipid tails, surrounding a hydrophilic, aqueous core. The discovery of liposomes can be traced back to the 1960’s, when Alec Bangham and R.W. Horne observed their formation when creating negatively stained phospholipid dispersions under electron microscopy at Babraham Institute in Cambridge [1]. In the decades that followed, research and understanding of liposomes led to their extensive utilization for fundamental studies and applications in industrial, agricultural, food production, consumer, and biomedical fields [2-9]. Their biomimetic properties resembling the phospholipid bilayer membrane of cells [10] also allow for investigations on the properties of cellular membranes and as a scaffold for reconstitution of membrane proteins, as well as studies on their biophysical and biological properties such as transport and interactions [11-13]. Apart from their characteristic spherical bilayer structure, liposomes are highly customizable with regards to their physical and chemical properties, making them suitable for a large variety of scientific, medical, and biotechnological applications.

## **Formation, Production, and Characterization of Liposomes**

The guiding principle of liposome formation resides in the energetic unfavourability of exposed hydrophobic components of phospholipids in aqueous solution. The phospholipid can be defined by two distinct molecular regions; a hydrophilic head composed of a phosphate and glycerol bridge, which is bound to a hydrophobic tail composed of fatty acids (Figure 1A) [14]. The simultaneous presence of the contrasting hydrophobic and hydrophilic regions defines it as an amphiphilic molecule. A fatty acid and aqueous interface drives grouping of like fatty acid tails to minimize the free energy of the system by self-assembling into structures such as micelles, monolayers, bilayers, unilamellar, and multilamellar liposomes (Figure 1B) [15-17].

Based on this principle, it was initially understood that upon simple hydration of a lipid film with an aqueous solution, spontaneous assembly of energetically favorable liposomes was possible [18]. Although there is still some speculation regarding the exact mechanism of vesicle formation upon aqueous hydration, it is generally agreed that the spherical enclosure of the bilayer is one of the most energetically favorable structures lipid film can attain upon exposure to water molecules, creating a local minima of the free energy of the system (Figure 2) [15, 16, 19].

It is, however, not enough to hydrate a lipid film with an aqueous solution to attain a sample of monodisperse and functional liposomes. Self-assembly resulting from passive exposure of lipid membranes to aqueous solution will result in formation of various energetically favorable lipid structures as previously mentioned. Liposomes will also exist in unilamellar and multilamellar form, that is, consisting of a single bilayer or

multiple concentric bilayers (Figure 1B), of various sizes. Further input of energy is required, whether it is through physical agitation or chemical environment alteration, to create a more uniform and functional sample of liposomes [15, 16, 19].

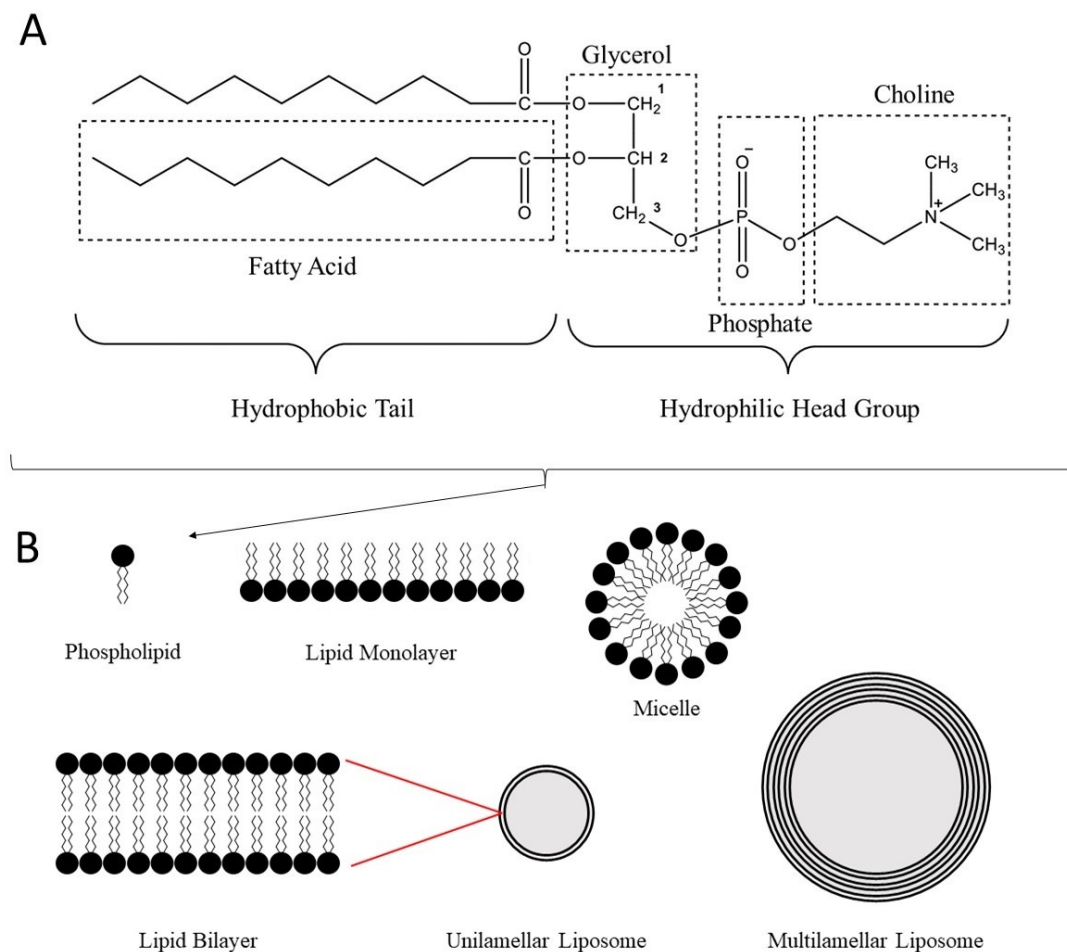


**Figure 1. Typical structure of a phospholipid and phospholipid structures formed upon hydration. (A) Phosphatidylcholine, a frequently used phospholipid in liposome preparation. Adapted from van Hoogvest, P. Review – An update on the use of oral phospholipid excipients [14]. Available under Creative Commons License. (B) Lipid structures typically formed upon hydration of dehydrated lipid films. This includes lipid monolayers, lipid bilayers, micelles, unilamellar and multilamellar liposomes, as well as aggregates of these structures.**

Mechanical dispersion and agitation methods utilize externally applied energy to reform and refine liposomes and lipid structures formed during hydration with an

aqueous solution. Two such methods which have prominently and dependably been used for decades includes extrusion and sonication [20-23]. Extrusion involves repeated refinement of liposomes formed by hydrated lipids by pushing them through pores of a specific size to create a uniform and monodisperse population of liposomes (Figure 3) [24, 25]. The understanding of the exact mechanism of liposome formation through sonication is still evasive, however it involves application of ultrasonic pulsation to a hydrated lipid solution to create a more uniform population of liposomes. It is likely that the high frequency vibration, physical agitation, and water cavitation induced by sonication results in shattering of large lipid structures to reform as small, unilamellar liposomes [26].

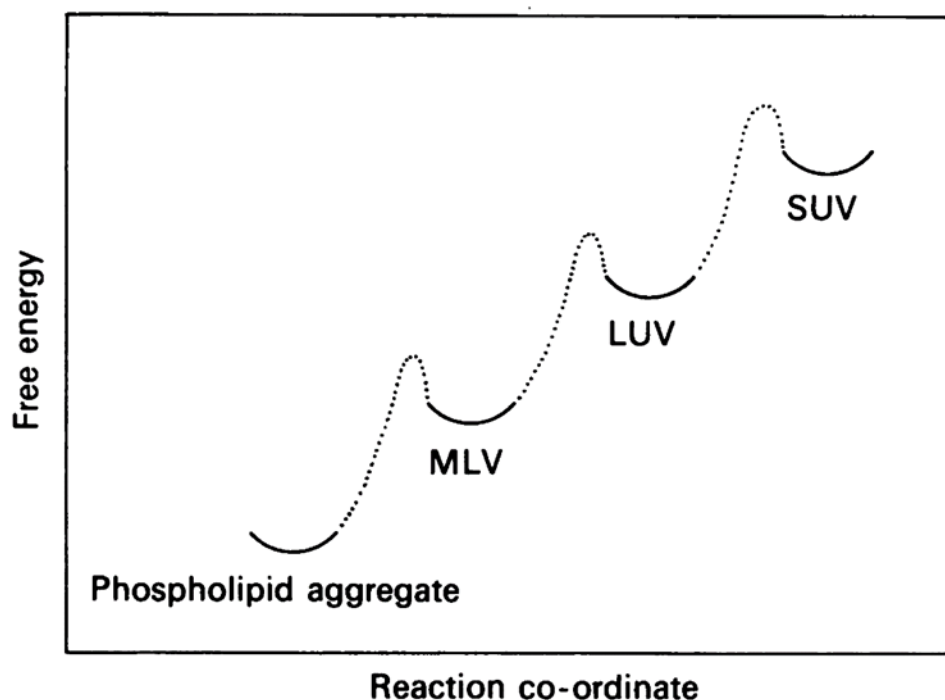


**Figure 1. Free energy diagram of liposome (vesicle) formation. Absolute relative minima of free energy seen with phospholipid aggregates, as compared to the local minima seen in formation of multilamellar vesicles (MLV), then large unilamellar vesicles (LUV), and finally small unilamellar vesicles (SUV). Figure originally from Lasic 1988 - The Mechanism of Vesicle Formation [16]. Used with permission from the publisher.**

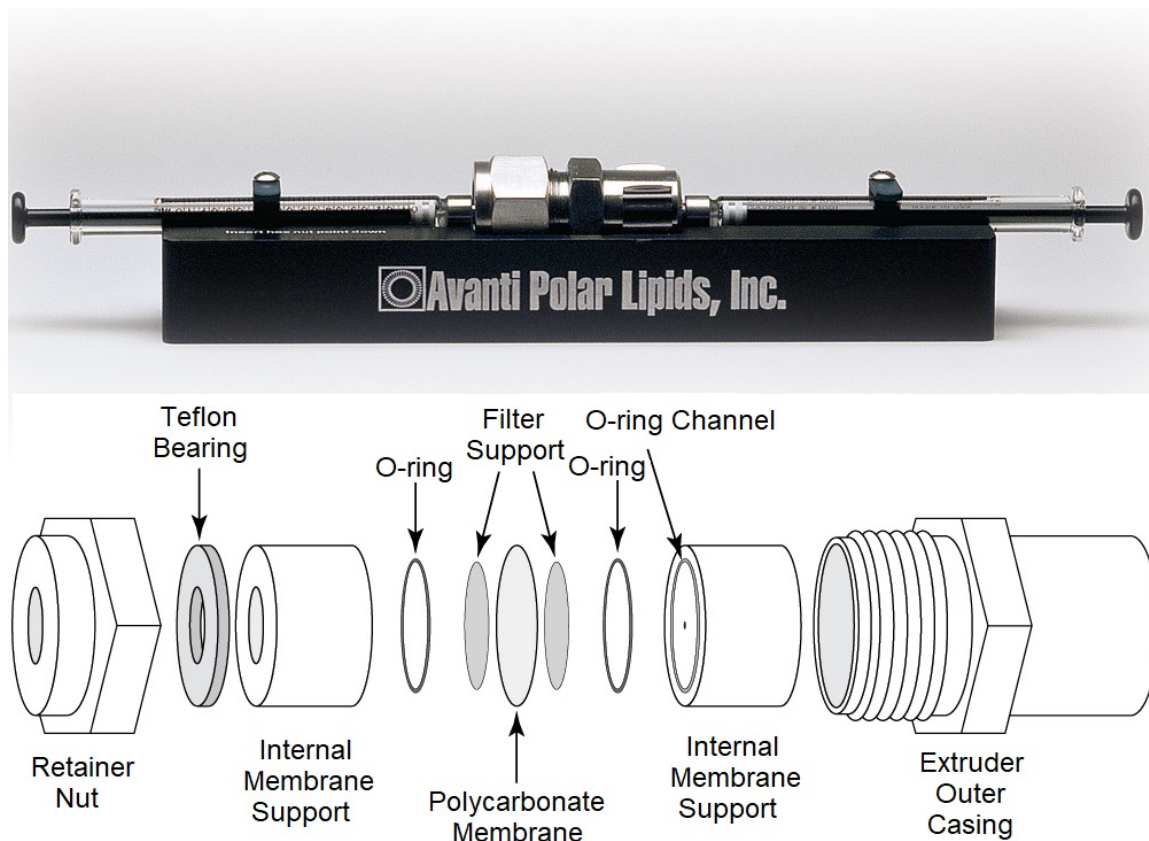


**Figure 2.** Example of an extrusion setup. The metallic block holds an extrusion assembly, which houses the polycarbonate membrane through which the polydisperse and multilamellar liposomes are extruded. Extruding action aides in creating a monodisperse and unilamellar sample of liposomes. Images acquired from the Avanti Polar Lipids website [<https://avantilipids.com/divisions/equipment-products>].

Beside these two original preparation methods of liposomes, numerous customizations and modifications have been made to better control their formation. It would take a whole book to properly describe the basis and exact science pertaining to each method, however many of the methods beyond some variations of the previously mentioned mechanical dispersion rely on the removal of organic solvents such as alcohol, ether, or detergent [27, 28].

Organic solvent removal techniques often require specialized custom devices and setups to rapidly dilute or remove organic solvents, such as ethanol from lipid/organic

solvent/loading molecule solutions, to create a sudden shift in the physical and chemical properties of the environment. This results in decreased lipid solubility, leading lipids to group their hydrophobic fatty acid tails when exposed to buffer solution, driving the formation of liposomes and simultaneous entrapment of cargo [29] (Figure 4). In a similar fashion, ether injection relies on the low boiling point of ether for evaporation from a lipid solution. Gradual removal of ether as an organic solvent through its evaporation drives self-assembly of liposomes in the aqueous solution the ether/lipid solution is initially injected into [30].

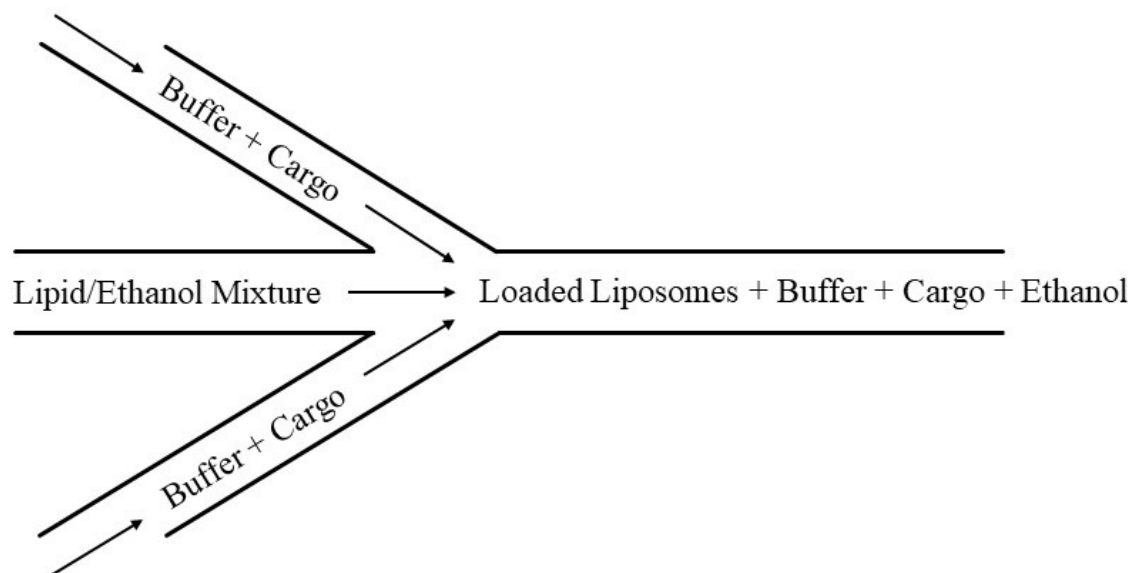


**Figure 4. Diagram of basic ethanol injecting setup. A solution of lipids with ethanol is rapidly diluted by an aqueous buffer to result in liposomes in buffer with diluted ethanol.**

Another well-established method involves the removal of a detergent from a lipid/detergent mixture [31]. This can be done by utilizing a few different techniques of detergent removal such as chromatography and dialysis; however, the principal of liposome formation lies in fusion of assembled lipid structures as the solution loses detergent to solubilize with. The fusion of these lipid structures creates lipid bilayer disks

with exposed hydrophobic edges. Further detergent elimination leads to fusion of adjacent disks, which evolve into spherical liposomes to decrease the span of, and eventually eliminate hydrophobic edges of the bilayer by curving [15, 16, 32].

It is important to note that the selection of a specific preparation technique cannot address all difficulties of liposome preparation, nor suit all needs. One method often surpasses the quality of another but may lack in other aspects. Several factors must be considered when using a particular method, such as encapsulation efficiency, size and size distribution of liposomes produced, compatibility with cargo or surface markers of liposomes, residual traces of solvent, as well as time, effort, and cost needed for production [2, 3]. This is especially important when creating biomedical products intended to be used on human patients, as quality and safety become of paramount importance.

When producing liposomes intended as carriers, it is vital to understand the properties of the cargo. Passive loading techniques involve formation of liposomes either entrapping cargo present in the surrounding environment [2, 33] or integrating hydrophilic or integral membrane components during lipid film drying or liposome formation. In a self-describing manner, this is a passive process and does not require any specific driving force or additional energy beyond that which is needed to form the liposomes.

A more exclusive technique, applicable only to molecules capable of changing from a membrane permeant to non-permeant state, is described by active loading. The existence of an electrochemical gradient between the internal and external environments of the liposomes allows changes in the properties of the loading molecules to modulate

their ability to permeate through the membrane. One such variation involves liposome preparation in one external pH environment, with an internal pH capable of adjusting the ionization of the cargo and its permeability. A buffer exchange, usually performed by using dialysis, is completed afterwards to generate a significant pH gradient [34]. As an example, in non-ionized form (neutral), some cargo molecules are membrane permeant and can diffuse freely through the membrane into the liposome from the external bulk solution. The diffusion process is often augmented by the established electrochemical gradients. Upon entering, the different pH drives ionization of the cargo molecule. The ionized form of the cargo is membrane impermeant, leaving it entrapped within the liposome. Although this can be a relatively time-consuming process requiring multiple steps, its desirability resides in its high loading efficiency (Figure 5) [33, 35]. An alternate approach for active loading utilizes the production of liposomes with a higher internal vs external concentration of ammonium sulfate to load chemotherapeutic doxorubicin (DOX). DOX, upon entering the liposome, forms gel-like aggregates due to loss of solubility when forming a complex with sulfate. As a result, it becomes incapable of escaping the liposome, leading to DOX concentrations hundred folds higher than those found outside. The bioavailability of the crystallized, membrane impermeant DOX molecules is retained [36-38].

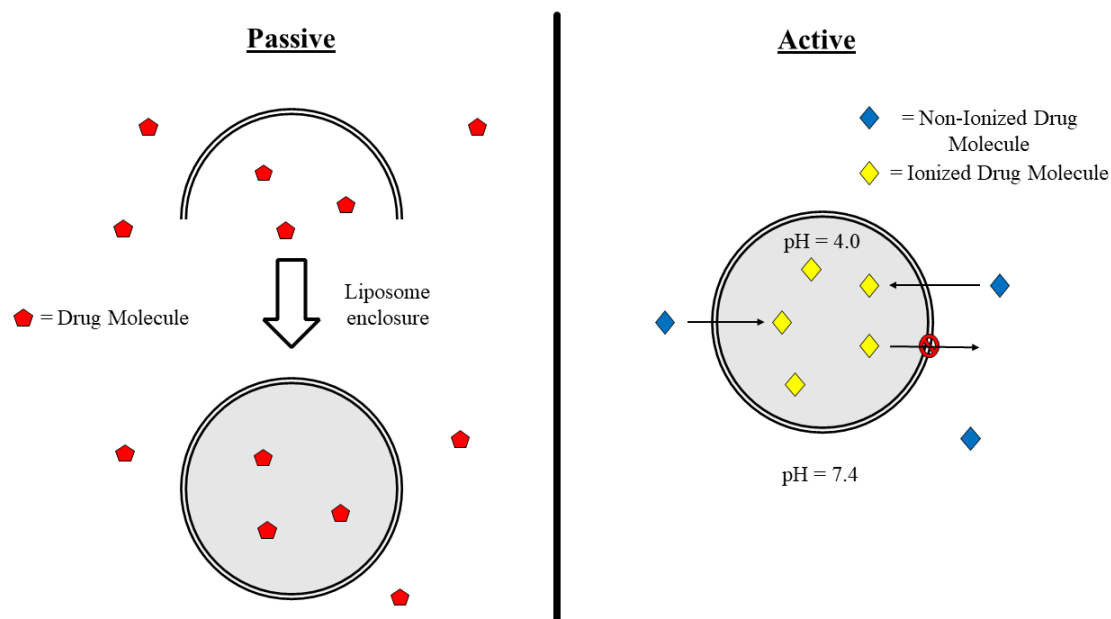


**Figure 5. Principal methods of liposome loading with hydrophilic cargo. Left side showing passive loading as formation of the liposome leads to encapsulation of drug molecules at the concentration present in the surrounding buffer. Right side showing active loading driven by electrochemical gradient (generated by pH difference in this example) which drives drug entrance into preformed liposome and ionization of drug molecule, preventing it from exiting the liposome.**

### Liposomes as Drug Carriers

Beyond furthering membrane studies by exploring protein membrane interactions, behavior, and characterization, liposomes serve as an excellent platform for carrying drugs in a protected state within the body [23, 29, 39, 40]. Substances intended for the treatment of diseases are seldom without unintended off-target effects. Drug molecules generally stimulate or inhibit behaviors of either foreign or host cells to achieve their desired effects, yet their activity is often indiscriminate. Systemic applications can be potentially hazardous and ineffective, as drug molecules are often reactive, unstable, and frequently target key biological components and processes. These issues are particularly concerning in instances such as treatment of maladies like fungal infections [41, 42] and malignant neoplasms [43, 44]. The systemic application of naked drug molecules not

only limits the amounts and concentrations of drugs that can be safely used to effectively treat the intended disease but is also often plagued by a short period of bioavailability. Drug carriers, such as liposomes, attempt to mitigate these issues by retaining and controlling release of a drug cargo intended for diseased tissue until reaching their desired target and prolonging their circulation within the body [45, 46]. In this light, using liposomes as drug carriers resulted in a fruitful and ever-expanding field of research (Figure 6).

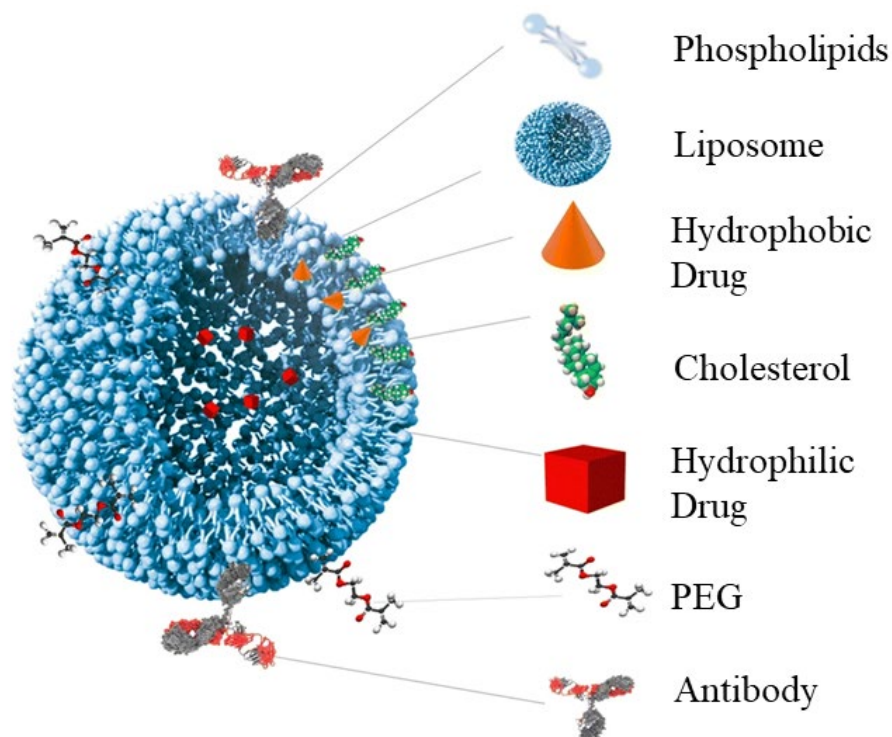


**Figure 6.** The versatile use and modification of liposomes as drug carriers.

Apart from drug loading in the core or membrane, liposomes are highly customizable. Surface modifications are frequently made to better reach and interact with their intended target (i.e., by using antibodies) as drug carriers or to avoid the immune system (PEG). Figure originally from Beltran-Gracia et al., 2019 - Nanomedicine review: clinical developments in liposomal applications [45]. Available under Creative Commons License.

One of the most obvious yet key aspects of liposomes pertaining to their usefulness as drug carriers is their isolated core. Beyond the ability of holding water soluble cargo in the core, the intramembranous space of the bilayer also creates a favorable environment for incorporating small hydrophobic molecules. The loading of drugs in the liposomes serves many purposes, key among them being the preservation of the drug cargo from the unstable and chemically active bloodstream environment. On the other hand, the prevention of premature drug action on non-target tissue, significantly reducing many side effects often seen from exposed, systemic treatment with the same drugs [46]. This preservation also acts to increase the overall long-term bioavailability of the drug and in some instances, increase effective concentrations [47].

In addition to their protective and stabilizing function, liposomes can be produced of sizes and physical properties that enable self-accumulation in intended regions, such as tumors, by the enhanced permeability and retention (EPR) effect (Figure 7) [48-50]. This can be seen by increased accumulation of small liposomes up to 200 nm diameter in tumor regions due to the porous, leaky capillaries developed among rapidly growing tumor tissue, as well as their lack of functional lymphatic drainage [51, 52]. Liposomes that are too small, somewhere around or below 50 nm in diameter, appear to have the tendency to also collect in the liver through fenestrated endothelium [53]. Contrarily, larger liposomes are easily detected and captured by the immune cells, resulting in both liver and spleen accumulation [54]. Furthermore, liposomes can be functionalized to target specific cells and tissues; for example, folate may be used to target cancer cells since tumor cells overexpress folate receptors on their surface [55, 56], while

functionalization with specific antibodies provide endless opportunities to target specific tissues [57-59].

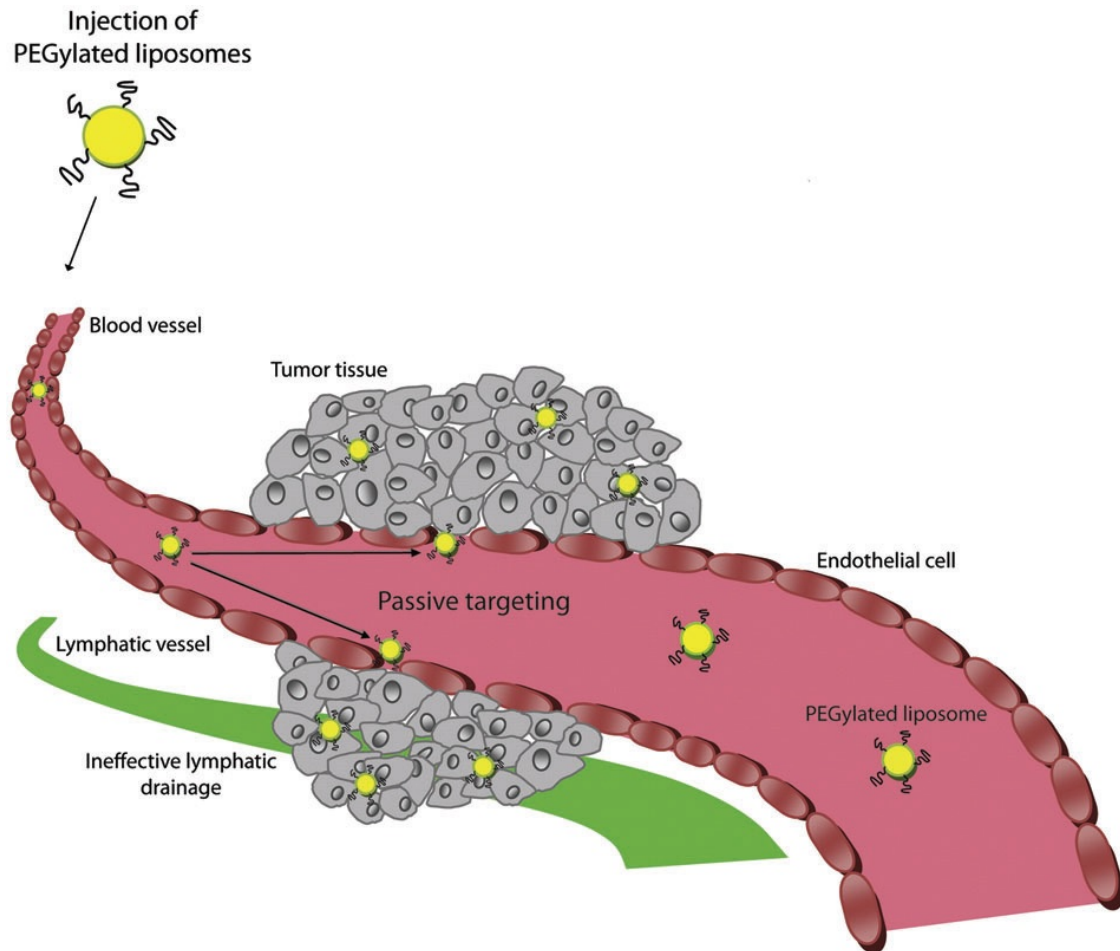


**Figure 3. The Enhanced Permeability and Retention (EPR) effect presented by small, PEGylated liposomes. The fenestrated endothelial lining of blood vessels developed by tumors allow entrance of small liposomes into the tumor tissue. Upon entrance, liposomes fail to escape because of the ineffective lymphatic drainage in tumors. Figure originally from Børresen et al., 2017 - Liposome-encapsulated chemotherapy: Current Evidence for its Use in Companion Animals [50]. Used with permission from the publisher.**

A prominent issue presented by the early attempt to use liposomes as drug carriers involved a strong immune response from the host upon injection into the bloodstream [60]. Liposomal membranes can be modified to minimize recognition by the host's

immune system mechanisms such as the mononuclear phagocyte system (MPS)/reticuloendothelial system (RES) [61-63]. Immune response can be evaded by creating a steric shield over the liposomal surfaces by utilizing polyethylene glycol (PEG) moieties protruding from the membrane (Figure 6) [64, 65], prolonging their circulation times to weeks. This revolutionized the study of liposomes as drug carriers as it allowed for their introduction into a host's bloodstream without immediate immune response.

An excellent example for liposomes-mediated drug delivery is shown by the liposomal formulation of doxorubicin. A powerful chemotherapeutic, doxorubicin, most effectively achieves shrinking tumor tissue at concentrations which are also cardio toxic [66, 67]. Doxil®, the first FDA approved liposomal drug carrier, uses active loading of doxorubicin into PEGylated liposomes to avoid immune system detection. Due to their sub-200 nm diameter, the EPR effect enables self-accumulation at tumor sites, resulting in a passive and local delivery of high concentration of doxorubicin [36, 68]. Some of the latest research and innovation pertaining to liposome drug and gene delivery involves the use of fusogenic liposomes expelling material into cellular cytosol [69, 70]. Finally, another prominent and potent technique involves producing liposomes that have membranes capable of changing permeability upon external stimulation, resulting in controlled or environmentally triggered release of cargo [71].

### **Triggered Release of Payload from Liposomes**

Beyond conventional treatments without the use of drug carriers, liposomes provide significant advantages and improvements which are already substantial on their own. It is well understood that beyond reaching a target, the amounts of a drug achieved

locally must go beyond threshold concentrations to effectively work. More so, it is often desirable that the high drug concentrations are attained in a short period of time.

PEGylated liposomes consisting of bilayers composed of relatively stable lipid compositions can take days to effectively release their contents [72]. In this regard, liposomes that can be triggered to release their cargo retain all the benefits offered by regular liposomal drug carriers, with the added benefit of being capable of delivering high concentration of drugs immediately upon application of external stimuli. This is of key significance especially when dealing with delivery of chemotherapeutics to tumor sites, where killing cancerous cells with the utmost urgency is often desired to eliminate their proliferation and potential metastatic behavior.

The need for controlled release is still an unmet challenge. However, efforts are being taken to better understand how the ability to create and utilize controlled release liposomes could potentially offer significant improvements in treatment outcomes. Greater understanding and abilities of synthetic chemistry, as well as nanoparticles, allows for the creation of lipids and lipid membranes capable of specific chemical or physical response to stimuli. Such stimuli come in the form of wavelength specific radiation [73, 74], pH change [75], ultrasound [76], magnetic actuation [77], and temperature [78]. Furthermore, particles embedded or loaded within liposomes can be triggered by external near-infrared or X-ray radiation to initiate a cascade of events leading to the release of the liposome content [79, 80].

## References

1. Bangham, A. D.; Horne, R. W., Negative staining of phospholipids and their structural modification by surface-active agents as observed in the electron microscope. *Journal of Molecular Biology* **1964**, *8* (5), 660-IN10.
2. Akbarzadeh, A.; Rezaei-Sadabady, R.; Davaran, S.; Joo, S. W.; Zarghami, N.; Hanifehpour, Y.; Samiei, M.; Kouhi, M.; Nejati-Koshki, K., Liposome: classification, preparation, and applications. *Nanoscale Res Lett* **2013**, *8* (1), 102.
3. Laouini, A.; Jaafar-Maalej, C.; Limayem-Blouza, I.; Sfar, S.; Charcosset, C.; Fessi, H., Preparation, Characterization and Applications of Liposomes: State of the Art. *Journal of Colloid Science and Biotechnology* **2012**, *1* (2), 147-168.
4. Lasic, D. D., Novel applications of liposomes. *Trends in Biotechnology* **1998**, *16* (7), 307-321.
5. Ghorbanzade, T.; Jafari, S. M.; Akhavan, S.; Hadavi, R., Nano-encapsulation of fish oil in nano-liposomes and its application in fortification of yogurt. *Food Chemistry* **2017**, *216*, 146-152.
6. Mohammadi, A.; Jafari, S. M.; Mahoonak, A. S.; Ghorbani, M., Liposomal/Nanoliposomal Encapsulation of Food-Relevant Enzymes and Their Application in the Food Industry. *Food and Bioprocess Technology* **2021**, *14* (1), 23-38.
7. Xing, H.; Hwang, K.; Lu, Y., Recent Developments of Liposomes as Nanocarriers for Theranostic Applications. *Theranostics* **2016**, *6* (9), 1336-1352.
8. Stano, P., Gene Expression Inside Liposomes: From Early Studies to Current Protocols. *Chemistry – A European Journal* **2019**, *25* (33), 7798-7814.
9. Ahmadi Ashtiani, H. R.; Bishe, P.; Lashgari, N.; Nilforoushzadeh, M. A.; Zare, S., Liposomes in Cosmetics. *J Skin Stem Cell* **2016**, *3* (3), e65815.
10. Rampioni, G.; D'Angelo, F.; Leoni, L.; Stano, P., Gene-Expressing Liposomes as Synthetic Cells for Molecular Communication Studies. *Frontiers in Bioengineering and Biotechnology* **2019**, *7* (1).

11. Shrestha, N.; Thomas, C. A.; Richtsmeier, D.; Bogard, A.; Hermann, R.; Walker, M.; Abatchev, G.; Brown, R. J.; Fologea, D., Temporary Membrane Permeabilization via the Pore-Forming Toxin Lysenin. *Toxins* **2020**, *12* (5).
12. Smirnova, I. A.; Ädelroth, P.; Brzezinski, P., Extraction and liposome reconstitution of membrane proteins with their native lipids without the use of detergents. *Scientific Reports* **2018**, *8* (1), 14950.
13. Daudey, G. A.; Zope, H. R.; Voskuhl, J.; Kros, A.; Boyle, A. L., Membrane-Fusion Distance Is Critical for Efficient Coiled-Coil-Peptide-Mediated Liposome Fusion. *Langmuir* **2017**, *33* (43), 12443-12452.
14. van Hoogevest, P., Review – An update on the use of oral phospholipid excipients. *European Journal of Pharmaceutical Sciences* **2017**, *108*, 1-12.
15. Lasic, D. D., A molecular model for vesicle formation. *Biochim Biophys Acta* **1982**, *692* (3), 501-2.
16. Lasic, D. D., The mechanism of vesicle formation. *The Biochemical journal* **1988**, *256* (1), 1-11.
17. Patil, Y. P.; Jadhav, S., Novel methods for liposome preparation. *Chem Phys Lipids* **2014**, *177*, 8-18.
18. Bangham, A. D.; Standish, M. M.; Watkins, J. C., Diffusion of univalent ions across the lamellae of swollen phospholipids. *Journal of Molecular Biology* **1965**, *13* (1), 238-IN27.
19. Winterhalter, M.; Lasic, D. D., Liposome stability and formation: experimental parameters and theories on the size distribution. *Chem Phys Lipids* **1993**, *64* (1-3), 35-43.
20. Cho, N.-J.; Hwang, L. Y.; Solandt, J. J. R.; Frank, C. W., Comparison of Extruded and Sonicated Vesicles for Planar Bilayer Self-Assembly. *Materials* **2013**, *6* (8).

21. Lapinski, M. M.; Castro-Forero, A.; Greiner, A. J.; Ofoli, R. Y.; Blanchard, G. J., Comparison of Liposomes Formed by Sonication and Extrusion: Rotational and Translational Diffusion of an Embedded Chromophore. *Langmuir* **2007**, *23* (23), 11677-11683.
22. Shah, V. M.; Nguyen, D. X.; Patel, P.; Cote, B.; Al-Fatease, A.; Pham, Y.; Huynh, M. G.; Woo, Y.; Alani, A. W. G., Liposomes produced by microfluidics and extrusion: A comparison for scale-up purposes. *Nanomedicine: Nanotechnology, Biology and Medicine* **2019**, *18*, 146-156.
23. Bozzuto, G.; Molinari, A., Liposomes as nanomedical devices. *International journal of nanomedicine* **2015**, *10*, 975-999.
24. Olson, F.; Hunt, C. A.; Szoka, F. C.; Vail, W. J.; Papahadjopoulos, D., Preparation of liposomes of defined size distribution by extrusion through polycarbonate membranes. *Biochimica et Biophysica Acta (BBA) - Biomembranes* **1979**, *557* (1), 9-23.
25. Ong, S. G.; Chitneni, M.; Lee, K. S.; Ming, L. C.; Yuen, K. H., Evaluation of Extrusion Technique for Nanosizing Liposomes. *Pharmaceutics* **2016**, *8* (4).
26. Richardson, E. S.; Pitt, W. G.; Woodbury, D. J., The Role of Cavitation in Liposome Formation. *Biophysical Journal* **2007**, *93* (12), 4100-4107.
27. Charcosset, C.; Juban, A.; Valour, J.-P.; Urbaniak, S.; Fessi, H., Preparation of liposomes at large scale using the ethanol injection method: Effect of scale-up and injection devices. *Chemical Engineering Research and Design* **2015**, *94*, 508-515.
28. Powers, D.; Nosoudi, N., Liposomes; from synthesis to targeting macrophages. **2019**.
29. Dimov, N.; Kastner, E.; Hussain, M.; Perrie, Y.; Szita, N., Author Correction: Formation and purification of tailored liposomes for drug delivery using a module-based micro continuous-flow system. In *Sci Rep*, England, 2018; Vol. 8, p 6762.
30. Deamer, D. W., Preparation and properties of ether-injection liposomes. *Ann NY Acad Sci* **1978**, *308*, 250-8.

31. Zumbuehl, O.; Weder, H. G., Liposomes of controllable size in the range of 40 to 180 nm by defined dialysis of lipid/detergent mixed micelles. *Biochimica et Biophysica Acta (BBA) - Biomembranes* **1981**, *640* (1), 252-262.
32. Peschka, R.; Purmann, T.; Schubert, R., Cross-flow filtration—an improved detergent removal technique for the preparation of liposomes. *International Journal of Pharmaceutics* **1998**, *162* (1), 177-183.
33. Cullis, P. R.; Mayer, L. D.; Bally, M. B.; Madden, T. D.; Hope, M. J., Generating and loading of liposomal systems for drug-delivery applications. *Advanced Drug Delivery Reviews* **1989**, *3* (3), 267-282.
34. Niu, G.; Cogburn, B.; Hughes, J., Preparation and characterization of doxorubicin liposomes. *Methods Mol Biol* **2010**, *624*, 211-9.
35. Cullis, P. R.; Hope, M. J.; Bally, M. B.; Madden, T. D.; Mayer, L. D.; Fenske, D. B., Influence of pH gradients on the transbilayer transport of drugs, lipids, peptides and metal ions into large unilamellar vesicles. *Biochim Biophys Acta* **1997**, *1331* (2), 187-211.
36. Barenholz, Y., Doxil®--the first FDA-approved nano-drug: lessons learned. *J Control Release* **2012**, *160* (2), 117-34.
37. Bolotin, E. M.; Cohen, R.; Bar, L. K.; Emanuel, N.; Ninio, S.; Barenholz, Y.; Lasic, D. D., Ammonium Sulfate Gradients for Efficient and Stable Remote Loading of Amphipathic Weak Bases into Liposomes and Ligandoliposomes. *Journal of Liposome Research* **1994**, *4* (1), 455-479.
38. Lasic, D. D.; Frederik, P. M.; Stuart, M. C.; Barenholz, Y.; McIntosh, T. J., Gelation of liposome interior. A novel method for drug encapsulation. *FEBS Lett* **1992**, *312* (2-3), 255-8.
39. Li, M.; Du, C.; Guo, N.; Teng, Y.; Meng, X.; Sun, H.; Li, S.; Yu, P.; Galons, H., Composition design and medical application of liposomes. *Eur J Med Chem* **2019**, *164*, 640-653.

40. Patra, J. K.; Das, G.; Fraceto, L. F.; Campos, E. V. R.; Rodriguez-Torres, M. d. P.; Acosta-Torres, L. S.; Diaz-Torres, L. A.; Grillo, R.; Swamy, M. K.; Sharma, S.; Habtemariam, S.; Shin, H.-S., Nano based drug delivery systems: recent developments and future prospects. *Journal of Nanobiotechnology* **2018**, *16* (1), 71.
41. Moen, M. D.; Lyseng-Williamson, K. A.; Scott, L. J., Liposomal amphotericin B: a review of its use as empirical therapy in febrile neutropenia and in the treatment of invasive fungal infections. *Drugs* **2009**, *69* (3), 361-92.
42. Groll, A. H.; Rijnders, B. J. A.; Walsh, T. J.; Adler-Moore, J.; Lewis, R. E.; Brüggemann, R. J. M., Clinical Pharmacokinetics, Pharmacodynamics, Safety and Efficacy of Liposomal Amphotericin B. *Clinical Infectious Diseases* **2019**, *68* (Supplement\_4), S260-S274.
43. Olusanya, T. O. B.; Haj Ahmad, R. R.; Ibegbu, D. M.; Smith, J. R.; Elkordy, A. A., Liposomal Drug Delivery Systems and Anticancer Drugs. *Molecules (Basel, Switzerland)* **2018**, *23* (4), 907.
44. Brown, P. D.; Patel, P. R., Nanomedicine: a pharma perspective. *Wiley Interdiscip Rev Nanomed Nanobiotechnol* **2015**, *7* (2), 125-30.
45. Beltrán-Gracia, E.; López-Camacho, A.; Higuera-Ciapara, I.; Velázquez-Fernández, J. B.; Vallejo-Cardona, A. A., Nanomedicine review: clinical developments in liposomal applications. *Cancer Nanotechnology* **2019**, *10* (1), 11.
46. Chang, C.-C.; Liu, D.-Z.; Lin, S.-Y.; Liang, H.-J.; Hou, W.-C.; Huang, W.-J.; Chang, C.-H.; Ho, F.-M.; Liang, Y.-C., Liposome encapsulation reduces cantharidin toxicity. *Food and Chemical Toxicology* **2008**, *46* (9), 3116-3121.
47. Medina-Alarcón, K. P.; Voltan, A. R.; Fonseca-Santos, B.; Moro, I. J.; de Oliveira Souza, F.; Chorilli, M.; Soares, C. P.; Dos Santos, A. G.; Mendes-Giannini, M. J. S.; Fusco-Almeida, A. M., Highlights in nanocarriers for the treatment against cervical cancer. *Mater Sci Eng C Mater Biol Appl* **2017**, *80*, 748-759.

48. Dawidczyk, C. M.; Kim, C.; Park, J. H.; Russell, L. M.; Lee, K. H.; Pomper, M. G.; Searson, P. C., State-of-the-art in design rules for drug delivery platforms: lessons learned from FDA-approved nanomedicines. *J Control Release* **2014**, *187*, 133-44.
49. Maeda, H.; Wu, J.; Sawa, T.; Matsumura, Y.; Hori, K., Tumor vascular permeability and the EPR effect in macromolecular therapeutics: a review. *Journal of Controlled Release* **2000**, *65* (1), 271-284.
50. Børresen, B.; Hansen, A. E.; Kjær, A.; Andresen, T. L.; Kristensen, A. T., Liposome-encapsulated chemotherapy: Current evidence for its use in companion animals. *Veterinary and Comparative Oncology* **2018**, *16* (1), E1-E15.
51. Ngoune, R.; Peters, A.; von Elverfeldt, D.; Winkler, K.; Pütz, G., Accumulating nanoparticles by EPR: A route of no return. *Journal of Controlled Release* **2016**, *238*, 58-70.
52. Hobbs, S. K.; Monsky, W. L.; Yuan, F.; Roberts, W. G.; Griffith, L.; Torchilin, V. P.; Jain, R. K., Regulation of transport pathways in tumor vessels: Role of tumor type and microenvironment. *Proceedings of the National Academy of Sciences* **1998**, *95* (8), 4607.
53. Litzinger, D. C.; Buiting, A. M. J.; van Rooijen, N.; Huang, L., Effect of liposome size on the circulation time and intraorgan distribution of amphipathic poly(ethylene glycol)-containing liposomes. *Biochimica et Biophysica Acta (BBA) - Biomembranes* **1994**, *1190* (1), 99-107.
54. Maruyama, K., Intracellular targeting delivery of liposomal drugs to solid tumors based on EPR effects. *Advanced Drug Delivery Reviews* **2011**, *63* (3), 161-169.
55. Gabizon, A.; Horowitz, A. T.; Goren, D.; Tzemach, D.; Mandelbaum-Shavit, F.; Qazen, M. M.; Zalipsky, S., Targeting Folate Receptor with Folate Linked to Extremities of Poly(ethylene glycol)-Grafted Liposomes: In Vitro Studies. *Bioconjugate Chemistry* **1999**, *10* (2), 289-298.

56. Soe, Z. C.; Thapa, R. K.; Ou, W.; Gautam, M.; Nguyen, H. T.; Jin, S. G.; Ku, S. K.; Oh, K. T.; Choi, H.-G.; Yong, C. S.; Kim, J. O., Folate receptor-mediated celastrol and irinotecan combination delivery using liposomes for effective chemotherapy. *Colloids and Surfaces B: Biointerfaces* **2018**, *170*, 718-728.
57. Arabi, L.; Badiee, A.; Mosaffa, F.; Jaafari, M. R., Targeting CD44 expressing cancer cells with anti-CD44 monoclonal antibody improves cellular uptake and antitumor efficacy of liposomal doxorubicin. *Journal of Controlled Release* **2015**, *220*, 275-286.
58. Belfiore, L.; Saunders, D. N.; Ranson, M.; Thurecht, K. J.; Storm, G.; Vine, K. L., Towards clinical translation of ligand-functionalized liposomes in targeted cancer therapy: Challenges and opportunities. *Journal of Controlled Release* **2018**, *277*, 1-13.
59. Crouch, C. H.; Bost, M. H.; Kim, T. H.; Green, B. M.; Arbuckle, D. S.; Grossman, C. H.; Howard, K. P., Optimization of Detergent-Mediated Reconstitution of Influenza A M2 Protein into Proteoliposomes. *Membranes (Basel)* **2018**, *8* (4).
60. Heath, T. D.; Edwards, D. C.; Ryman, B. E., The Adjuvant Properties of Liposomes. *Biochemical Society Transactions* **1976**, *4* (1), 129-133.
61. Gabizon, A.; Papahadjopoulos, D., Liposome formulations with prolonged circulation time in blood and enhanced uptake by tumors. *Proc Natl Acad Sci U S A* **1988**, *85* (18), 6949-53.
62. Caron, W. P.; Lay, J. C.; Fong, A. M.; La-Beck, N. M.; Kumar, P.; Newman, S. E.; Zhou, H.; Monaco, J. H.; Clarke-Pearson, D. L.; Brewster, W. R.; Van Le, L.; Bae-Jump, V. L.; Gehrig, P. A.; Zamboni, W. C., Translational Studies of Phenotypic Probes for the Mononuclear Phagocyte System and Liposomal Pharmacology. *Journal of Pharmacology and Experimental Therapeutics* **2013**, *347* (3), 599.

63. Kao, Y. J.; Juliano, R. L., Interactions of liposomes with the reticuloendothelial system. Effects of reticuloendothelial blockade on the clearance of large unilamellar vesicles. *Biochim Biophys Acta* **1981**, *677* (3-4), 453-61.
64. Papahadjopoulos, D.; Allen, T. M.; Gabizon, A.; Mayhew, E.; Matthay, K.; Huang, S. K.; Lee, K. D.; Woodle, M. C.; Lasic, D. D.; Redemann, C., Sterically stabilized liposomes: improvements in pharmacokinetics and antitumor therapeutic efficacy. *Proceedings of the National Academy of Sciences* **1991**, *88* (24), 11460.
65. Klibanov, A. L.; Maruyama, K.; Torchilin, V. P.; Huang, L., Amphipathic polyethyleneglycols effectively prolong the circulation time of liposomes. *FEBS Letters* **1990**, *268* (1), 235-237.
66. Songbo, M.; Lang, H.; Xinyong, C.; Bin, X.; Ping, Z.; Liang, S., Oxidative stress injury in doxorubicin-induced cardiotoxicity. *Toxicology Letters* **2019**, *307*, 41-48.
67. Tahover, E.; Patil, Y. P.; Gabizon, A. A., Emerging delivery systems to reduce doxorubicin cardiotoxicity and improve therapeutic index: focus on liposomes. *Anti-Cancer Drugs* **2015**, *26* (3).
68. Gabizon, A.; Catane, R.; Uziely, B.; Kaufman, B.; Safra, T.; Cohen, R.; Martin, F.; Huang, A.; Barenholz, Y., Prolonged Circulation Time and Enhanced Accumulation in Malignant Exudates of Doxorubicin Encapsulated in Polyethylene-glycol Coated Liposomes. *Cancer Research* **1994**, *54* (4), 987.
69. Scriboni, A. B.; Couto, V. M.; Ribeiro, L. N. d. M.; Freires, I. A.; Groppo, F. C.; de Paula, E.; Franz-Montan, M.; Cogo-Müller, K., Fusogenic Liposomes Increase the Antimicrobial Activity of Vancomycin Against *Staphylococcus aureus* Biofilm. *Frontiers in Pharmacology* **2019**, *10* (1401).
70. Kube, S.; Hersch, N.; Naumovska, E.; Gensch, T.; Hendriks, J.; Franzen, A.; Landvogt, L.; Siebrasse, J.-P.; Kubitscheck, U.; Hoffmann, B.; Merkel, R.; Csiszár, A., Fusogenic Liposomes as Nanocarriers for the Delivery of Intracellular Proteins. *Langmuir* **2017**, *33* (4), 1051-1059.

71. Bibi, S.; Lattmann, E.; Mohammed, A. R.; Perrie, Y., Trigger release liposome systems: local and remote controlled delivery? *Journal of Microencapsulation* **2012**, *29* (3), 262-276.
72. Barenholz, Y., Liposome application: problems and prospects. *Current Opinion in Colloid & Interface Science* **2001**, *6* (1), 66-77.
73. Wang, J.-Y.; Wu, Q.-F.; Li, J.-P.; Ren, Q.-S.; Wang, Y.-L.; Liu, X.-M., Photo-sensitive liposomes: chemistry and application in drug delivery. *Mini reviews in medicinal chemistry* **2010**, *10* (2), 172-181.
74. Yavlovich, A.; Singh, A.; Blumenthal, R.; Puri, A., A novel class of photo-triggerable liposomes containing DPPC:DC8,9PC as vehicles for delivery of doxorubicin to cells. *Biochimica et Biophysica Acta (BBA) - Biomembranes* **2011**, *1808* (1), 117-126.
75. Jiang, L.; Li, L.; He, B.; Pan, D.; Luo, K.; Yi, Q.; Gu, Z., Anti-Cancer Efficacy of Paclitaxel Loaded in pH Triggered Liposomes. *Journal of Biomedical Nanotechnology* **2016**, *12* (1), 79-90.
76. Schroeder, A.; Honen, R.; Turjeman, K.; Gabizon, A.; Kost, J.; Barenholz, Y., Ultrasound triggered release of cisplatin from liposomes in murine tumors. *Journal of Controlled Release* **2009**, *137* (1), 63-68.
77. Amstad, E.; Kohlbrecher, J.; Müller, E.; Schweizer, T.; Textor, M.; Reimhult, E., Triggered Release from Liposomes through Magnetic Actuation of Iron Oxide Nanoparticle Containing Membranes. *Nano Letters* **2011**, *11* (4), 1664-1670.
78. Kono, K.; Nakashima, S.; Kokuryo, D.; Aoki, I.; Shimomoto, H.; Aoshima, S.; Maruyama, K.; Yuba, E.; Kojima, C.; Harada, A.; Ishizaka, Y., Multi-functional liposomes having temperature-triggered release and magnetic resonance imaging for tumor-specific chemotherapy. *Biomaterials* **2011**, *32* (5), 1387-1395.
79. Fologea, D.; Salamo, G.; Henry, R.; Borrelli, M. J.; Corry, P., X-Ray Controlled Drug Release from Liposomes. *Biophysical Journal* **2016**, *110* (3), 200a.

80. Wu, G.; Mikhailovsky, A.; Khant, H. A.; Fu, C.; Chiu, W.; Zasadzinski, J. A., Remotely Triggered Liposome Release by Near-Infrared Light Absorption via Hollow Gold Nanoshells. *Journal of the American Chemical Society* **2008**, *130* (26), 8175-8177.

## CHAPTER TWO: PREPARATION, LOADING, AND CHARACTERIZATION OF LIPOSOMES MADE BY SONICATION AND EXTRUSION

Widely recognized as classic preparation methods of liposomes, extrusion and sonication are reliably and frequently used, decades after their inception [1-4]. In this respect, this chapter will discuss the production and further physical characterization of common liposomes by employing microscopy imaging and Dynamic Light Scattering. Apart from formation, liposomes were also passively or actively loaded with drug simulating dyes or chemotherapeutic doxorubicin, and successful loading was confirmed by fluorescence microscopy and spectroscopy. Further analysis of loading was performed by using fluorescence spectroscopy analysis, which exploited fluorescence self-quenching to monitor dye concentration changes upon liposome membrane solubilization with non-ionic detergent.

### **Materials and Methods**

#### Lipids, Loading Molecules, and Buffers

Asolectin (Aso, Sigma-Aldrich), cholesterol (Chol, Sigma-Aldrich), 1,2-distearoyl-sn-glycero-3-phosphocholine (DSPC, Avanti Polar Lipids), and 1,2-distearoyl-sn-glycero-3-phosphoethanolamine-N-[methoxy(polyethyleneglycol)-2000] (DSPE-PEG, Avanti Polar Lipids) (Figure 8) were purchased either in powder or chloroform solubilized form. The powder lipids were solubilized in chloroform, mixed with the other lipids at the desired weight ratios in glass vials, then had the solvent removed by placing

the open vials placed under vacuum for at least 12 hours. Formed lipid films not used immediately were stored in a freezer at -20 °C. The precursors to all liposome preparations were the dried lipid films prepared from a mixture of lipids at specified dry-weight ratios. The dye molecules used to demonstrate loading included calcein (CAL), rhodamine 6G (R6G), and acridine orange (AO) (all from ThermoFisher Scientific). An actual chemotherapeutic loaded into extruded liposomes was doxorubicin (DOX, Sigma-Aldrich) (Figure 9). The buffers used for all experiments included phosphate-buffered saline 1x (PBS, Fisher Scientific), 135 mM KCl + 20 mM HEPES prepared from KCl in dry form (ThermoFisher Scientific) and 1 M HEPES (Sigma-Aldrich), or 150 mM citrate buffer prepared from sodium citrate dihydrate and citric acid (Fisher Scientific) brought to pH 4.24 using 1 M HCl.

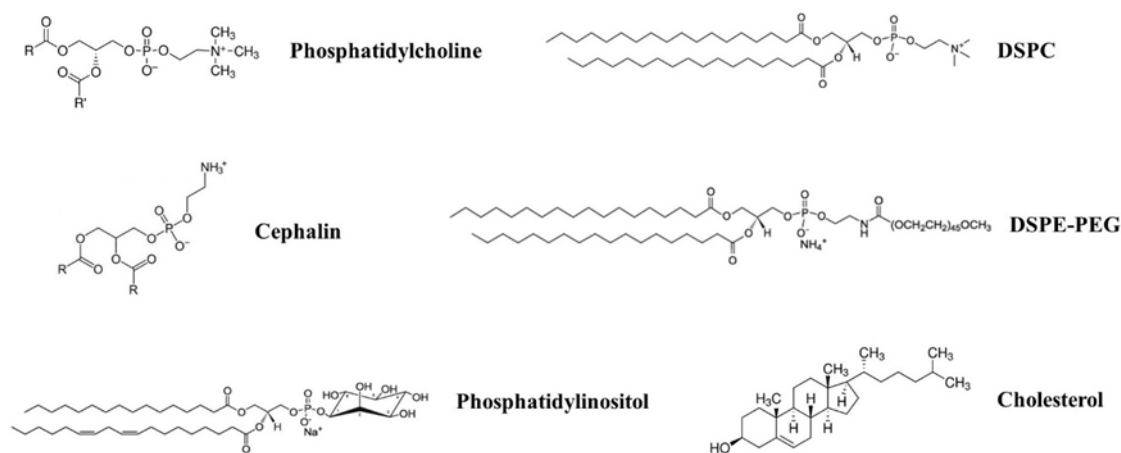


**Figure 8. Structural details of phospholipids and cholesterol used for preparation of liposomes. Naturally derived asolectin is a combination of equal parts lecithin [phosphatidylcholine], cephalin, and phosphatidylinositol, with small amounts of other phospholipids and polar lipids (“R” indicates possible variable structure in fatty acid tail). Synthetic lipids 1,2-distearoyl-sn-glycero-3-phosphocholine (DSPC) and 1,2-distearoyl-sn-glycero-3-phosphoethanolamine-N-[methoxy(polyethyleneglycol)-2000] (DSPE-PEG) and cholesterol were also utilized for liposome production.**

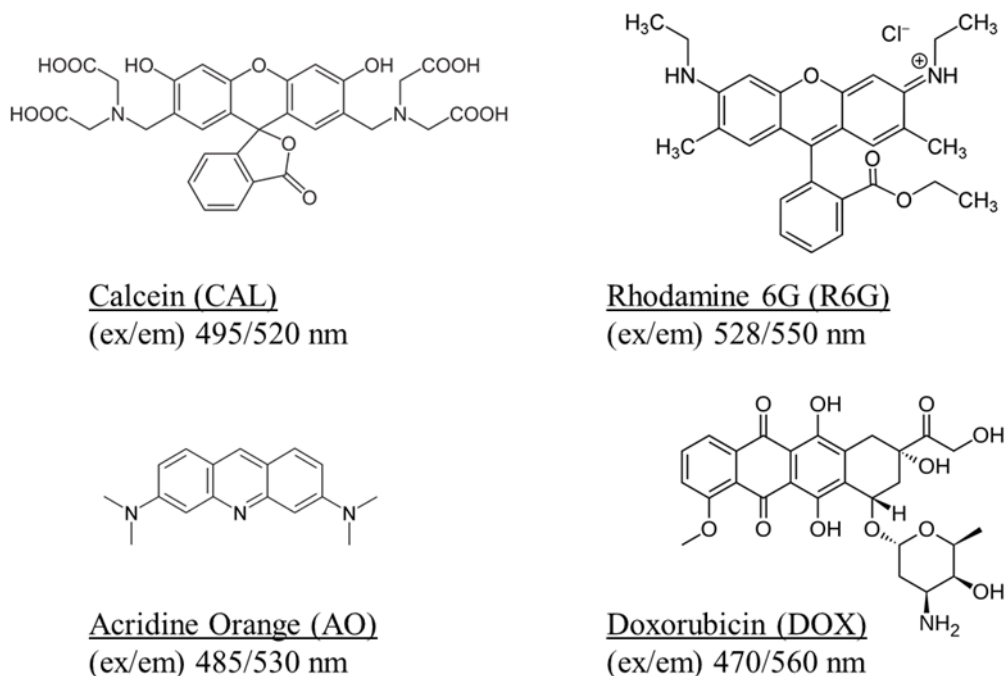


**Figure 9. Chemical and optical properties of dye and drug molecules passively and actively loaded into sonication and extrusion prepared liposomes. Fluorescent dyes calcein (CAL) (ex/em) 495/520 nm, and rhodamine 6G (R6G) (ex/em) 528/550 nm were passively loaded. Fluorescent dye acridine orange (AO) (ex/em) 485/530 nm was both passively and actively loaded. Anthracycline chemotherapeutic doxorubicin (DOX) (ex/em) 470/560 nm was actively loaded.**

### Liposome Preparation

Prior to extrusion, the lipid films in the glass vials were slowly hydrated with appropriate buffer/dye for a minimum of 30 minutes at 45 °C. To complete hydration and homogenize the mixture, the hydrated samples underwent two freeze/thaw cycles. Freezing brought the hydrated lipids to -20 °C, and thawing quickly warmed the samples to 45 °C. Upon final thawing, lipid hydration mixtures were brought to 60 °C right before placement into the extrusion syringe. The liposomes were extruded at 70 °C with an Avanti Polar Lipids extruder equipped with specified pore size polycarbonate membrane filters for a minimum of 61 passes

Liposome preparation by sonication was completed with a Misonix S-4000 probe sonicator (Misonix) equipped with a micro-tip. Lipid film hydration was completed in the same manner as described previously for hydration before extrusion. Immediately prior to sonication, hydrated mixtures were brought up to 60°C then allowed to cool to room temperature. Subsequently, the hydrated lipid mixtures were placed into small glass vials and sonicated on ice for 15 minutes in manual mode at 25% amplitude and a power transfer of 6-7 W.

#### Liposome Loading and Dialysis Purification

Passively loaded liposomes were purified of excess dye using dialysis. CAL loaded liposomes were passively loaded at 3 mM concentration, and R6G liposomes were loaded at 1 mM dye concentration. Liposome samples were loaded into Float-A-Lyzer G2 dialysis devices (Spectrum Spectra/Por), Slide-A-Lyzer cassettes (Thermo Fisher Scientific), or an Ultra-Fast Dialyzer chamber sealed with 100 nm polycarbonate membranes (Harvard Apparatus). The dialysis devices were placed into pristine buffer (identical to the hydration buffer) for at least 24 hours. For particularly concentrated dye in bulk that required thorough liposome purification, dialysis was complete with multiple rounds of buffer exchange.

For samples being actively loaded, hydration and liposome preparation was completed in a 150 mM citrate buffer at pH 4.24. Buffer exchange with neutral pH buffer (PBS 1X or KCl 135 mM + HEPES 20 mM) was completed by overnight dialysis using the same procedure as for purification of passively loaded liposomes. Active loading for AO was allowed for a minimum of 24 hours for AO and 48 hours for DOX at 4 °C before further analysis by microscopy or fluorescence spectroscopy. The external concentration

of dye/drug active loading was 50  $\mu\text{M}$  for AO and 25  $\mu\text{M}$  for DOX; at these concentrations, the amount of dye left in the bulk was negligible, and no further purification was performed.

#### Liposome Characterization with Microscopy and Dynamic Light Scattering

Imaging was completed with an Olympus IX71 fluorescence microscope (Olympus Scientific Solutions Americas Corp) equipped with appropriate filter sets. The emission spectrum of each dye was determined with a FluoroMax4 spectrofluorometer (Horiba) set in emission mode. The release of encapsulated dyes was observed with the spectrofluorometer set in kinetics acquisition mode. To verify the load, 100  $\mu\text{L}$  of 5% v/v Triton X-100 (Sigma-Aldrich) was added to the liposomal solutions in cuvettes.

Size characterization of the liposomes was performed by dynamic light scattering (DLS) with the Zetasizer Nano ZS (Malvern Instruments) for determination of average hydrodynamic diameter and size distribution (PDI, polydispersity index) at room temperature. For each liposome sample we analyzed three sets, and each set consisted of 13 consecutive runs. Each set provided the corresponding average diameter and PDI, from which the mean values and standard deviations were calculated.

### **Results and Discussions**

#### Size and Size Distribution: Liposomes Prepared by Hydration, Sonication, and Extrusion

The fate of liposomes in vivo heavily depends on their physical and chemical attributes. Two such very pertinent and important features are size and size distribution [5, 6]. Although there does not appear to be a strict numerical cut-off or standard that is required of liposomes regarding their size or size distribution for biomedical applications, these factors are key in designating their suitability and safety for such use [6, 7].

Biodistribution and clearance are greatly influenced by the size of the particles injected into the bloodstream or subcutaneous tissue of a subject [5, 6, 8-12]. In addition, liposomes used in such applications must have predictable characteristics, such as a uniform size distribution, to complete their intended purpose and minimize unintended side effects from their application [5, 7]. Beyond safety, poor size distributions have been implicated in impeding pharmacological and pharmacokinetic studies involving liposomes [6, 13]. In this regard, it is important to assess these two physical properties of liposomes soon after they are produced. This was done by analyzing the PDI and average hydrodynamic diameter of samples as analyzed by DLS.

Liposome production is initiated with the hydration of a lipid deposit [13, 14]. Hydration can be utilized only for the preparation of polydisperse and multilamellar liposomes, therefore further procedures must be taken to improve the quality of liposomes (i.e., lamellarity, size, and size distribution), such as extrusion and sonication. The first set of analyses included comparing the average hydrodynamic diameter and PDI of liposomes prepared by hydration (H), probe sonication (S), and extrusion (E) through 400 nm polycarbonate membranes. The measurements included liposomes composed of either a regular lipid composition (dry weight ratio of Aso:Chol at 10:4, designated R) or long circulating PEGylated formulation (dry weight ratio of DSPC:Chol:DSPE-PEG of 8.2:3.8:2.6, designated P) (Table 1). Because the used PEGylated formulation had a higher lipid phase transition temperature, hydration was completed at 70 °C, rather than the 45 °C used for regular formulation lipids.

**Table 1. Physical characterization of liposomes by DLS analysis. Average hydrodynamic diameter and polydispersity index (PDI) of liposomes composed of either a regular or PEGylated formulation using hydration, sonication, or extrusion. \*Liposomes were denoted by a two-letter code with the first letter representing preparation method (hydration = H, sonication = S, extrusion = E) and a second letter denoting lipid formulation (regular = R, PEGylated = P).**

	Composition (mg/mL) Aso:DSPC:Chol:DSPE-PEG	Average Diameter, nm (Mean $\pm$ SD)	PDI (Mean $\pm$ SD)	Preparation Method
HR	10:0:4:0	2352 $\pm$ 315	1.0	Hydration
HP	0:8.2:3.8:2.6	17160 $\pm$ 4436	0.333 $\pm$ 0.06	Hydration
SR	10:0:4:0	139 $\pm$ 1	0.194 $\pm$ 0.02	Sonication
SP	0:8.2:3.8:2.6	83 $\pm$ 1	0.154 $\pm$ 0.02	Sonication
ER	10:0:4:0	267 $\pm$ 7	0.162 $\pm$ 0	Extrusion
EP	0:8.2:3.8:2.6	317 $\pm$ 5	0.015 $\pm$ 0.01	Extrusion

As expected, liposomes prepared only by hydration resulted in large and polydisperse products with inconclusive estimates (Table 1). DLS is well able to analyze nanoparticles generally ranging in diameter from a few nanometers to several microns. However, due to the way hydrodynamic radius is calculated based on laser light scattering in DLS and how sensitive the technique is to aggregates [15, 16], readings falling outside the range of resolution results in inaccurate and inconclusive data. This is exemplified by comparison of R and P liposomes prepared by hydration. A Z-average hydrodynamic diameter calculation is not capable of providing accurate values with poorly distributed data. This issue is further compounded by the way PDI is calculated based on the hydrodynamic radius approximation, which is frequently used to assess size distribution quality. Therefore, the acceptable PDI seen in the hydrated P sample is essentially nonsensical and is not sufficient for their accurate appraisal.

To confirm the hydrated sample is indeed very polydisperse and of poor size quality overall, the formed liposomes were assessed using light microscopy (Figure 10). In contrast to a very monodisperse (mean PDI < 0.1, Figure 10B) sample of liposomes prepared by extrusion with the same P lipid composition, the hydrated sample appears to be a lot more polydisperse and contain more large, non-uniform aggregates (Figure 10A). This demonstrates that liposomes prepared with only hydration are not suitable for biomedical and drug delivery application, highlighting the need for further refinement of hydrated lipids to attain suitable drug carriers.

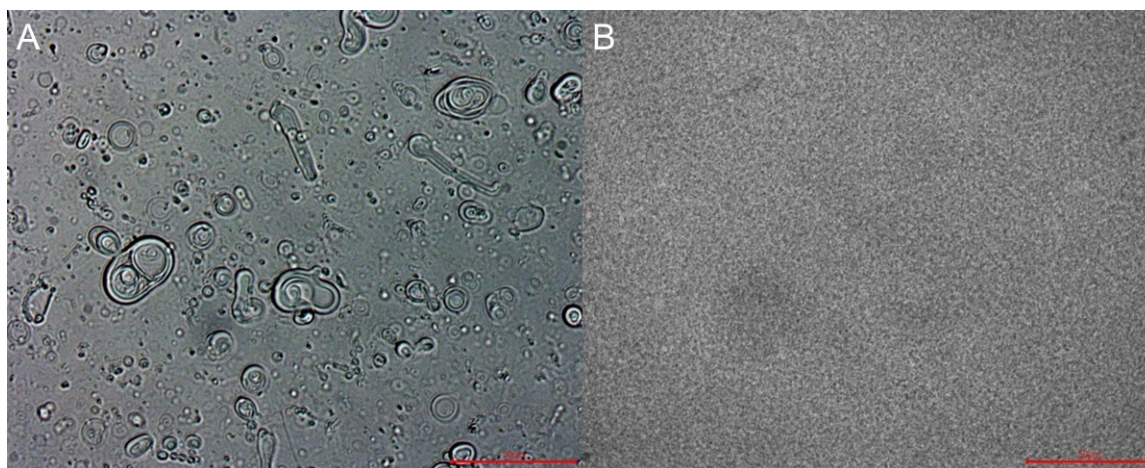


**Figure 10. Light microscopy images of liposomes. P formulated liposomes prepared by hydration (A) and extrusion through 400 nm polycarbonate membranes (B). Edits were made to remove foreign particles in the foreground from view. Scale bars are 50  $\mu$ M.**

Analysis of size characterization of liposomes prepared by sonication and extrusion show much more acceptable values of the physical parameters and trends with both regular and PEGylated formulations for biomedical purposes. Both formulations and preparation methods result in PDI averages below 0.2, suggesting suitability as drug carriers [3, 7]. Sonication prepared liposomes appeared to be suitable for decreased immune detection, as well as capable of exploiting the EPR effect in tumors given their

average hydrodynamic radius was below 150 nm in both lipid compositions [17-20]. It is, however, important to note that extrusion prepared liposomes were made using 400 nm polycarbonate membranes, partially accounting for the significant difference in size between sonication and extrusion prepared liposomes. Nonetheless, given the greater versatility of extrusion, it can prepare small unilamellar liposomes resembling the sizes we achieved with sonication [2, 21] and provides an overall gentler method of liposome preparation. Although the selection of a polycarbonate membrane pore diameter allows for partial control of liposome size prepared during extrusion, it does not result in liposomes exactly reflecting the size of pore diameter [22]. Because of the small sizes of the prepared samples, imaging with standard light microscopy provides very little information as even under ideal conditions, the diameter is at or below the limit of resolution for sonication or extrusion prepared liposomes that serve as drug carriers. Microscopy serves to confirm the lack of aggregates and absence of large fragments (Figure 10), which is initially suggested by DLS (Figure 11).

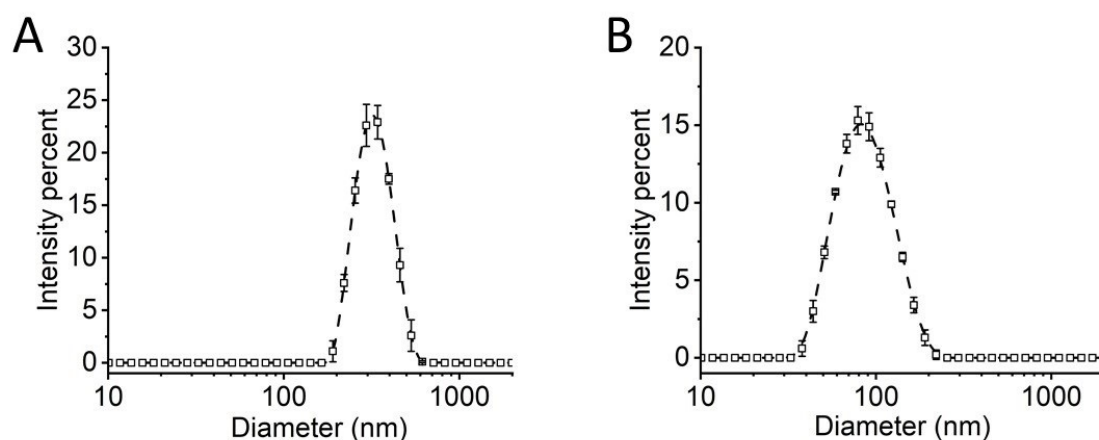


**Figure 11. Size distribution of liposomes prepared by sonication and extrusion. Graphical size representation on a logarithmic scale of EP liposomes made by extrusion with a 400 nm polycarbonate membrane (A) and SP liposomes prepared with 15 minutes of probe sonication.**

Polyethylene glycol (PEG) significantly advances the capabilities and stability of liposomes by being fused to lipids utilized in membranes for liposome preparation (Figure 12) [23]. Apart from the immune system evasion capabilities of PEGylated liposomes [24, 25], the steric properties of PEGylated moieties protruding from membranes translate into decreased aggregation and a more uniformly sized population of liposomes [26, 27]. This phenomenon can be observed when comparing regular with PEGylated formulation liposomes prepared with the same method. For sonication, average PDI was approximately 20% lower in PEGylated liposomes, and an over 90% decrease in PDI was observed between PEGylated and regular formulation extrusion prepared liposomes.

It is, however, improper to assume the differences between regular and PEGylated lipid composition liposomes can be solely attributed to the presence of PEG on the surface of the liposomal membrane. The composition of the regular liposomes is dominated by a mixture of phospholipids, predominantly phosphatidylcholine, cephalin, and phosphatidylinositol, accompanied by cholesterol. The PEGylated formulation has a membrane composed only of synthetically made 1,2-distearoyl-sn-glycero-3-phosphocholine (DSPC) and 1,2-distearoyl-sn-glycero-3-phosphoethanolamine (DSPE) as membrane components besides cholesterol. This difference results in slight variations in membrane properties such as fluidity at a given temperature. This is responsible for the need for preparation at slightly higher temperatures when dealing with R formulation lipid films in comparison to P formulations.

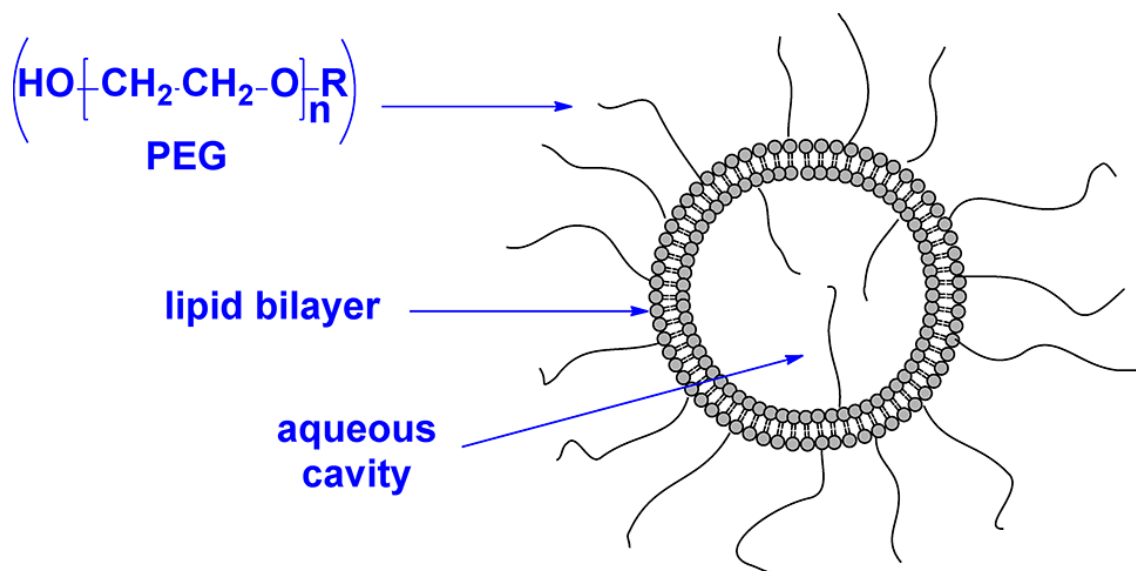


**Figure 12. PEGylated liposomes. Liposome with protruding polyethylene glycol moieties from the phospholipid bilayer membrane. Figure taken from Labruere et al., Anti-Methicillin-Resistant *Staphylococcus aureus* Nanoantibiotics [23]. Available under Creative Commons License.**

#### Passive and Active Loading of Liposomes

A key aspect of preparing liposomes as drug carriers includes loading them with a drug cargo. This can be simulated with a range of dyes that often resemble physical and chemical properties of drugs encapsulated into liposomes; however, they are cheaper, offer better visualization capabilities, and are suitable for both passive and active loading [28, 29]. Both passive and active methods were used for either extrusion or sonication prepared liposomes.

For the preparation of passively loaded liposomes, dried lipid films were hydrated with buffer mixed with desired dye concentration (3 mM CAL, or 1 mM R6G). During formation, some of the molecules are passively entrapped into the aqueous core at varying efficiencies depending on size, lamellarity, and lipid composition [30, 31]. After using the designated liposome preparation technique, the liposomes were purified using dialysis to purge their surrounding solution of unencapsulated cargo. The resulting inner

dye concentrations were higher than that of their external environment, as confirmed by the contrast observed under fluorescence microscopy for CAL (Figure 13A) and R6G (Figure 13B) loaded liposomes.

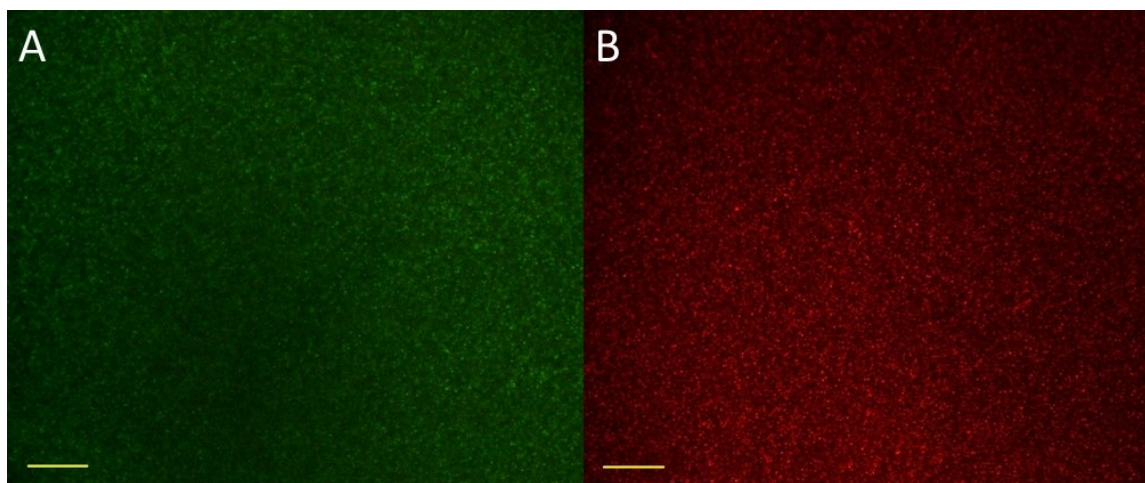


**Figure 13. Fluorescence microscopy of PEGylated liposomes passively loaded with drug simulating fluorescent dyes. CAL loaded (A) and R6G loaded (B) liposomes prepared with extrusion. Scale bar is 30  $\mu$ M.**

Active loading involves creating an electrochemical gradient between the internal and external environments of the liposomes. To do this, liposomes were initially hydrated and prepared in an acidic 150 mM citrate buffer of pH 4.24. Afterwards, liposomes underwent an overnight external buffer exchange with 1X PBS buffer of pH 7.4. AO, a membrane permeant dye at neutral pH, was introduced to the formed liposomes by adding it to the neutral, external solution. The electrochemical gradient created by the difference in external vs internal pH environments drives the unionized, membrane permeant molecules through the membranes of the liposome [32]. Upon entrance, AO becomes ionized, making it membrane impermeant. Using this method, one may load concentrations of dye up to several times above the initial concentration of which it was introduced [33]. In an identical fashion, liposomes were also loaded with DOX, for which

the main substitution was the use of 135 mM KCl + 20 mM HEPES solution for buffer exchange. External starting concentration in the external buffers for actively loaded AO was 50  $\mu$ M, and 25  $\mu$ M for DOX, respectively.

It is important to note that if non-permeant cargo is loaded during liposome formation, the cargo can effectively be loaded passively, although that does result in significantly reduced loading efficiency. This is because the driving force of the electrochemical gradient is not utilized, and drug solubility is limited. Large pH gradients of a few units between inside and outside the liposome can result in very effective final loading concentrations (thousands of times higher than final external molecule concentrations [32, 34]). A common method for active loading of DOX uses an ammonium sulfate gradient inside prepared liposomes. Upon entering the liposomes, DOX complexes with sulfate and crystallizes due to the compound's poor solubility, resulting in failure to permeate through the liposomal membrane and its prolonged containment [35, 36].

#### Cargo Release from Liposomes

Having trace amounts of intended content loaded into liposomes does not qualify them as useful for many purposes, in particular drug delivery. The success of liposome preparation often considers the encapsulation efficiency of the cargo into the liposomes [37, 38]. Although the exact loading efficiency of the sonication and extrusion prepared liposomes was not assessed, we determined if a significant amount of fluorescent dye was loaded into our liposomes. This was done by exploiting self-quenching fluorescence properties of dyes and drugs we used to approximate the loaded concentrations for both actively and passively loaded liposomes. The phenomenon of self-quenching can be

observed beyond a threshold fluorescent molecule concentration. Counterintuitively, beyond a certain concentration, fluorescence signal diminishes with further increase in concentration (Figure 14). CAL, AO, R6G, and DOX all present self-quenching at bulk concentrations ranging from 10  $\mu\text{M}$  to 120  $\mu\text{M}$ . Under specific concentrations, the fluorescence of the dyes increases upon dye addition; however, once the self-quenching level is achieved, dye addition leads to a significant decrease in fluorescence. Although the exact mechanism behind this is still somehow unclear, it is understood that the proximity of the dye molecules interferes with their fluorescent properties, resulting in a diminished fluorescence emission [39, 40]. Exploiting this unique characteristic, we attempted to gauge the concentration of fluorescent molecules loaded into the liposomes after their preparation. Determining whether self-quenching concentrations were achieved was done by solubilizing the liposomal membrane using a small amount of a non-ionic detergent, Triton X-100 [41], which releases the cargo into the bulk, leads to its dilution, and consequently adjusts the fluorescence signal.

Both regular and long circulating liposome formulations and three of the loading molecules were utilized for this investigation (Figure 15). All samples presented a sharp increase in fluorescence immediately after detergent addition, indicative of loading beyond the self-quenching concentration. This suggests that all the liposomes contained enough cargo to diffuse in the bulk, dilute, and lead to the observed increase in fluorescence. However, we also observed different evolutions for the different formulations, which allowed us to better understand the influence of lipid composition on loading by interpreting the fluorescence spectroscopy data. The extrusion (E) prepared liposomes of regular (R) formulation, ER, were passively loaded with 3 mM CAL. E

prepared liposomes of both R and PEGylated (P) formulations were actively loaded with AO by its addition to buffer exchanged liposomes to concentrations of 50  $\mu\text{M}$  concentrations. DOX was actively loaded into E prepared P formulation buffer exchanged liposomes at 25  $\mu\text{M}$  concentration. In every instance, 50  $\mu\text{L}$  of liposomes were added to 1 mL of buffer and allowed to equilibrate, and liposomes were solubilized by adding to the cuvettes 100  $\mu\text{L}$  of 5% v/v Triton X-100 (Figure 15).

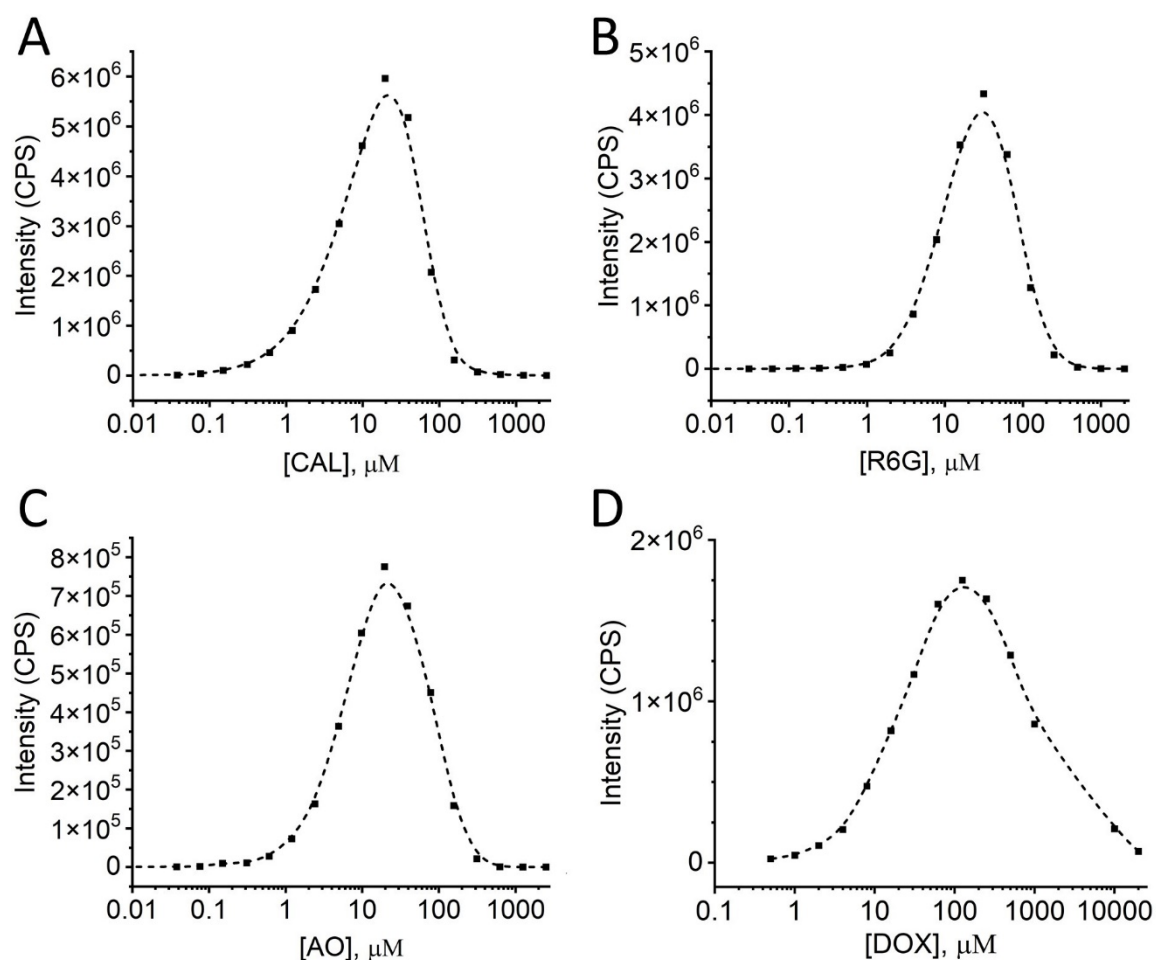


**Figure 4. Self-Quenching curves of used drug and dyes. Graphs show how fluorescence increases with concentration up until a peak fluorescence, at which point increasing molecular concentration results in a diminished fluorescence concentration for CAL (A), R6G (B), AO (C), and DOX (D).**

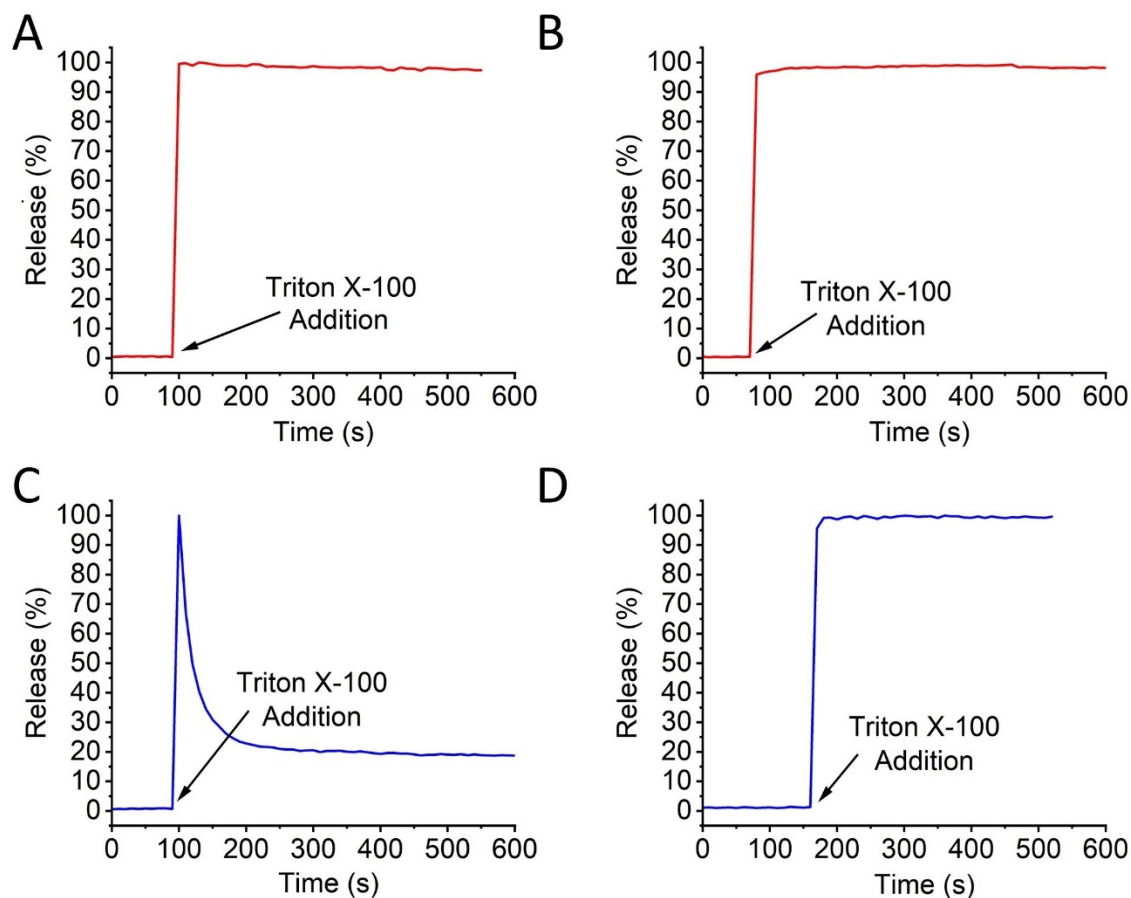


**Figure 15. Analysis of dye and drug loading into liposomes. Non-ionic detergent induced CAL (A) and actively loaded AO (B and C) and DOX (D) release from regular liposome formulations (red) and PEGylated formulations (blue) induced by addition of Triton X-100.**

Passively loaded ER CAL liposomes showed a rapid increase and sustained, stable fluorescence resulting from CAL release upon detergent addition (Figure 15A). Similarly, ER liposomes loaded with AO (Figure 15B) and EP liposomes loaded with DOX (Figure 15D) showed a sharp increase then plateau in fluorescence, suggesting large loading concentrations since bulk dilution did not bring the fluorescence signal under the peak fluorescence intensity (which would be seen as a further gradual decrease in fluorescence). In contrast, EP liposomes loaded with AO at the identical 50  $\mu\text{M}$  concentration used in ER liposomes showed a sharp increase, followed by a decay in

fluorescence, suggesting loading concentrations of cargo high enough to exhibit self-quenching behavior, yet low enough to fall below peak fluorescence concentrations after being released into the bulk (Figure 15C). The contrast in formulation (regular vs PEGylated) and resulting release of liposomes prepared and loaded with identical AO concentrations exemplifies how liposome formulation influences loading efficiency [31].

### **Conclusions**

With the performed set of experiments, a solid baseline for liposome preparation using extrusion and sonication along with active and passive loading is established. Moreover, the produced liposomes are analyzed and characterized to better understand some of the key characteristics such as their hydrodynamic radius, size distribution, visual characteristics, and loading efficiency. Finally, liposomes are confirmed to be loaded at close to intended concentration with both drug simulating dyes and the drug doxorubicin both through microscopy and fluorescence spectroscopy.

Sonication and extrusion could produce liposomes composed of either regular or PEGylated formulation that were suitable for either active or passive loading. Sonication offers less variety in selecting a desired size of the produced liposomes. Although it was predictably near 100 nm with both regular and PEGylated lipid membranes, it is questionable whether liposome diameter can easily be adjusted by modifying sonication parameters and settings. Although sonication can be used to prepare liposomes with minimal effort and in short periods of time, size distribution is not predictable, and quality often suffers. Consistently extrusion provides better size distribution (inferred from a lower PDI) than sonication prepared with identical lipid composition. Extrusion also offers the added benefit of offering more control pertaining to the sizing of

liposomes produced by allowing selection of pore sizes in the polycarbonate membranes used for extrusion. Finally, extrusion is generally recognized as a gentler method of preparation, as sonication can easily damage fragile cargo and other membrane components.

Sonication and extrusion have been extensively used and continue to be used as they have a proven record of reliably producing liposomes. However, there are aspects to be further improved, such as time commitment and effort, expenses, and scale of production, all while preserving quality and reliability. In this light, as liposome research gathers traction and realizes greater application, developments are constantly being made to address these concerns. A new technique developed by our lab [42] and described in the next chapter offers simultaneous production, loading, and purification of liposomes in a matter of hours.

## References

1. Cho, N.-J.; Hwang, L. Y.; Solandt, J. J. R.; Frank, C. W., Comparison of Extruded and Sonicated Vesicles for Planar Bilayer Self-Assembly. *Materials* **2013**, *6* (8).
2. Lapinski, M. M.; Castro-Forero, A.; Greiner, A. J.; Ofoli, R. Y.; Blanchard, G. J., Comparison of Liposomes Formed by Sonication and Extrusion: Rotational and Translational Diffusion of an Embedded Chromophore. *Langmuir* **2007**, *23* (23), 11677-11683.
3. Shah, V. M.; Nguyen, D. X.; Patel, P.; Cote, B.; Al-Fatease, A.; Pham, Y.; Huynh, M. G.; Woo, Y.; Alani, A. W. G., Liposomes produced by microfluidics and extrusion: A comparison for scale-up purposes. *Nanomedicine: Nanotechnology, Biology and Medicine* **2019**, *18*, 146-156.
4. Bozzuto, G.; Molinari, A., Liposomes as nanomedical devices. *International journal of nanomedicine* **2015**, *10*, 975-999.
5. Kanášová, M.; Nesměrák, K., Systematic review of liposomes' characterization methods. *Monatshefte für Chemie - Chemical Monthly* **2017**, *148* (9), 1581-1593.
6. Peretz Damari, S.; Shamrakov, D.; Varenik, M.; Koren, E.; Nativ-Roth, E.; Barenholz, Y.; Regev, O., Practical aspects in size and morphology characterization of drug-loaded nano-liposomes. *International Journal of Pharmaceutics* **2018**, *547* (1), 648-655.
7. Danaei, M.; Dehghankhold, M.; Ataei, S.; Hasanzadeh Davarani, F.; Javanmard, R.; Dokhani, A.; Khorasani, S.; Mozafari, M. R., Impact of Particle Size and Polydispersity Index on the Clinical Applications of Lipidic Nanocarrier Systems. *Pharmaceutics* **2018**, *10* (2), 57.
8. Corvo, M. L.; Boerman, O. C.; Oyen, W. J. G.; Jorge, J. C. S.; Cruz, M. E. M.; Crommelin, D. J. A.; Storm, G., Subcutaneous Administration of Superoxide Dismutase Entrapped in Long Circulating Liposomes: In Vivo Fate and Therapeutic Activity in an Inflammation Model. *Pharmaceutical Research* **2000**, *17* (5), 600-606.

9. Juliano, R. L.; Stamp, D., The effect of particle size and charge on the clearance rates of liposomes and liposome encapsulated drugs. *Biochem Biophys Res Commun* **1975**, *63* (3), 651-8.
10. Litzinger, D. C.; Buiting, A. M. J.; van Rooijen, N.; Huang, L., Effect of liposome size on the circulation time and intraorgan distribution of amphipathic poly(ethylene glycol)-containing liposomes. *Biochimica et Biophysica Acta (BBA) - Biomembranes* **1994**, *1190* (1), 99-107.
11. Gabizon, A.; Goren, D.; Cohen, R.; Barenholz, Y., Development of liposomal anthracyclines: from basics to clinical applications | This paper is based on a lecture presented at the 8th International Symposium on recent Advances in Drug Delivery Systems (Salt Lake City, UT, USA, 1997).1. *Journal of Controlled Release* **1998**, *53* (1), 275-279.
12. Charrois, G. J. R.; Allen, T. M., Rate of biodistribution of STEALTH® liposomes to tumor and skin: influence of liposome diameter and implications for toxicity and therapeutic activity. *Biochimica et Biophysica Acta (BBA) - Biomembranes* **2003**, *1609* (1), 102-108.
13. Olson, F.; Hunt, C. A.; Szoka, F. C.; Vail, W. J.; Papahadjopoulos, D., Preparation of liposomes of defined size distribution by extrusion through polycarbonate membranes. *Biochimica et Biophysica Acta (BBA) - Biomembranes* **1979**, *557* (1), 9-23.
14. Zhang, H., Thin-Film Hydration Followed by Extrusion Method for Liposome Preparation. In *Liposomes: Methods and Protocols*, D'Souza, G. G. M., Ed. Springer New York: New York, NY, 2017; pp 17-22.
15. Stetefeld, J.; McKenna, S. A.; Patel, T. R., Dynamic light scattering: a practical guide and applications in biomedical sciences. *Biophysical Reviews* **2016**, *8* (4), 409-427.
16. Uskoković, V., Dynamic Light Scattering Based Microelectrophoresis: Main Prospects and Limitations. *Journal of Dispersion Science and Technology* **2012**, *33* (12), 1762-1786.

17. Hobbs, S. K.; Monsky, W. L.; Yuan, F.; Roberts, W. G.; Griffith, L.; Torchilin, V. P.; Jain, R. K., Regulation of transport pathways in tumor vessels: Role of tumor type and microenvironment. *Proceedings of the National Academy of Sciences* **1998**, *95* (8), 4607.
18. Maruyama, K., Intracellular targeting delivery of liposomal drugs to solid tumors based on EPR effects. *Advanced Drug Delivery Reviews* **2011**, *63* (3), 161-169.
19. Ngoune, R.; Peters, A.; von Elverfeldt, D.; Winkler, K.; Pütz, G., Accumulating nanoparticles by EPR: A route of no return. *Journal of Controlled Release* **2016**, *238*, 58-70.
20. Maeda, H.; Wu, J.; Sawa, T.; Matsumura, Y.; Hori, K., Tumor vascular permeability and the EPR effect in macromolecular therapeutics: a review. *Journal of Controlled Release* **2000**, *65* (1), 271-284.
21. Berger, N.; Sachse, A.; Bender, J.; Schubert, R.; Brandl, M., Filter extrusion of liposomes using different devices: comparison of liposome size, encapsulation efficiency, and process characteristics. *International Journal of Pharmaceutics* **2001**, *223* (1), 55-68.
22. Ong, S. G.; Chitneni, M.; Lee, K. S.; Ming, L. C.; Yuen, K. H., Evaluation of Extrusion Technique for Nanosizing Liposomes. *Pharmaceutics* **2016**, *8* (4).
23. Labruère, R.; Sona, A. J.; Tuross, E., Anti-Methicillin-Resistant Staphylococcus aureus Nanoantibiotics. *Front Pharmacol* **2019**, *10*, 1121.
24. Klibanov, A. L.; Maruyama, K.; Torchilin, V. P.; Huang, L., Amphipathic polyethyleneglycols effectively prolong the circulation time of liposomes. *FEBS Letters* **1990**, *268* (1), 235-237.
25. Papahadjopoulos, D.; Allen, T. M.; Gabizon, A.; Mayhew, E.; Matthay, K.; Huang, S. K.; Lee, K. D.; Woodle, M. C.; Lasic, D. D.; Redemann, C., Sterically stabilized liposomes: improvements in pharmacokinetics and antitumor therapeutic efficacy. *Proceedings of the National Academy of Sciences* **1991**, *88* (24), 11460.

26. Immordino, M. L.; Dosio, F.; Cattell, L., Stealth liposomes: review of the basic science, rationale, and clinical applications, existing and potential. *International journal of nanomedicine* **2006**, *1* (3), 297-315.
27. Needham, D.; McIntosh, T. J.; Lasic, D. D., Repulsive interactions and mechanical stability of polymer-grafted lipid membranes. *Biochim Biophys Acta* **1992**, *1108* (1), 40-8.
28. Ahmed, S. E.; Moussa, H. G.; Martins, A. M.; Abbas, Y.; Al-Sayah, M. H.; Husseini, G. A., Factors Affecting the Acoustic In Vitro Release of Calcein from PEGylated Liposomes. *Journal of Nanoscience and Nanotechnology* **2019**, *19* (11), 6899-6906.
29. Maherani, B.; Arab-Tehrany, E.; Kheirilomoom, A.; Geny, D.; Linder, M., Calcein release behavior from liposomal bilayer; influence of physicochemical/mechanical/structural properties of lipids. *Biochimie* **2013**, *95* (11), 2018-2033.
30. Brandl, M., Liposomes as drug carriers: a technological approach. In *Biotechnology Annual Review*, Elsevier: 2001; Vol. 7, pp 59-85.
31. Eloy, J. O.; Claro de Souza, M.; Petrilli, R.; Barcellos, J. P. A.; Lee, R. J.; Marchetti, J. M., Liposomes as carriers of hydrophilic small molecule drugs: Strategies to enhance encapsulation and delivery. *Colloids and Surfaces B: Biointerfaces* **2014**, *123*, 345-363.
32. Cullis, P. R.; Mayer, L. D.; Bally, M. B.; Madden, T. D.; Hope, M. J., Generating and loading of liposomal systems for drug-delivery applications. *Advanced Drug Delivery Reviews* **1989**, *3* (3), 267-282.
33. Cullis, P. R.; Hope, M. J.; Bally, M. B.; Madden, T. D.; Mayer, L. D.; Fenske, D. B., Influence of pH gradients on the transbilayer transport of drugs, lipids, peptides and metal ions into large unilamellar vesicles. *Biochim Biophys Acta* **1997**, *1331* (2), 187-211.

34. Gubernator, J., Active methods of drug loading into liposomes: recent strategies for stable drug entrapment and increased in vivo activity. *Expert Opinion on Drug Delivery* **2011**, 8 (5), 565-580.
35. Barenholz, Y., Doxil®--the first FDA-approved nano-drug: lessons learned. *J Control Release* **2012**, 160 (2), 117-34.
36. Bolotin, E. M.; Cohen, R.; Bar, L. K.; Emanuel, N.; Ninio, S.; Barenholz, Y.; Lasic, D. D., Ammonium Sulfate Gradients for Efficient and Stable Remote Loading of Amphipathic Weak Bases into Liposomes and Ligandoliposomes. *Journal of Liposome Research* **1994**, 4 (1), 455-479.
37. Has, C.; Sunthar, P., A comprehensive review on recent preparation techniques of liposomes. *Journal of Liposome Research* **2020**, 30 (4), 336-365.
38. Mayer, L. D.; Bally, M. B.; Cullis, P. R., Uptake of adriamycin into large unilamellar vesicles in response to a pH gradient. *Biochim Biophys Acta* **1986**, 857 (1), 123-6.
39. Amado, A. M.; Ramos, A. P.; Silva, E. R.; Borissevitch, I. E., Quenching of acridine orange fluorescence by salts in aqueous solutions: Effects of aggregation and charge transfer. *Journal of Luminescence* **2016**, 178, 288-294.
40. Hamann, S.; Kiilgaard, J. F.; Litman, T.; Alvarez-Leefmans, F. J.; Winther, B. R.; Zeuthen, T., Measurement of Cell Volume Changes by Fluorescence Self-Quenching. *Journal of Fluorescence* **2002**, 12 (2), 139-145.
41. Jimah, J. R.; Schlesinger, P. H.; Tolia, N. H., Liposome Disruption Assay to Examine Lytic Properties of Biomolecules. *Bio-protocol* **2017**, 7 (15), e2433.
42. Abatchev, G.; Bogard, A.; Hutchinson, Z.; Ward, J.; Fologea, D., Rapid Production and Purification of Dye-Loaded Liposomes by Electrodialysis-Driven Depletion. *Membranes* **2021**, 11 (6).

CHAPTER THREE: RAPID PRODUCTION AND PURIFICATION OF DYE -  
LOADED LIPOSOMES BY ELECTRODIALYSIS-DRIVEN DEPLETION

Gamid Abatchev <sup>1,2,\*</sup>, Andrew Bogard <sup>1,2</sup>, Zoe Hutchinson <sup>1</sup>, Jason Ward <sup>1</sup> and  
Daniel Fologea <sup>1,2,\*</sup>

<sup>1</sup> Department of Physics, Boise State University, Boise, ID 83725, USA

<sup>2</sup> Biomolecular Sciences Graduate Program, Boise State University, Boise, ID 83725,  
USA

\*Correspondence: gamidabatchev@u.boisestate.edu, danielfologea@boisestate.edu



Original work published under Creative Commons License: MDPI, Membranes, Rapid  
Production and Purification of Dye-Loaded Liposomes by Electrodialysis-Driven  
Depletion, Abatchev *et al*, (2021)

<https://doi.org/10.3390/membranes11060417>

<https://www.mdpi.com/2077-0375/11/6/417>

## Abstract

Liposomes are spherical-shaped vesicles that enclose an aqueous milieu surrounded by bilayer or multilayer membranes formed by self-assembly of lipid molecules. They are intensively exploited as either model membranes for fundamental studies or as vehicles for delivery of active substances in vivo and in vitro. Irrespective of the method adopted for production of loaded liposomes, obtaining the final purified product is often achieved by employing multiple, time-consuming steps. To alleviate this problem, we propose a simplified approach for concomitant production and purification of loaded liposomes by exploiting the Electrodialysis-Driven Depletion of charged molecules from solutions. Our investigations show that electrically-driven migration of charged detergent and dye molecules from solutions that include natural or synthetic lipid mixtures leads to rapid self-assembly of loaded, purified liposomes, as inferred from microscopy and fluorescence spectroscopy assessments. In addition, the same procedure was successfully applied for incorporating PEGylated lipids into the membranes for the purpose of enabling long-circulation times needed for potential in vivo applications. Dynamic Light Scattering analyses and comparison of electrically-formed liposomes with liposomes produced by sonication or extrusion suggest potential use for numerous in vitro and in vivo applications.

## Introduction

Liposomes are spherical vesicles that enclose an aqueous interior cavity protected by a unilamellar or multilamellar shell made of lipids, and the exploitation of their features has enabled the development of myriads of scientific and biomedical applications [1–6]. The liposome membrane is made of lipids commonly found in cell

membranes, and their compositions may be adjusted by addition of specific lipids and sterols to better simulate the lipid partition of a particular membrane host. Such mimicking provides a simplified experimental system for surveying transport properties of membranes [4,7]. More fundamental exploration options are presented by the ability to reconstitute membrane receptors directly into membranes [8,9] or to functionalize the membrane surface by chemical addition of specific recognition elements [10–12].

Another important set of applications of liposomes originates in their ability to function as carriers for ions and molecules. Liposomes may transport hydrophilic, water-soluble cargo within their aqueous inner volume, and non-polar compounds embedded within the hydrophobic core of the membrane. These excellent transport capabilities led to the idea of using liposomes for transport and delivery of drugs to diseased organs and tissues in the human body [13]. The ability to adjust the physio-chemical properties of liposomes for drug delivery purposes is greatly exemplified by their FDA-approved clinical application for cancer therapy [14,15]. Liposome PEGylation significantly improves their circulation time by preventing recognition by the reticuloendothelial system (RES) / mononuclear phagocyte system (MPS) [16–18], while a small size enables self-accumulation into solid tumors by the Enhanced Permeability and Retention (EPR) effect [19–21]. Active loading of drugs such as doxorubicin enables the achievement of high local drug concentrations, greatly reducing systemic distribution by self-accumulating at the tumor site [22].

All production methods of liposomes used as carriers employ liposome preparation and loading. Irrespective of the production approach adopted, liposome preparation relies on the self-assembly of lipids, which is driven by their amphiphilic

nature and interactions with water. Hydration from thin lipid films usually leads to the formation of multilamellar liposomes, which are further down-sized and rendered unilamellar by extrusion or sonication [23–26]. In this case, passive drug loading may be realized by direct addition to the hydrating solution, while active loading by electrochemical gradients may be achieved after liposome formation [27,28]. In a different approach, liposome preparation is achieved by further dilution of a solvent utilized to solubilize the lipids, which may be performed by organic solvent injection [29–31] or detergent removal [32–36]. These methods are well established, and each one has advantages and disadvantages with respect to equipment requirements, achievement of desired size, loading protocol and efficacy, and time. A major bottleneck common among multiple production methods is the time needed to complete the procedures and obtain loaded liposomes devoid of unloaded cargo in the bulk.

To alleviate this problem, we propose producing loaded and purified liposomes by Electrodialysis-Driven Depletion (EDD) of detergent. Detergent removal has long been understood to create bilayers [33,37] and established as a method for preparing unilamellar liposomes [33–36,38]. Upon solubilizing lipids with a detergent, a mixed micelle formation consisting of detergent and lipids appear. Removal of the detergent results in fusion of micelles and bilayer disk formation. As the disk becomes larger, it will curve to minimize edge circumference to reduce hydrocarbon tail exposure to aqueous solution and eventually enclose to form a bilayer sphere, eliminating exposed edges [39,40].

Based on this body of evidence, we hypothesized that electrophoresis may lead to rapid depletion of ionic detergents from detergent-lipid mixtures and liposome formation.

In addition, we anticipated that charged molecules intended as cargo may be trapped inside the formed liposomes before being cleared from the bulk by the action of the electric field. Our experimental results strongly support the applicability of EDD for fast liposome formation, loading, and purification.

### **Materials and Methods**

Asolectin (Aso, Sigma-Aldrich, St. Louis, MO, USA), cholesterol (Chol, Sigma-Aldrich), brain sphingomyelin (SM, Avanti Polar Lipids, Alabaster, AL, USA), 1,2-distearoyl-sn-glycero-3-phosphocholine (DSPC, Avanti Polar Lipids), and 1,2-distearoyl-sn-glycero-3-phosphoethanolamine-N-[methoxy(polyethyleneglycol)-2000] (DSPE-PEG, Avanti Polar Lipids) were purchased either in powder or chloroform-solubilized form. The powder lipids were solubilized in chloroform, mixed with the other lipids at the desired ratios in a glass vial, and had the solvent removed by being placed under vacuum for at least 12 h. Formed lipid films not used immediately were stored in a freezer at -20 °C. The precursors to all liposome preparations were the dried lipid films prepared from mixture of lipids at dry-weight ratios specified in the results section. KCl (ThermoFisher Scientific, Waltham, MA, USA), a stock solution of 1M HEPES (Sigma-Aldrich) of pH 7.4, and cholic acid (CA, ThermoFisher Scientific) were used to prepare buffered ionic solutions (20 mM KCl, 5 mM Hepes) with or without addition of acridine orange (AO) or rhodamine 6G (R6G) (both from ThermoFisher Scientific) at 1 mM final concentration. The emission spectrum of each dye was determined with a FluoroMax4 spectrofluorometer (Horiba Scientific, Piscataway, NJ, USA) set in emission mode. The same instrument was used to establish the AO self-quenching plot, monitor AO and R6G

migration under exposure to electric field, and measure the release kinetics of dyes loaded into liposomes.

The electrodialysis-driven depletion (EDD) experiments employed a traditional use of the ElectroPrep Electrodialysis System (product #: 74-1196, Harvard Apparatus, Holliston, MA, USA), which was also adapted for real-time assessment of dye migration from the Ultra-Fast Dialyzer chamber (Harvard Apparatus) under exposure to electric fields in order to establish the time required to complete dye depletion from the chamber. The modified experimental setup (Figure 16) included the ElectroPrep Electrodialysis System completed with a custom fluidic system which continuously re-circulated the solution from either reservoir with a multi-port Gilson MiniPuls 3 peristaltic pump (Gilson Inc., Middleton, WI, USA) and fed a constant-volume flow cell (cuvette) for monitoring of fluorescence with the spectrofluorometer. Specific emission of each dye was measured in kinetics mode at 0.1 s integration time and a sampling rate of six samples/minute. The solution in the dialysis chamber mounted in the insulating separation wall was the only conducting pathway between the reservoirs. Consequently, charged molecules migrated from the dialysis chamber into the corresponding reservoir as dictated by the electrophoretic force. The Pt electrodes of the ElectroPrep Electrodialysis System were wired to a VWR Power Source 300V electrophoresis power supply (VWR International, Radnor, PA, USA) set to constant current, and the solutions in the reservoirs were continuously stirred with magnetic stir bars.

Liposome production by EDD comprised hydration and solubilization of lipid mixtures in 1 mL ionic solutions containing 2% (w/v) CA. To aid homogenization, the samples underwent a brief sonication (10 s) in a bath sonicator (Fisher Scientific),

followed by 10 min heating at 75 °C and another brief sonication. After solubilization, the solutions were transferred into the double sided Ultra-Fast Dialyzer chamber equipped at both ends with polycarbonate membranes (10 nm pores, Harvard Apparatus), and mounted in the insulating separation wall of the ElectroPrep Electrodesialysis tank filled with electrolyte solutions.

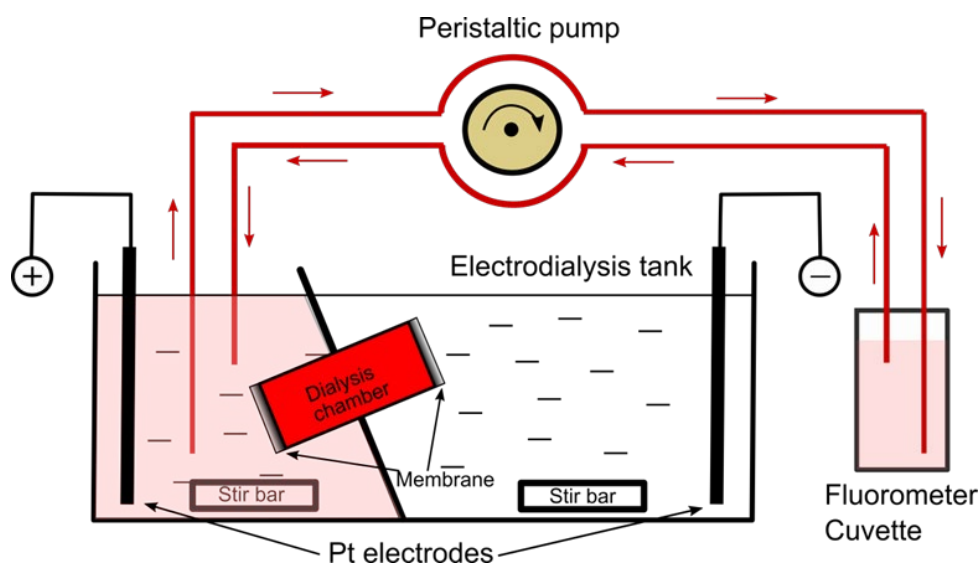


**Figure 5. Experimental setup for liposome production by electrodesialysis-driven depletion (EDD) and fluorescence monitoring. The custom setup includes the electrodesialysis tank (ElectroPrep Electrodesialysis System), an Ultra-Fast Dialyzer chamber, and a microfluidic setup to recirculate the solutions through a constant volume fluorometer cuvette for real-time fluorescence measurements. This specific setup describes migration and quantification of an anionic dye transferred from the dialysis chamber to the left reservoir. The solutions in the two reservoirs were continuously stirred with magnetic bars. The diagram is not to scale.**

Liposome preparation by sonication was performed with a Misonix S-4000 probe sonicator (Misonix, Farmingdale, NY, USA) equipped with a micro-tip. The lipid mixtures (with, and without dyes) were hydrated in warm electrolyte solutions, then placed into small glass vials and sonicated on ice for 15 min in manual mode at 25% amplitude, and a power transfer of 6–7 W.

For extrusion, the lipid films in the glass vials were slowly hydrated for a few hours at 45 °C. To complete hydration and homogenize the mixture, the hydrated samples underwent four freeze/thaw cycles. The liposomes were extruded at 70 °C with an Avanti Polar Lipids extruder equipped with 200 nm polycarbonate filters for a total of 61 passes. Imaging was completed with an Olympus IX71 fluorescence microscope (Olympus Scientific Solutions Americas Corp, Waltham, MA, USA) equipped with filter sets specific for the used dyes. The release of encapsulated dyes was monitored from the fluorescence changes elicited by membrane permeabilization with 0.5% Triton X-100 (Sigma-Aldrich) [41,42]. A similar procedure was utilized to assess the unilamellarity of EDD-produced liposomes by inducing permeabilization with the pore-forming toxin lysenin (Sigma-Aldrich).

For comparison between the three distinct production methods, liposomes were characterized by dynamic light scattering (DLS) with the Zetasizer Nano ZS (Malvern Panalytical Inc., Westborough, MA, USA) for determination of average hydrodynamic diameter and size distribution (PDI, polydispersity index) at room temperature. For each liposome sample we analyzed three sets, with each set consisting of 13 consecutive runs. Each set provided the corresponding average diameter and PDI, from which we calculated the mean values and standard deviations.

## **Results and Discussions**

### Dye Separation by Electrodialysis

Successful separation by electrodialysis requires the detergent and dye molecules to possess an effective electric load. The used detergent (CA) is acidic ( $pK_a = 4.8$  [43]) and completely ionized near neutral pH; although many of the common fluorescent dyes

are also charged for a large range of pHs, we did not know how long they would take to migrate from the dialysis chamber to the reservoirs upon exposure to an external electric field. A potential issue with the electrical conditions is that the electrical currents may lead to redox reactions at the electrodes (i.e.,  $H^+$  and  $HO^-$  production, as well as other products that may also lead to undesired side reactions in solutions), and an increased temperature through the Joule effect. pH changes may affect the ionization status of the molecules and their migration, and they may also modulate the fluorescence of the dyes. To alleviate such potential issues, we sought to reduce the electrical currents in order to prevent major temperature and pH changes. While this may be simply realized by reducing the applied voltage, such an approach will also diminish the magnitude of the electrophoretic force, which may lengthen the time required for migration. After some experimentation, we established that the 20 mM KCl/5 mM HEPES (pH = 7.4) led to minor variations of temperature of the bulk ( $\sim 2^\circ C$ ) and pH in the dialysis chamber ( $\sim 0.3$  units) at 75 mA constant current applied for 45 min.

To determine the time required for dye migration, we loaded the electro dialysis chamber with 1 mM of AO or R6G. The electro dialysis tank reservoirs were filled with dye-free ionic solutions and dye migration was estimated by employing the fluidic system described in the Materials and Methods section. The evolution of the fluorescence in reservoirs was estimated from kinetics measurements by employing the flow cell and the fluorometer. The wavelengths for excitation/emission were set apart for each of the dyes (AO: 485 nm/530 nm, R6G: 528 nm/550 nm), with a 1 nm slit for both excitation and emission. The power supply was set to 75 mA constant current, and the fluorescence measurements started  $\sim 10$  s after applying the voltage. Both dyes started migrating from

the chamber shortly after application of the electric field and the fluorescence monotonically increased until reaching a plateau indicative of migration completion (Figure 17). The kinetics profiles (i.e., the characteristic time) for the dyes were different, and AO migrated faster than R6G. However, the maximum signal was achieved in less than 40 min for both dyes, which set a reference time frame for further electro dialysis experiments.

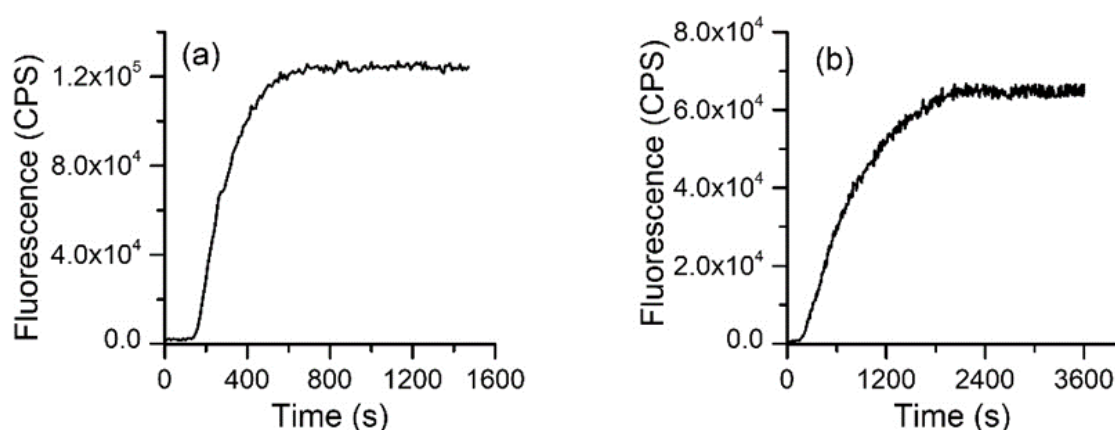


**Figure 6. Electro dialysis leads to rapid depletion of charged dyes from solutions. Acridine orange (AO) (a) migrates faster than rhodamine 6G (R6G) (b) but both are depleted from the dialysis chamber and transferred into the reservoirs in less than 40 min.**

#### Simultaneous Liposome Formation, Loading, and Purification by EDD

Detergent removal from the lipid-containing mixtures by dialysis drives the formation of self-enclosed structures [33,44]. We hypothesized that during enclosure, dye molecules can also be entrapped within the formed liposomes. Therefore, fast and concomitant liposome formation and loading may be achieved if the detergent and dye are electrophoretically driven outside the dialysis chamber.

To test this hypothesis, we prepared lipid mixtures (Aso:Chol, 10:4 weight ratio) in ionic solutions containing 2% (w/v) CA to which 1 mM AO or R6G was added. The

samples were subjected to electro dialysis at 75 mA constant current for up to 40 min. Figure 18 shows that simultaneous clearance of detergent and dye molecules leads to formation of loaded liposomes.

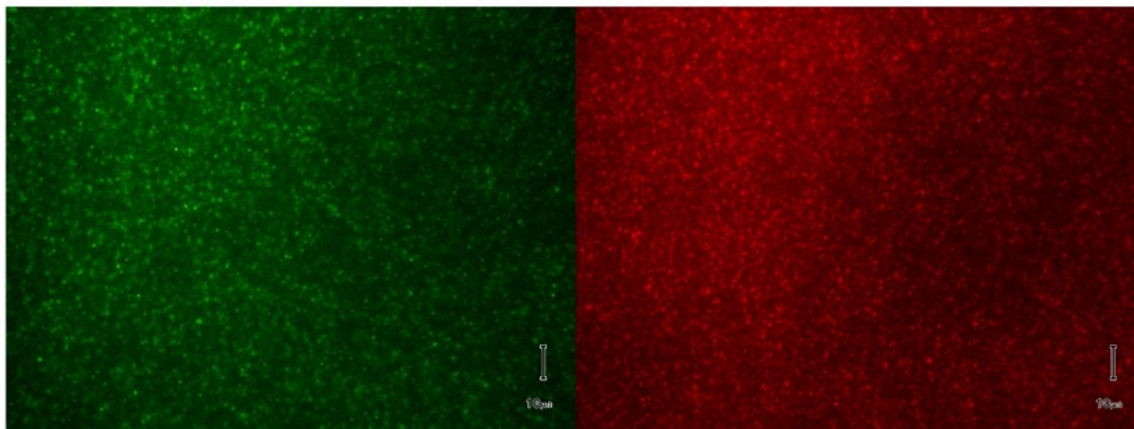


**Figure 7. Microscopy imaging of fluorescent liposomes produced and purified by EDD. The liposomes are composed of asolectin and cholesterol and are loaded with AO (left panel) and R6G (right panel). The scale bar is 10  $\mu\text{m}$ .**

#### Production of Long-Circulating Liposomes by Electrodialysis

The rapid clearance of liposomes from circulation constitutes a major roadblock for in vivo biomedical applications [45–47]. However, substantially improved circulation times are attained by adjusting the lipid composition of the membrane in order to minimize the undesired interactions with the defense system of the host. Addition of PEGylated lipids to the self-assembled membranes is often employed to extend the lifetime of liposomes in circulation, and such compositions are used for producing liposomes intended for cancer therapy and other in vivo applications [16–18,46,48,49]. To verify if electro dialysis is suitable for formation and loading of long-circulating liposomes, we prepared lipid mixtures containing DSPC, Chol, and DSPE-PEG (8.2:3.8:2.6 weight ratios). The lipids were solubilized in the buffered solution containing 2% CA and 1 mM AO, heated for 20 min at 75 °C, introduced into the Ultra-Fast

Dialyzer chamber and subjected to a constant current of 75 mA for 20 min. Microscopy imaging revealed the formation of AO-loaded liposomes (Figure 19) and the good contrast ratio between liposomes and background suggested successful elimination of non- incorporated AO.

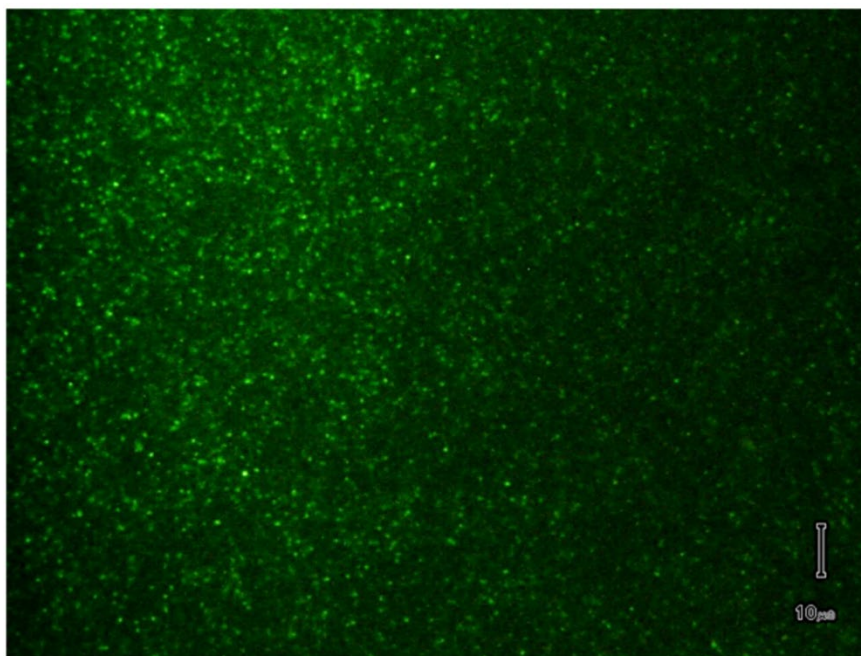


**Figure 8.** Microscopy image of PEGylated liposomes loaded with AO, prepared, and purified by EDD. The scale bar is 10  $\mu\text{m}$ .

#### Verification of Dye Loading

There is no doubt that some of the dye present in the solubilization buffer is lost during the exposure to electrical currents due to migration before being trapped in the formed liposomes. To provide a rough estimation of the residual AO concentration inside PEGylated liposomes, we performed a release experiment that employed solubilization of liposomal membranes by addition of the non-ionic detergent Triton X-100 [41,42]. AO fluorescence presents self-quenching, i.e., a significant decrease in fluorescence manifested upon increase in dye concentration over 10  $\mu\text{M}$  [50]. Although the exact

mechanisms of self-quenching are not elucidated, it is considered that the intermolecular interactions occurring at high concentrations lead to a diminished fluorescence emission [50–52]. If self-quenching concentrations are attained inside liposomes, membrane solubilization leads to dye dissipation into the bulk, and the decrease in concentration over time is monitored from the increase in fluorescence [53].

The changes in AO fluorescence intensity recorded upon addition of 100  $\mu\text{L}$  of 5% Triton-X-100 to a 1.0 mL buffer solution containing 20  $\mu\text{L}$  PEGylated liposomes produced by electrodialysis indicated that the AO concentration inside liposomes attained self-quenching levels (Figure 20). In addition, the fluorescence continually increased upon membrane solubilization, indicating that the AO concentration in the bulk did not fall below self-quenching level.

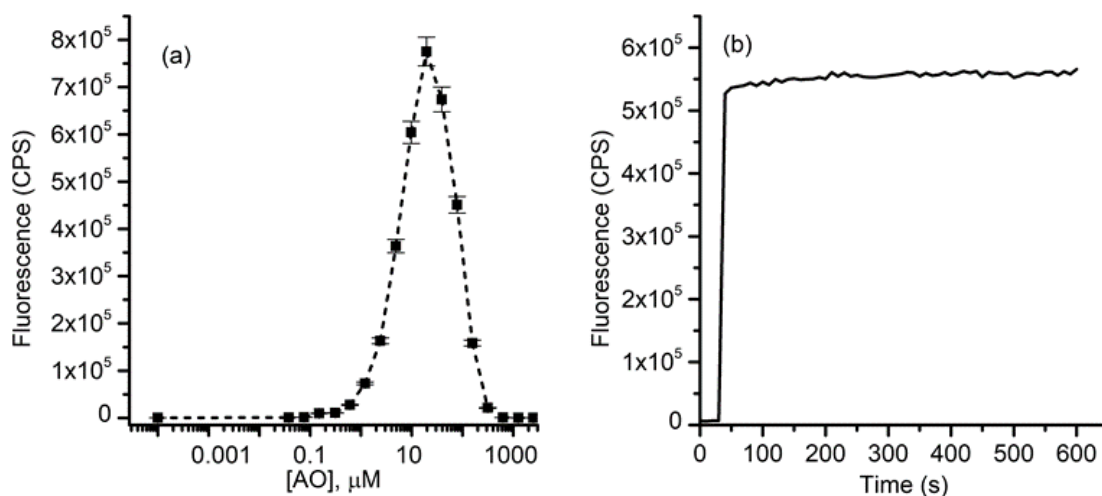


**Figure 20.** AO release from PEGylated liposomes produced, loaded, and purified by EDD. (a) AO fluorescence indicates self-quenching at bulk concentrations over 10  $\mu\text{M}$ . (b) The sustained release of AO from liposomes solubilized by addition of Triton X-100 indicates successful loading.

### Unilamellar or Multilamellar?

Our next investigation addressed the lamellarity of the liposomes produced by EDD. Irrespective of the production method, a fraction of the liposomes will have the

membrane consisting of multiple layers, which may impede their further application for purposes that require unilamellar liposomes. The fundamental difference between unilamellar and multilamellar liposomes is the number of lipid layers they consist of. Determining the number of layers in the membrane is not an easy task and may require sophisticated instruments and extensive preparatory tasks [54,55]. To answer this question, we proceeded with exploring the interactions between liposomal membranes and pore-forming toxins. This approach is based on the significant changes in the membrane permeability induced by the conductive pathways produced by the pore-forming toxins interacting with the target membranes; the leaky membrane leads to the release of incorporated dyes, which can be assessed by microscopy or fluorescence spectroscopy. For our investigations we used the prototype pore-forming toxin lysenin, which introduces large-conductance pores in artificial and natural membranes containing sphingomyelin [56–59]. However, for relevancy with regards to the membrane thickness, one may assume that lysenin may not span multiple bilayers [60], therefore the changes in membrane permeability are specific to unilamellar liposomes. Liposomes consisting of Aso, SM, and Chol (10:4:4 weight ratio) were produced and loaded with AO by electro dialysis as described in the previous sections and analyzed by fluorescence spectroscopy. The release of the dye was monitored from the changes in AO's fluorescence upon addition of lysenin (~20 ng) to the cuvette containing 2mL buffer and 100  $\mu$ L liposomes. As inferred from the recorded kinetics (Figure 6), the release of the dye started immediately after lysenin addition, and monotonically increased for the total duration of the record (3,000 s). As anticipated, the lysenin-induced release was slower than the detergent-induced release since lysenin channels must first interact with the

target membranes and oligomerize into functional pores to induce release of the dye. The fluorescence asymptotically approached a steady state, which corresponds to ~80 % of the total release induced by Triton X-100 addition (Figure 21).

This experiment suggests that most of the target membranes are unilamellar; nonetheless, this is not irrefutable proof that all the membranes are solely consisting of lipid bilayers. Unilamellar and multilamellar patches may be present within the same liposomes, and the unilamellar portion of the membrane may facilitate lysenin-induced permeabilization and dye release.

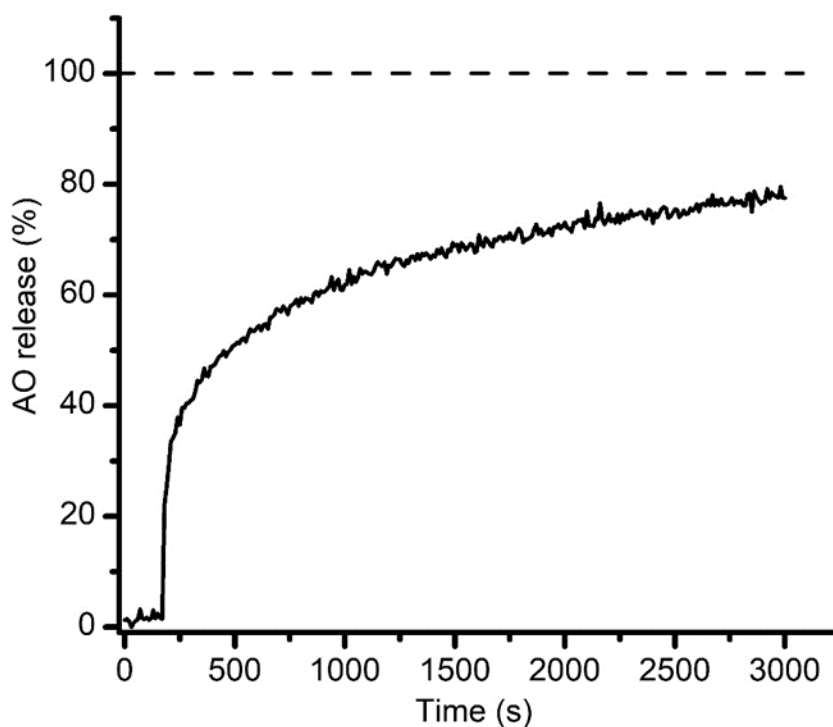


**Figure 9.** Lysenin-induced permeabilization of sphingomyelin-based liposomes. The sustained release of AO (~80 % in less than one hour, relative to 100% release achieved by Triton X-100 addition) suggests that the target membranes are unilamellar. The dashed line shows the 100% release achieved by Triton X-100 addition.

### EDD Comparison to Extrusion and Sonication

Two well-established methods of liposome preparation are extrusion and sonication [23], which have been widely and successfully used for decades [61]. Extrusion refines liposomes formed by hydration and self-assembly to render them unilamellar and adjust their size by passage through membrane filter pores of a particular size [25,26]. Sonication also generates relatively consistent and evenly distributed populations of unilamellar liposomes in a short period of time with low effort, although their size is not easily controlled. However, production of loaded liposomes by either method requires further purification steps to remove the unincorporated molecules from bulk. When charged cargo is used for liposome loading, EDD may eliminate the necessity of further purification and significantly reduce the time required for preparation of loaded liposomes. To further assess the quality of liposomes prepared by the three different methods (extrusion, sonication, and EDD), we compared their physical characteristics by DLS. The three experiments utilized identical lipid compositions (10:4 mass ratio of Aso to Chol) and ionic solutions; only electrodialysis comprised addition of CA for solubilization. For consistency, all the lipids were first mixed in chloroform, placed in glass vials, vacuumed overnight for solvent removal, and the formed thin films were hydrated for 2 h at 45 °C. Liposomes were prepared by extrusion, sonication, and EDD as described in the methods section. DLS analysis (Figure 22) indicated that extrusion provided an average diameter of  $259.6 \pm 2.4$  nm and the narrowest size distribution with a PDI of  $0.077 \pm 0.029$ . Liposomes obtained by sonication presented a significantly smaller average diameter of  $114.2 \pm 1.8$  nm with a larger size distribution, having a PDI of  $0.250 \pm 0.013$ . EDD led to formation of liposomes characterized by an

intermediate size, with an average diameter of  $134.8 \pm 0.7$  nm and a PDI of  $0.214 \pm 0.011$ .

A simple comparison between the three methods shows the most uniform size distribution is achieved by extrusion. This method also enables controlling the average diameter of the liposomes by choosing appropriate membrane filters, which are available in a large range of pore sizes. Both sonication and EDD are fast, simple, and provide satisfactory size distribution of produced liposomes. In both cases however, the size of the produced liposomes is not easily adjusted from experimental conditions.

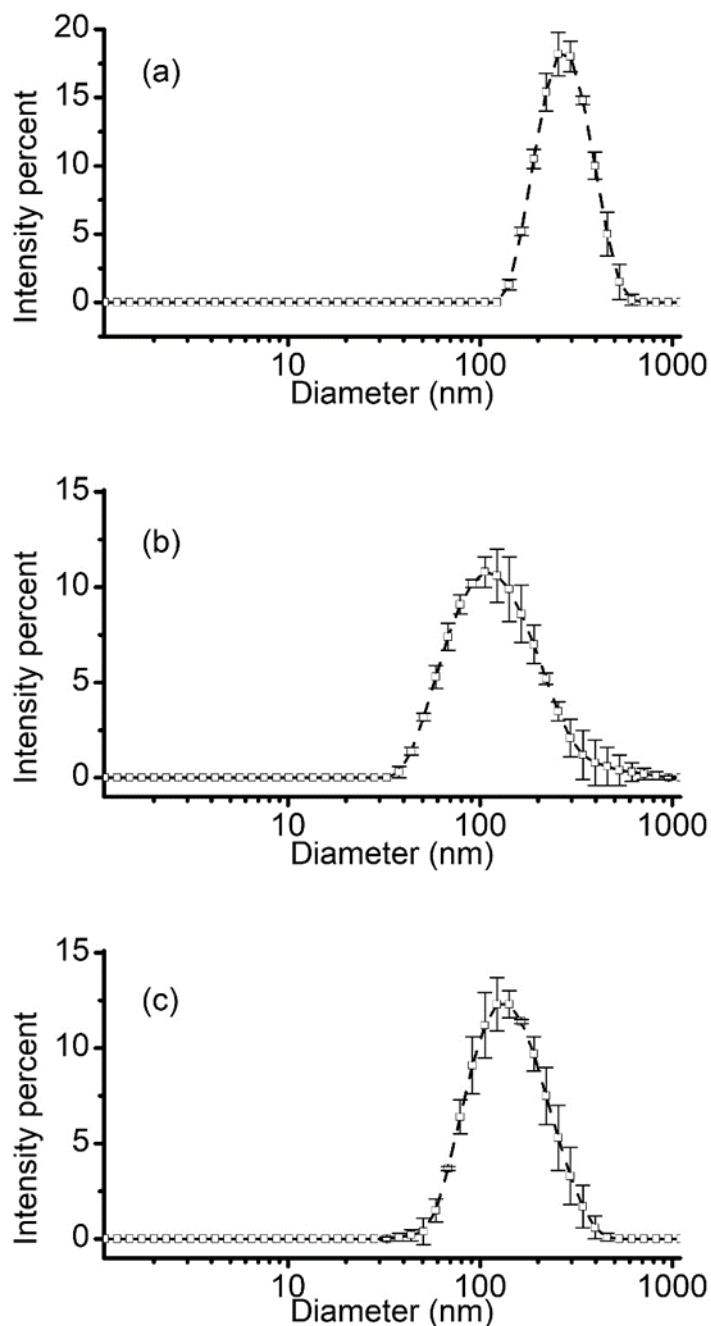


**Figure 22. Dynamic light scattering characterization of liposomes produced by extrusion (a), probe sonication (b), and EDD (c). Each plot shows the mean intensity percent  $\pm$  SD ( $n = 3$ ) determined as a function of diameter.**

The physical characteristics of the EDD-produced liposomes together with the ability to utilize lipid compositions that improve their circulation time suggest that they are suitable for a large variety of scientific and biomedical applications [62]. An

advantage of the EDD method over others is its ability to simultaneously form, load, and separate liposomes from the non-incorporated cargo, therefore significantly reducing the time needed for purification. However, beside the necessity of using charged detergents and dyes, liposome production by EDD has other potential limitations. Changes in pH and solution compositions during electro dialysis may alter the physical and chemical properties of the molecules (i.e., ionization state, or fluorescence). This is particularly concerning if the cargo molecules are heavily reliant on such properties for their intended purpose and efficacy. A simple solution to address this problem was the use of a low ionic strength electrolyte solution. Such solutions may lead to osmotic balance issues, but they may be mitigated by including neutral molecules (i.e., sugars) in the solutions to ensure iso-osmolarity. Although EDD is similar to other solvent-removal methods (including detergent removal by simple dialysis), we do not have an estimate of the amount of detergent left in solutions or membranes. We successfully tested several lipid/dye compositions but one universal setting for successful EDD might be elusive. Therefore, pretreatment conditions, such as temperature and solution agitation, as well as solution and electrical conditions may need to be tailored to other lipids and cargo used for EDD preparation of loaded liposomes.

### **Conclusion**

In summary, EDD may be employed for fast and cost-effective production of loaded and purified liposomes. The size and distribution quality of the liposomes attainable with EDD are comparable to extrusion and sonication. Further investigations of the various settings and parameters and their influence on liposome formation and

loading may provide a better understanding of the limitations and full potential presented by this method for scientific and biomedical applications.

## References

1. Ajeeshkumar, K.K.; Aneesh, P.A.; Raju, N.; Suseela, M.; Ravishankar, C.N.; Benjakul, S. Advancements in liposome technology: Preparation techniques and applications in food, functional foods, and bioactive delivery: A review. *Compr Rev Food Sci Food Saf* **2021**, *20*, 1280–1306, doi:10.1111/1541-4337.12725.
2. Bozzuto, G.; Molinari, A. Liposomes as nanomedical devices. *Int J Nanomedicine* **2015**, *10*, 975–999, doi:10.2147/IJN.S68861.
3. Laouini, A.; Jaafar-Maalej, C.; Limayem-Blouza, I.; Sfar, S.; Charcosset, C.; Fessi, H.; Preparation, Characterization and Applications of Liposomes: State of the Art. *J Colloid Sci Biotechnol* **2012**, *1*, 147–168, doi:10.1166/jcsb.2012.1020.
4. Martinez-Crespo, L.; Sun-Wang, J.L.; Sierra, A.F.; Aragay, G.; Errasti-Murugarren, E.; Bartoccioni, P.; Palacin, M.; Ballester, P. Facilitated Diffusion of Proline across Membranes of Liposomes and Living Cells by a Calix[4]pyrrole Cavitand. *Chem* **2020**, *6*, 3054–3070, doi:10.1016/j.chempr.2020.08.018.
5. Pick, H.; Alves, A.C.; Vogel, H. Single-Vesicle Assays Using Liposomes and Cell-Derived Vesicles: From Modeling Complex Membrane Processes to Synthetic Biology and Biomedical Applications. *Chem Rev* **2018**, *118*, 8598–8654, doi:10.1021/acs.chemrev.7b00777.
6. Routledge, S.J.; Linney, J.A.; Goddard, A.D. Liposomes as models for membrane integrity. *Biochem Soc Trans* **2019**, *47*, 919–932, doi:10.1042/bst20190123.
7. Srivastava, A.; Eisenthal, K.B. Kinetics of molecular transport across a liposome bilayer. *Chem Phys Lett* **1998**, *292*, 345–351, doi:10.1016/S0009-2614(98)00662-9.
8. Aronson, M.R.; Medina, S.; Mitchell, M.J. Peptide functionalized liposomes for receptor targeted cancer therapy. *APL Bioeng* **2021**, *5*, 011501, doi:10.1063/5.0029860.

9. Brea, R.J.; Cole, C.M.; Lyda, B.R.; Ye, L.; Prosser, R.S.; Sunahara, R.K.; Devaraj, N.K. In Situ Reconstitution of the Adenosine A2A Receptor in Spontaneously Formed Synthetic Liposomes. *J Am Chem Soc* **2017**, *139*, 3607–3610, doi:10.1021/jacs.6b12830.
10. Zhang, X.; Qi, J.; Lu, Y.; He, W.; Li, X.; Wu, W. Biotinylated liposomes as potential carriers for the oral delivery of insulin. *Nanomedicine* **2014**, *10*, 167–176, doi:10.1016/j.nano.2013.07.011.
11. Gabizon, A.; Horowitz, A.T.; Goren, D.; Tzemach, D.; Mandelbaum-Shavit, F.; Qazen, M.M.; Zalipsky, S. Targeting Folate Receptor with Folate Linked to Extremities of Poly(ethylene glycol)-Grafted Liposomes: In Vitro Studies. *Bioconjug Chem* **1999**, *10*, 289–298, doi:10.1021/bc9801124.
12. Soe, Z.C.; Thapa, R.K.; Ou, W.; Gautam, M.; Nguyen, H.T.; Jin, S.G.; Ku, S.K.; Oh, K.T.; Choi, H.-G.; Yong, C.S.; et al. Folate receptor-mediated celastrol and irinotecan combination delivery using liposomes for effective chemotherapy. *Colloids Surf B* **2018**, *170*, 718–728, doi:10.1016/j.colsurfb.2018.07.013.
13. Yingchoncharoen, P.; Kalinowski, D.S.; Richardson, D.R. Lipid-Based Drug Delivery Systems in Cancer Therapy: What Is Available and What Is Yet to Come. *Pharmacol Rev* **2016**, *68*, 701–787, doi:10.1124/pr.115.012070.
14. Dawidczyk, C.M.; Kim, C.; Park, J.H.; Russell, L.M.; Lee, K.H.; Pomper, M.G.; Searson, P.C. State-of-the-art in design rules for drug delivery platforms: Lessons learned from FDA-approved nanomedicines. *J Control Release* **2014**, *187*, 133–144, doi:10.1016/j.jconrel.2014.05.036.
15. Bulbake, U.; Doppalapudi, S.; Kommineni, N.; Khan, W. Liposomal Formulations in Clinical Use: An Updated Review. *Pharmaceutics* **2017**, *9*, doi:10.3390/pharmaceutics9020012.
16. Beltran-Gracia, E.; Lopez-Camacho, A.; Higuera-Ciajara, I.; Velazquez-Fernandez, J.B.; Vallejo-Cardona, A.A. Nanomedicine review: Clinical developments in liposomal applications. *Cancer Nanotechnol* **2019**, *10*, 11, doi:10.1186/s12645-019-0055-y.

17. Klibanov, A.L.; Maruyama, K.; Torchilin, V.P.; Huang, L. Amphipathic polyethyleneglycols effectively prolong the circulation time of liposomes. *FEBS Lett* **1990**, 268, 235–237, doi:10.1016/0014-5793(90)81016-H.
18. Najlah, M.; Said Suliman, A.; Tolaymat, I.; Kurusamy, S.; Kannappan, V.; Elhissi, A.M.A.; Wang, W. Development of Injectable PEGylated Liposome Encapsulating Disulfiram for Colorectal Cancer Treatment. *Pharmaceutics* **2019**, 11, 610.
19. Hobbs, S.K.; Monsky, W.L.; Yuan, F.; Roberts, W.G.; Griffith, L.; Torchilin, V.P.; Jain, R.K. Regulation of transport pathways in tumor vessels: Role of tumor type and microenvironment. *Proc Natl Acad Sci U S A* **1998**, 95, 4607–4612, doi:10.1073/pnas.95.8.4607.
20. Golombek, S.K.; May, J.-N.; Theek, B.; Appold, L.; Drude, N.; Kiessling, F.; Lammers, T. Tumor targeting via EPR: Strategies to enhance patient responses. *Adv Drug Deliv Rev* **2018**, 130, 17–38, doi:10.1016/j.addr.2018.07.007.
21. Rosenblum, D.; Joshi, N.; Tao, W.; Karp, J.M.; Peer, D. Progress and challenges towards targeted delivery of cancer therapeutics. *Nat Commun* **2018**, 9, 1410, doi:10.1038/s41467-018-03705-y.
22. Gabizon, A.; Catane, R.; Uziely, B.; Kaufman, B.; Safra, T.; Cohen, R.; Martin, F.; Huang, A.; Barenholz, Y. Prolonged Circulation Time and Enhanced Accumulation in Malignant Exudates of Doxorubicin Encapsulated in Polyethylene-glycol Coated Liposomes. *Cancer Res* **1994**, 54, 987.
23. Cho, N.-J.; Hwang, L.Y.; Solandt, J.J.R.; Frank, C.W. Comparison of Extruded and Sonicated Vesicles for Planar Bilayer Self-Assembly. *Materials* **2013**, 6, doi:10.3390/ma6083294.
24. Johnson, S.M.; Bangham, A.D.; Hill, M.W.; Korn, E.D. Single bilayer liposomes. *Biochim Biophys Acta - Biomembr* **1971**, 233, 820–826, doi:10.1016/0005-2736(71)90184-2.

25. Olson, F.; Hunt, C.A.; Szoka, F.C.; Vail, W.J.; Papahadjopoulos, D. Preparation of liposomes of defined size distribution by extrusion through polycarbonate membranes. *Biochim Biophys Acta - Biomembr* **1979**, 557, 9–23, doi:10.1016/0005-2736(79)90085-3.
26. Ong, S.G.; Chitneni, M.; Lee, K.S.; Ming, L.C.; Yuen, K.H. Evaluation of Extrusion Technique for Nanosizing Liposomes. *Pharmaceutics* **2016**, 8, doi:10.3390/pharmaceutics8040036.
27. Abraham, S.A.; Waterhouse, D.N.; Mayer, L.D.; Cullis, P.R.; Madden, T.D.; Bally, M.B. The liposomal formulation of doxorubicin. *Methods Enzymol* **2005**, 391, 71–97, doi:10.1016/s0076-6879(05)91004-5.
28. Cullis, P.R.; Mayer, L.D.; Bally, M.B.; Madden, T.D.; Hope, M.J. Generating and loading of liposomal systems for drug-delivery applications. *Adv Drug Deliv Rev* **1989**, 3, 267–282, doi:10.1016/0169-409X(89)90024-0.
29. Batzri, S.; Korn, E.D. Single bilayer liposomes prepared without sonication. *Biochim Biophys Acta - Biomembr* **1973**, 298, 1015–1019, doi:10.1016/0005-2736(73)90408-2.
30. Deamer, D.W. Preparation and properties of ether-injection liposomes. *Ann N Y Acad Sci* **1978**, 308, 250–258, doi:10.1111/j.1749-6632.1978.tb22027.x.
31. Sala, M.; Miladi, K.; Agusti, G.; Elaissari, A.; Fessi, H. Preparation of liposomes: A comparative study between the double solvent displacement and the conventional ethanol injection - From laboratory scale to large scale. *Colloids Surf Physicochem Eng Aspects* **2017**, 524, 71–78, doi:10.1016/j.colsurfa.2017.02.084.
32. Liu, D.; Huang, L. Role of cholesterol in the stability of pH-sensitive, large unilamellar liposomes prepared by the detergent-dialysis method. *Biochim et Biophys Acta - Biomembr* **1989**, 981, 254–260, doi:10.1016/0005-2736(89)90035-7.

33. Milsmann, M.H.; Schwendener, R.A.; Weder, H.G. The preparation of large single bilayer liposomes by a fast and controlled dialysis. *Biochim Biophys Acta – Biomembr* **1978**, 512, 147–155, doi:10.1016/0005-2736(78)90225-0.
34. Ollivon, M.; Lesieur, S.; Grabielle-Madelmont, C.C.; Paternostre, M.Ì.t. Vesicle reconstitution from lipid-detergent mixed micelles. *Biochim Biophys Acta - Biomembr* **2000**, 1508, 34–50, doi:10.1016/S0304-4157(00)00006-X.
35. Schubert, R.; Liposome preparation by detergent removal. *Methods Enzymol* **2003**, 367, 46–70, doi:10.1016/s0076-6879(03)67005-9.
36. Yao, X.; Fan, X.; Yan, N. Cryo-EM analysis of a membrane protein embedded in the liposome. *Proc Natl Acad Sci* **2020**, 117, 18497, doi:10.1073/pnas.2009385117.
37. Helenius, A.; Simons, K. Solubilization of membranes by detergents. *Biochim Biophys Acta – Rev Biomembr* **1975**, 415, 29–79, doi:10.1016/0304-4157(75)90016-7.
38. Schubert, R.; Beyer, K.; Wolburg, H.; Schmidt, K.H. Structural changes in membranes of large unilamellar vesicles after binding of sodium cholate. *Biochemistry* **1986**, 25, 5263–5269, doi:10.1021/bi00366a042.
39. Lasic, D.D.; A molecular model for vesicle formation. *Biochim Biophys Acta – Biomembr* **1982**, 692, 501–502, doi:10.1016/0005-2736(82)90404-7.
40. Lichtenberg, D.; Ahyayauch, H.; Goñi, Félix, M. The Mechanism of Detergent Solubilization of Lipid Bilayers. *Biophys J* **2013**, 105, 289–299, doi:10.1016/j.bpj.2013.06.007.
41. Jimah, J.R.; Schlesinger, P.H.; Tolia, N.H. Liposome Disruption Assay to Examine Lytic Properties of Biomolecules. *Bio-protocol* **2017**, 7, e2433, doi:10.21769/BioProtoc.2433.
42. Zagana, P.; Mourtas, S.; Basta, A.; Antimisiaris, S.G.; Preparation, Physicochemical Properties, and In Vitro Toxicity towards Cancer Cells of Novel Types of Arsonoliposomes. *Pharmaceutics* **2020**, 12, 327 doi:103390/pharmaceutics12040327.

43. Cabral, D.J.; Hamilton, J.A.; Small, D.M. The ionization behavior of bile acids in different aqueous environments. *J Lipid Res* **1986**, *27*, 334–343, doi:10.1016/S0022-2275(20)38839-8.
44. Rigaud, J.-L.; Lévy, D. Reconstitution of Membrane Proteins into Liposomes. *Methods Enzymol*, **2003**, *372*, 65–86, doi:0.1016/S0076-6879(03)72004-7.
45. Agrawal, A.K.; Gupta, C.M.; Tuftsin-bearing liposomes in treatment of macrophage-based infections. *Adv Drug Del Rev* **2000**, *41*, 135-146, doi:10.1016/S0169-409X(99)00061-7.
46. Caron, W.P.; Lay, J.C.; Fong, A.M.; La-Beck, N.M.; Kumar, P.; Newman, S.E.; Zhou, H.; Monaco, J.H.; Clarke-Pearson, D.L.; Brewster, W.R.; et al. Translational Studies of Phenotypic Probes for the Mononuclear Phagocyte System and Liposomal Pharmacology. *J Pharmacol Exp Ther* **2013**, *347*, 599, doi:10.1124/jpet.113.208801.
47. Kao, Y.J.; Juliano, R.L. Interactions of liposomes with the reticuloendothelial system. Effects of reticuloendothelial blockade on the clearance of large unilamellar vesicles. *Biochim Biophys Acta – Gen Subj* **1981**, *677*, 453–461, doi:10.1016/0304-4165(81)90259-2.
48. McSweeney, M.D.; Shen, L.; DeWalle, A.C.; Joiner, J.B.; Ciociola, E.C.; Raghuwanshi, D.; Macauley, M.S.; Lai, S.K. Pre-treatment with high molecular weight free PEG effectively suppresses anti-PEG antibody induction by PEG-liposomes in mice. *J Control Release* **2021**, *329*, 774–781, doi:10.1016/j.jconrel.2020.10.011.
49. Papahadjopoulos, D.; Allen, T.M.; Gabizon, A.; Mayhew, E.; Matthay, K.; Huang, S.K.; Lee, K.D.; Woodle, M.C.; Lasic, D.D.; Redemann, C. Sterically stabilized liposomes: Improvements in pharmacokinetics and antitumor therapeutic efficacy. *Proc Nat Acad Sci* **1991**, *88*, 11460, doi:10.1073/pnas.88.24.11460.

50. Amado, A.M.; Ramos, A.P.; Silva, E.R.; Borissevitch, I.E. Quenching of acridine orange fluorescence by salts in aqueous solutions: Effects of aggregation and charge transfer. *J Lumin* **2016**, *178*, 288–294, doi:10.1016/j.jlumin.2016.06.006.
51. Bae, W.; Yoon, T.-Y.; Jeong, C. Direct evaluation of self-quenching behavior of fluorophores at high concentrations using an evanescent field. *PLoS ONE* **2021**, *16*, e0247326, doi:10.1371/journal.pone.0247326.
52. Hamann, S.; Kiilgaard, J.F.; Litman, T.; Alvarez-Leefmans, F.J.; Winther, B.R.; Zeuthen, T. Measurement of Cell Volume Changes by Fluorescence Self-Quenching. *J Fluoresc* **2002**, *12*, 139–145, doi:10.1023/A:1016832027325.
53. Needham, D.; Anyarambhatla, G.; Kong, G.; Dewhirst, M.W. A New Temperature-sensitive Liposome for Use with Mild Hyperthermia: Characterization and Testing in a Human Tumor Xenograft Model. *Cancer Res* **2000**, *60*, 1197.
54. Wang, T.; Deng, Y.; Geng, Y.; Gao, Z.; Zou, J.; Wang, Z. Preparation of submicron unilamellar liposomes by freeze-drying double emulsions. *Biochim Biophys Acta - Biomembr* **2006**, *1758*, 222–231, doi:10.1016/j.bbamem.2006.01.023.
55. Tejera-Garcia, R.; Ranjan, S.; Zamotin, V.; Sood, R.; Kinnunen, P.K.J. Making Unilamellar Liposomes Using Focused Ultrasound. *Langmuir* **2011**, *27*, 10088–10097, doi:10.1021/la201708x.
56. Ide, T.; Aoki, T.; Takeuchi, Y.; Yanagida, T. Lysenin forms a voltage-dependent channel in artificial lipid bilayer membranes. *Biochem Biophys Res Commun* **2006**, *346*, 288–292, doi:10.1016/j.bbrc.2006.05.115.
57. Ishitsuka, R.; Kobayashi, T. Lysenin: A new tool for investigating membrane lipid organization. *Anat Sci Int* **2004**, *79*, 184–190, doi:10.1111/j.1447-073x.2004.00086.x.

58. Kulma, M.; Hereć, M.; Grudziński, W.; Anderluh, G.; Gruszecki, W.I.; Kwiatkowska, K.; Sobota, A. Sphingomyelin-rich domains are sites of lysenin oligomerization: Implications for raft studies. *Biochim Biophys Acta - Biomembr* **2010**, 1798, 471–481, doi.org/10.1016/j.bbamem.2009.12.004.
59. Yamaji-Hasegawa, A.; Makino, A.; Baba, T.; Senoh, Y.; Kimura-Suda, H.; Sato, S.B.; Terada, N.; Ohno, S.; Kiyokawa, E.; Umeda, M.; et al. Oligomerization and pore formation of a sphingomyelin-specific toxin, lysenin. *J Biol Chem* **2003**, 278, 22762–22770, doi.org/10.1074/jbc.M213209200.
60. Shrestha, N.; Thomas, C.A.; Richtsmeier, D.; Bogard, A.; Hermann, R.; Walker, M.; Abatchev, G.; Brown, R.J.; Fologea, D. Temporary Membrane Permeabilization via the Pore-Forming Toxin Lysenin. *Toxins* **2020**, 12, 343, doi:10.3390/toxins12050343.
61. Lapinski, M.M.; Castro-Forero, A.; Greiner, A.J.; Ofoli, R.Y.; Blanchard, G.J. Comparison of Liposomes Formed by Sonication and Extrusion: Rotational and Translational Diffusion of an Embedded Chromophore. *Langmuir* **2007**, 23, 11677–11683, doi:10.1021/la7020963.
62. Danaei, M.; Dehghankhold, M.; Ataei, S.; Hasanzadeh Davarani, F.; Javanmard, R.; Dokhani, A.; Khorasani, S.; Mozafari, M.R. Impact of Particle Size and Polydispersity Index on the Clinical Applications of Lipidic Nanocarrier Systems. *Pharmaceutics* **2018**, 10, 57, doi:10.3390/pharmaceutics100200

## CHAPTER FOUR: CONTROLLED RELEASE FROM PHOTOCCLICK AND PH- SENSITIVE LIPOSOMES

### **Introduction**

The use of liposomes as enclosed, protective structures, capable of delivering their cargo is often marred by their passive and uncontrolled release [1-3]. Encapsulation and preservation of payload is one of the major purposes of liposome technology, however experimenters and producers must often compromise. One must choose between leaky liposomes that release too quickly, or liposomes made to avoid leakage completely, resulting in very slow and insignificant release. Ideally, release would occur only at a desired time, however controlled release of cargo from liposomes is an unmet challenge that can limit their use in many applications, particularly in the realms of scientific research and medical use [4, 5].

A key area of interest pertaining to controlled release involves chemotherapeutic delivery for the treatment of cancers [6, 7]. The slow passive leakage of chemotherapeutics within a few weeks after accumulation at tumor sites is often ineffective in stopping the rapid division of cancer cells [1]. To address this issue, the past decades have investigated numerous bioengineering approaches and stimuli for inducing drug release from liposomes in a localized and efficient manner [2]. Investigations on controlled release from liposomes have ranged from using mild hyperthermia [8, 9], photo-activation [10, 11], focused ultrasound [12, 13], nanoparticles and molecules embedded or co-loaded with the main cargo to aid in liposome leakage

upon near-infrared [7, 14] or magnetic field exposure [15-17], as well as pH change to be triggered by external microenvironment conditions of tumor tissue [18, 19]. Although the intended outcome of content release is achieved, the efficiency and degree of release is questionable; as a matter of fact, no method of controlled drug release from liposomes is included in current clinical practices.

In addition to the proposed mechanisms pertaining to cargo release upon stimulation by radiation (usually UV, VIS, and IR), an attractive subcategory is presented by the utilization of photosensitive lipids endowed with additional chemical bonding capabilities upon radiation exposure. In this endeavor, photopolymerizable lipids allow successful control of membrane permeability. Upon UV or visible light stimulation, photosensitive lipids undergo covalent bonding and polymerization [10, 11, 20, 21]. The loss of fluidity resulting from the de novo created bonds translates into a significant increase in permeability, which allows the transport of ions and molecules through the otherwise impermeable membranes [22]. Apparently, this process is augmented by the segregation of photopolymerizable lipids into domains (rafts), which promotes radiation-induced polymerization and leads to increased membrane permeability [10, 22]. Considering PhotoClick membrane components have been insufficiently studied for use in photo-responsive liposomes, we decided to further investigate their potential in this regard. PhotoClick chemistry involves the activation of diazirine moieties in specially modified sphingosine and cholesterol to become activated upon exposure to UV light at approximately 365 nm [23]. Photoactivation leads to diazirine reactions, resulting in a covalently reactive carbene (Figure 23) [24]. Furthermore, sphingosine and cholesterol are understood to accumulate in lipid rafts in membranes [25-28]. This suggests increased

likelihood of crosslinking between these components considering their increased proximity in such areas, making them an excellent candidate for being used in the intended manner.

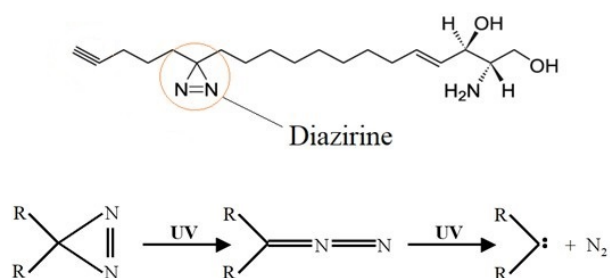


**Figure 10. PhotoClick reaction of diazirine. The diazirine moiety on PhotoClick sphingomyelin, one of the UV sensitive components used in our liposomes, releases nitrogen and results in reactive carbene formation upon UV exposure. Carbene readily covalently bonds, allowing for crosslinking in the membranes, and leading to permeabilization. Similar chemical process occurs in PhotoClick cholesterol, the other UV sensitive component used.**

Although the response to visible and UV light has been demonstrated to induce release from photosensitive liposomes made with other photopolymerizable lipids [21, 29], an obvious issue remains when considering their application for the use as chemotherapeutic delivery vehicles to tumors. Light and UV are not very capable of penetrating tissue. Deep seated tumors are therefore not going to benefit from photosensitive liposomes, as light and UV will not be capable of triggering release of loaded chemotherapy. However, O'Brien et al. reported that some liposomes made with photopolymerizable components are also X-ray responsive [30]. This prompted us to investigate the possibility that liposomes composed with PhotoClick components are also responsive to X-ray irradiation. This would be a momentous advancement in controlled release from liposomes, as an actinic beam utilized for radiotherapy can be used to also

serve as a controlled, effective, and highly localized trigger for release of chemotherapeutics [31, 32]. Although the postulated benefits of concomitant radiation and chemotherapy are still unclear due to the lack of sufficient investigations, evidence suggests such an approach has the potential to treat tumors at a significantly higher efficiency than either treatment alone [33-36]. Furthermore, simultaneous radio-chemotherapy is strongly limited by its combined toxicity [35, 37]; targeted release of local chemotherapy using liposomes capable of release upon X-ray exposure would have the potential to significantly reduce the toxicity of systemic chemotherapy treatment while improving the overall clinical outcome.

Our further investigations looked into pH sensitive liposomes, which we redesigned to be triggered to release their payload by pH changes induced by irradiation. Stealth liposomes sensitive to pH changes have been long foreseen as candidates for drug delivery into tumors [38-42]. Stealth liposomes, already utilized for drug delivery, present a reduced uptake by cells of the reticuloendothelial system (RES)/ mononuclear phagocyte system (MPS). This results in a long circulation median lifetime [43, 44] and accumulation into tumors by the enhanced permeability and retention (EPR) effect [45, 46]. The added pH sensitivity creates the means to release an incorporated drug upon pH variation (usually increase of acidity), therefore ensuring delivery. The primary design of these specialized vehicles was based on the hypothesis that pH decreases dramatically inside a tumor; however, this decrease is not uniform, and it has been proven to be rather modest [47]. Therefore, controlling the pH of the environment by external stimuli may add the benefit of controlled drug release from pH sensitive liposomes.

Most pH-sensitive liposome formulations described in the literature are prepared with unsaturated phospholipids in combination with mildly acidic amphiphiles, and their ability to deliver incorporated drugs upon decreasing pH is well documented [18, 38, 39, 41, 42]. Since the ability to release the drug from such vehicles directly depends on pH, a mechanism to control the local intra-liposomal pH is required. In this endeavor, we sought a mechanism by which acidification would be produced upon interaction with ionizing radiation, thus allowing concomitant radio and chemotherapy.

To achieve our scientific goals, we propose using organic halogens to induce acidification upon X-ray exposure to gain local pH control. Chemical changes upon irradiation of organic halogens were an important topic in the 50s and 60s [48-56], when scientists were looking for simple, meaningful ways to determine doses of radiation. Although the advent of solid-state physics and electronics led to the almost total abandonment of such approaches, the scientific explorations for dosimetry purposes led to new knowledge, useful for our purposes. Many organic halogen compounds liberate the corresponding halogen acid when irradiated in water solutions [48-56]. Although the exact mechanism is not known, there is evidence that the action is indirect, through radicals produced from water upon irradiation. The chief ionizable product formed after exposure to X-ray was demonstrated to be the halogenated acid. From all organic halogens suitable for our purpose, we focused our attention on bromal hydrate; since the 1950s, water solutions of bromal hydrate have been proposed to be used as radiation dosimeters based on HBr release upon irradiation [53].

## Materials and Methods

### Lipids, Loading Molecules, and Solutions

The lipids used for liposome preparation included 1,2-distearoyl-sn-glycero-3-phosphocholine (DSPC, Avanti Polar Lipids), cholesterol (Chol, Sigma-Aldrich), sphingomyelin (SM, Avanti Polar Lipids), PhotoClick sphingosine (P-SM, Avanti Polar Lipids), PhotoClick cholesterol (P-Chol, Avanti Polar Lipids), phosphatidylethanolamine (PE, Avanti Polar Lipids), and oleic acid (OA, Avanti Polar Lipids). Lipids were purchased either in powder or chloroform-solubilized form. The powder lipids were solubilized in chloroform as concentrated stock solutions, mixed with the other lipids at the desired ratios in glass vials (amber, and covered with Al foil for all light sensitive compounds), and had the solvent removed by being placed under vacuum at room temperature for at least 12 h. The formed lipid cakes were stored in the freezer until further use. Structural details of the used lipids are presented in Figure 24.

Electrolyte buffered solutions were prepared with KCl, NaCl (ThermoFisher Scientific), and HEPES (additions from a 1M stock solution of pH 7.4, Sigma-Aldrich). Calcein (CAL, ThermoFisher Scientific) and cisplatin (CIS, ThermoFisher Scientific) were diluted to desired concentration in the hydrating buffers for passive loading. For the preparation of liposomes intended for active loading with doxorubicin (DOX, Sigma-Aldrich) we used a 150 mM citrate buffer made from sodium citrate dihydrate and citric acid (both from Fisher Scientific); the pH was adjusted to pH 4.24 by adding small aliquots of 1 M HCl. Anhydrous bromal (TCI America) mixed with water was re-crystallized under vacuum, hydrated to 1M final concentration, then further reduced to 150 mM concentration and stored in a sealed amber container in the refrigerator. KCl

solutions (135 mM, pH 7.2) as well as stock solutions of HCl (concentrations ranging from 0.1 mM to 100 mM) were used for investigations of pH-sensitive liposomes. All the other common chemicals were purchased from various producers and prepared according to their recommendations.

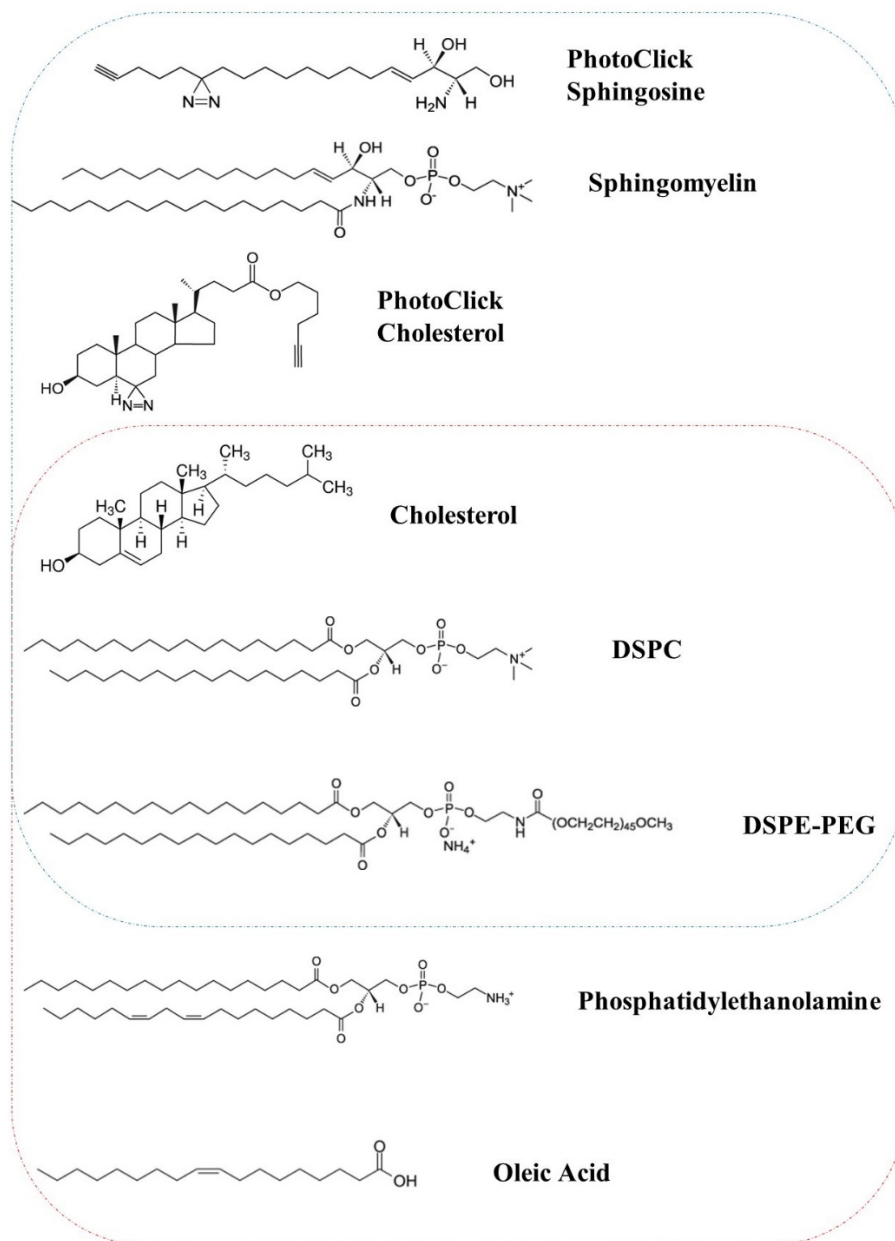


**Figure 24. Lipid components used in the production of liposomes used for investigations on controlled release. Cholesterol (Chol) and 1,2-distearoyl-sn-glycero-3-phosphocholine (DSPC) were used for both UV/X-ray and pH sensitive liposomes. PhotoClick sphingosine (P-SM), PhotoClick cholesterol (P-Chol), and sphingomyelin (SM) were used specifically for UV/X-ray sensitive liposomes (DSPE-PEG was used in one variation of PhotoClick composed liposomes with DOX loading. Phosphatidylethanolamine (PE), oleic acid (OA), and 1,2-distearoyl-sn-glycero-3-phosphoethanolamine-N-[methoxy(polyethyleneglycol)-2000] (DSPE-PEG) were used specifically for pH sensitive liposomes. UV/X-ray sensitive components are outlined in dashed blue line; the dotted red line outlines the components used for preparation of pH sensitive liposomes.**

### Liposomes Preparation

Slow hydration of lipids in the desired buffered solutions (with or without cargo) was achieved by adding the solutions over the lipid cakes in sealed glass vials, after which the mixtures were gradually heated from 45 °C to 68 °C over a few hours. The large aggregates that were easily visible in the hydration vials were dispersed by either brief sonication (5 seconds in a bath sonicator, Fisher Scientific) or a few cycles of freezing/thawing.

Liposome preparation was performed exclusively by employing the extrusion technique [57-59]. An Avanti Polar Lipids extruder with a proper set of polycarbonate filter membranes (pore size of 400 nm and 800 nm, as indicated for each specific experiment) was placed on a hot plate preheated to ensure a temperature of the extruder body greater than the transition temperature of the used lipids (generally, a temperature of 70 °C was sufficient for all the experiments). To avoid any potential interactions between the photo-sensitive lipids and light, the syringes were covered with aluminum foil during extrusion. The syringes were filled with hydrated lipid mixtures for both passive and active loading of dyes or drugs, as detailed next. Each extrusion protocol comprised at least 41 passes through the polycarbonate membrane.

### Liposome Loading and Purification

Passive loading of the liposomes was achieved by adding the cargo at the intended concentrations mixed into hydration buffer; after extrusion, the non-incorporated load was removed by extensive dialysis in cassettes against 0.5 L – 2 L of dye-free buffered solution. For active loading of DOX, first an electrochemical gradient was created by dialysis-exchange of the acidic external buffer with a neutral or near-

neutral one. After buffer exchange, active loading was initiated by addition of 125  $\mu\text{M}$  DOX to the bulk. The loading process lasted for at least 48 hours, after which the unloaded DOX was removed by dialysis against a DOX-free buffered solution (neutral or near-neutral pH).

### Fluorescence and Spectral Characterization

Fluorescence spectroscopy was utilized for establishing the self-quenching plots of CAL and DOX, and for determining the kinetics of the drug release upon liposome exposure to physical and chemical stimuli. For these purposes, we utilized a FluoroMax4 spectrofluorometer (Horiba) set in either emission or kinetics mode. For these release characterizations, the normalized efficiency  $E_N$  was calculated by considering the fluorescence of the sample before exposure ( $F_0$ ), the fluorescence of the sample after exposure and at different time intervals ( $F$ ), and the maximal fluorescence ( $F_{100}$ ) determined upon total release of the considered dye from liposomes in the presence of Triton X-100 (Sigma Aldrich) [60]. This was used to analyze release data at multiple time points. For relative release efficiency ( $E_R$ ), the initial fluorescence ( $F_0$ ) was not subtracted to allow better visual comparison of controls and experimental samples in the single point bar graphs used. The release efficiency is given in percent. The formulas used for release efficiency are:

$$E_N\% = 100 \times (F - F_0) / (F_{100} - F_0) \quad \text{or} \quad E_R\% = (F / F_{100}) \times 100$$

Since CIS is non-fluorescent, we adopted the optical absorption quantification method from prior work reported elsewhere [61-63]. For establishment of a CIS concentration standard curve o-phenylenediamine (OPDA, Fisher Scientific) and dimethylformamide (DMF, Fisher Scientific) were used to complex with CIS for optical

absorption analysis with a Varian Carry 5000 spectrophotometer. A stock solution of CIS was obtained by dissolving 10 mg CIS in 100 mL potassium phosphate buffer (135 mM, pH 7.2) at 65° C. Working standard solutions were prepared by using 1 mL OPDA at 1.4 mg/mL in DMF and further filled with phosphate buffer to a total volume of 3 mL. The solutions were heated in a water bath at 100° C for 10 minutes to develop the green color. After cooling at room temperature, the final volume was adjusted to 10 mL with DMF and the absorption at 704 nm was determined with the spectrometer [61-63]. The reaction responsible for CIS complex formation is summarized in Figure 25.

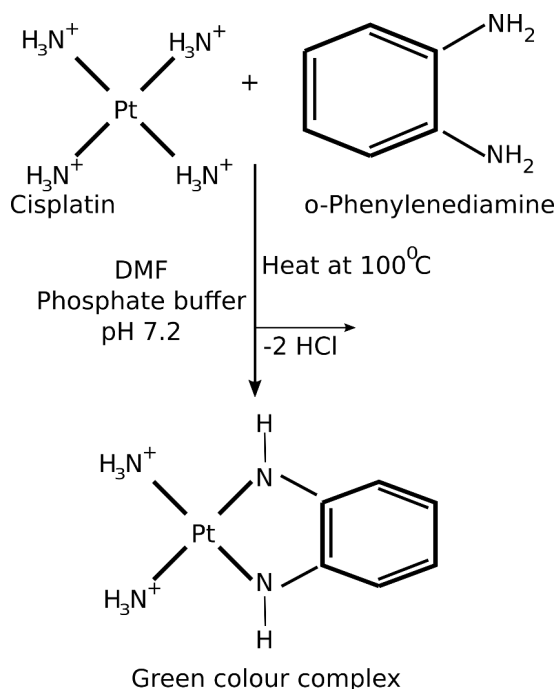


**Figure 11. Optically absorbing complex formation of Cisplatin. Reaction with o-phenylenediamine (OPDA) and dimethylformamide (DMF) results in increased absorbance at 704 nm.**

### UV and X-Ray Irradiation

Preliminary testing under UV irradiation conditions was completed with a highly directional UV LED (SETI, 365 nm). The LED was mounted into the lid of a spectrometer cuvette and powered from a custom constant current generator; the

approximate UV power emitted by the LED was only 0.5 mW. X-ray irradiation of samples was performed with a Quantum CS-1 X-ray system, equipped with a Quantum 40kW/125 kVp "Q-Vision" high frequency radiographic generator; the irradiation conditions are detailed in the results and discussions section.

## **Results and Discussions**

### Self-Quenching of Calcein and Doxorubicin

The emission spectra of CAL and DOX solutions as a function of concentrations were measured with the Fluoromax4 fluorometer set in emission mode for excitation wavelengths of 495 nm (CAL) and 470 nm (DOX). The magnitude of the emission was determined from the recorded spectra at 520 nm for CAL, and 570 nm for DOX. The excitation and emission slits were set at 1 nm. Both dyes presented a concentration-dependent increase in fluorescence in the low concentration range (Figure 26). CAL reached a maximum in fluorescence at around 20  $\mu\text{M}$ , while DOX achieved the maximum fluorescence at around 100  $\mu\text{M}$ . However, both dyes encountered a massive concentration-dependent fluorescence decrease over these concentration values, specific to self-quenching [64, 65]. This behavior points out the basic principles for the determination of dye release from fluorescence measurements; liposomes loaded with dyes at high concentrations will present a low fluorescence owing to self-quenching [66] (Figures 26 A and B). However, the destabilization of the membrane leads to an increase of membrane permeability, allowing loaded dyes to leak out. The significant dilution upon dye release from permeabilized liposomes leads to a prominent increase in fluorescence. This procedure also enables fast determination of maximum loading; fast destabilization of the membrane with detergent (i.e., Triton X-100, Figures 26 C and D)

leads to 100% release of the loaded dye, which may be further used to assess the efficacy of specific release upon membrane destabilization by physical or chemical stimuli.

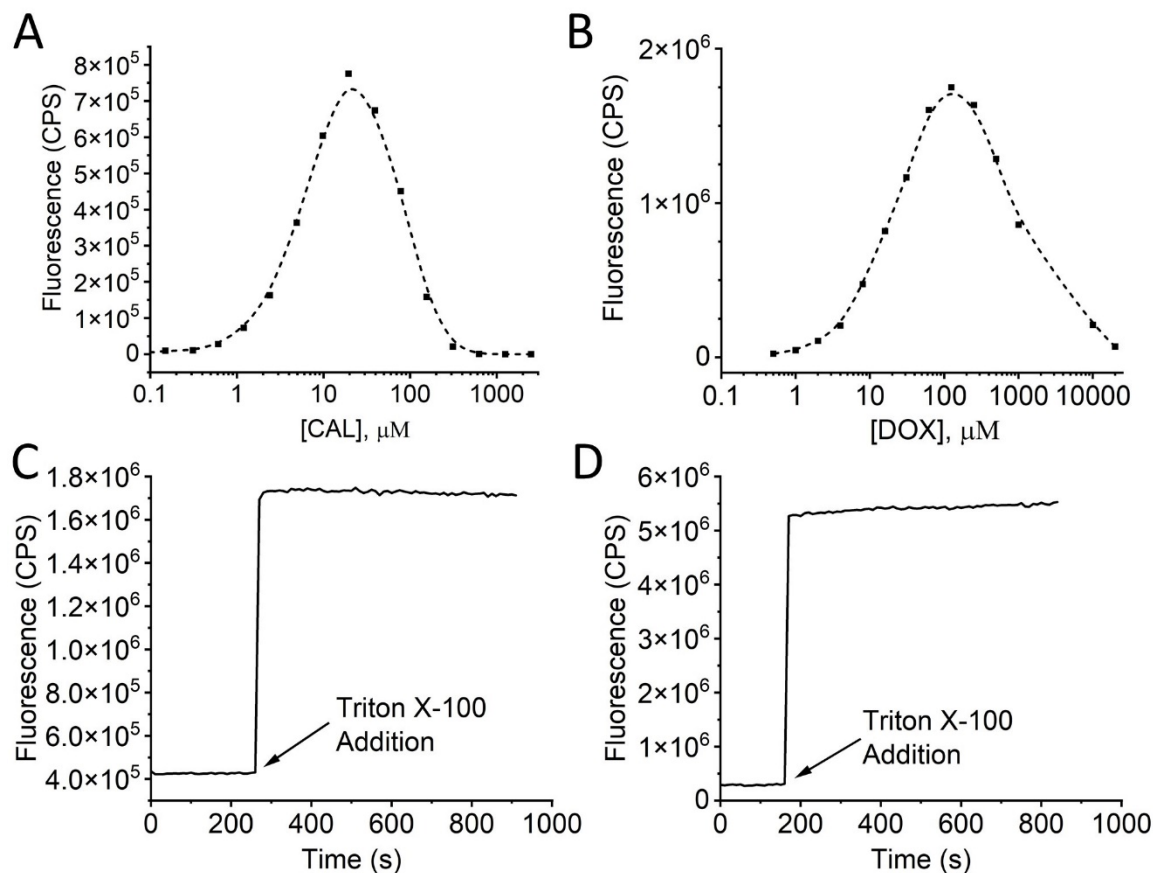


**Figure 12. Self-quenching of CAL and DOX, followed by detergent induced release measurements from loaded liposomes. We established maximum fluorescence concentration for CAL of about  $20 \mu\text{M}$  (A) and DOX of about  $100 \mu\text{M}$  (B) characterizing their concentration dependent quenching behaviors. Maximum release of CAL (C) and DOX (D) was induced by Triton-X 100 addition, showing loaded and purified liposomes in dye/drug free buffer.**

For the preparation of PhotoClick liposomes, DSPC, Chol, SM, P-Chol, and P-SM have been dissolved in chloroform at a mass ratio of 10:1:2:1.2:0.8. The mixture was vacuum dried for 48 hours and the resulting lipid films were hydrated with 135 mM NaCl, 20 mM HEPES (pH 7.2), and 30 mM CAL (self-quenching concentration). The final concentration of DSPC in the hydration buffer was 10 mg/mL. A control sample

consisted of DSPC, Chol, and SM only (10:2:4 mass ratio). After hydration, 800 nm liposomes were produced by extrusion (41 passes) through stacked polycarbonate filters and the non-incorporated CAL was removed by overnight cassette dialysis against 1 L of dye-free buffered electrolyte solution. The samples were stored in amber vials at 4 °C until use.

In order to identify PhotoClick responsiveness of the liposomes containing P-SM and P-Chol in their membrane, we performed a preliminary test that employed CAL release upon exposure to the UV light (365 nm) provided by the LED. The fluorometer was set in kinetics mode (Ex/Em: 495/520 nm), 1 s integration time, with the anti-photobleaching option activated, and 10 s sampling time. Three cuvettes were filled with 1.9 mL buffered electrolyte solution and 100  $\mu$ L liposomes. The sample cuvette contained PhotoClick liposomes, while the control comprised liposomes made without PhotoClick components. Another control containing PhotoClick liposomes was set for measuring the 100% CAL release upon addition of 50  $\mu$ L of 5% v/v Triton X-100; the relative release efficacy was determined for the sample and control liposomes (Figure 27).

Upon exposure to the UV light from the UV LED, CAL quickly started leaking out from the liposomes, as indicated by the increasing fluorescent signal. However, negligible leakage was determined from the UV-exposed liposomes lacking PhotoClick components, suggesting that the PhotoClick components are needed to render liposomes sensitive to UV radiation. UV exposure initiates CAL release from PhotoClick liposomes and results in approximately 70% release of the incorporated dye in less than one hour. Seeing the sigmoidal trend of CAL release likely suggests a multistep or cooperative

process in membrane permeabilization. Upon UV exposure, the diazirine groups within the PhotoClick sphingosine and cholesterol are photo-activated, resulting in the formation of reactive carbene [24]. This reactive species results in formation of covalent crosslinking among membrane components, resulting in a loss of membrane fluidity and allowing the leakage of cargo. It is worth mentioning that our results suggest that covalent crosslinking occurs without any need for proteins embedded in the liposome membrane, and this result may be explained based on the lipid self-organization in lipid rafts [26, 67]. The particular composition of the membranes includes SM and Chol, which are known to segregate in SM-rich domains (lipid rafts) [27, 28]. The local high density of bonds prone to crosslinking possibly promote covalent bonding without the necessity of membrane proteins; nonetheless, it is not clear if the leakage occurs through the more rigid domains resulted after crosslinking or at the edge between the rigid rafts and the more fluidic bulk phase [68].

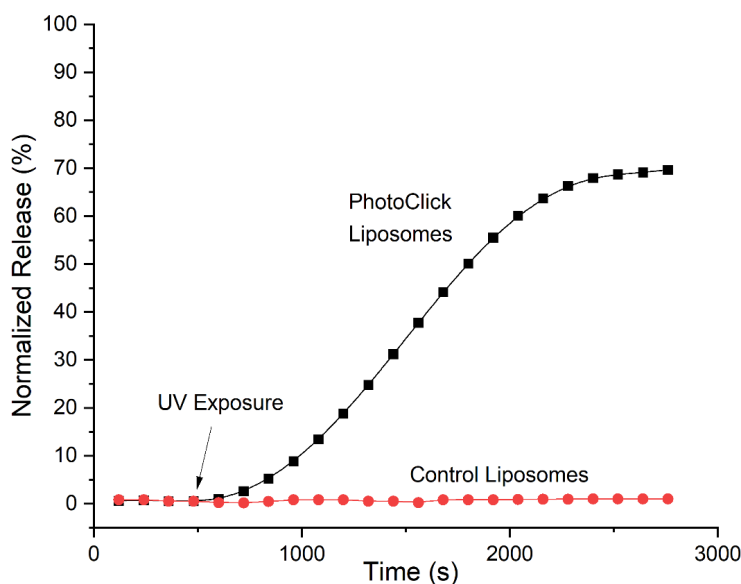


**Figure 27. UV induced release of CAL from liposomes. 100  $\mu$ L of CAL loaded PhotoClick liposomes exposed to UV light resulted in ~70% release. Comparatively, liposomes lacking PhotoClick components showed negligible release (~1%) over the time span measurements were taken. 100% release was achieved by treating PhotoClick liposomes with Triton X-100.**

#### Calcein Release from PhotoClick Liposomes Upon X-ray Exposure

As observed, UV exposure elicited a significant release of CAL in comparison to the control lacking PhotoClick components. Although this may find immediate in vitro applications, a prominent shortcoming of using UV to trigger release in liposomes involves the simple fact that UV light is not capable of significant tissue penetration. Many tumors needing drug delivery are deeply seated within the body; in this respect, X-ray has the benefit of not only being able to penetrate deeply into tissue, but also offer a major improvement with regards to local and loco-regional control and better clinical outcome in combination with chemotherapy [36, 69, 70]. Concomitant application of chemotherapy and radiation have been shown to significantly improve destruction of tumor tissue, however, it is limited by an increased toxicity [35, 37]. Local release of

chemotherapy from liposomes triggered by X-ray radiation could allow for highly localized concomitant radiation and chemotherapy treatment, compounding the efficacy of tumor destruction, while reducing the immense stress on the body resulting from systemic chemotherapy and simultaneously added radiotoxicity.

Although it is shown that PhotoClick liposomes respond to UV light, there is no evidence of PhotoClick lipids having sensitivity to X-ray radiation. However, according to O'Brien et al, photopolymerizable lipids (which are similarly responsive to UV light) also respond to ionizing radiation (i.e., X-ray) [30]. Prompted by these prior findings, we tested whether the PhotoClick liposomes also respond to X-ray radiation, which may prove fruitful for future biomedical applications of this technology for drug delivery and cancer therapy. To answer these questions, we prepared 800 nm PhotoClick liposomes with lipid compositions identical to the previous experiment and filled them with 30 mM CAL solubilized in a buffer containing 50 mM KCl and 50 mM Hepes (pH 7.2). The X-ray exposure was performed by applying a succession of 20 pulses from the X-ray equipment (0.125 MeV, 320 mA). The fluorescence of the sample and control liposomes was recorded before and after irradiation, and the maximum (100%) relative efficacy determined based on the maximum release recorded for the non-irradiated PhotoClick sample solubilized by addition of 100  $\mu$ L 5% v/v Triton X-100 (Figure 28). Our results indicate that approximately 60% of the CAL dye was released from the exposed PhotoClick sample in less than one hour. Within the same time interval, the exposed control showed negligible release, suggesting that the PhotoClick components are essential to initiating and sustaining cargo release from liposomes upon X-ray exposure.

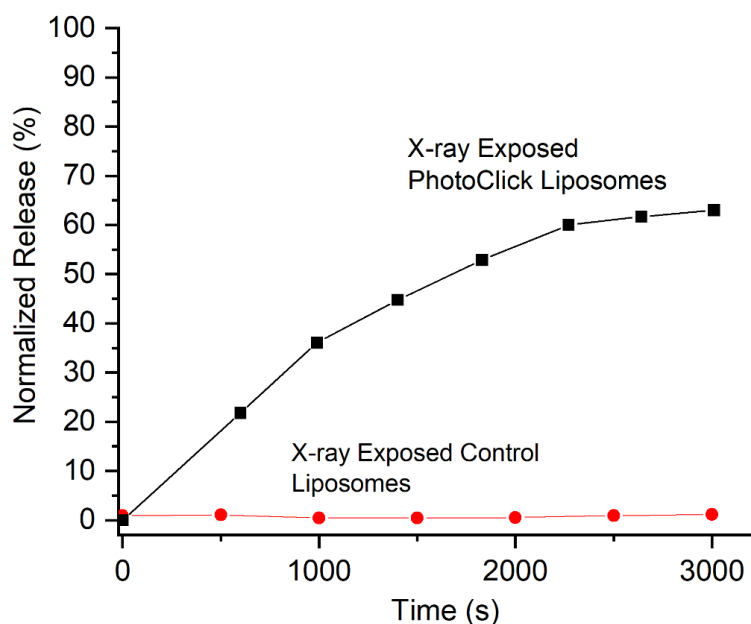


**Figure 13.** Normalized release percent of CAL from PhotoClick liposomes in X-ray. Comparatively, liposomes lacking PhotoClick components showed negligible release over the time span measurements were taken. 100% release was achieved by treating Photoclick liposomes with Triton X-100.

#### DOX Release from PhotoClick Liposomes After X-ray Exposure

Next, we focused on investigating the release of DOX from PhotoClick liposomes. 400 nm Stealth liposomes were prepared by extrusion in an acidic environment based on the citrate buffer. The first buffer exchange with a neutral buffer (pH 7.2) was performed by overnight cassette dialysis. Liposomes were actively loaded with DOX by adding the drug to the bulk solution at 125  $\mu\text{M}$  final concentration after the buffer exchange. The active loading procedure lasted for four days, after which the non-incorporated DOX was removed by overnight cassette dialysis against 2 L of drug-free buffer (pH 7.2).

The experiment for X-ray controlled drug release comprised exposure to radiation of 100  $\mu\text{L}$  PhotoClick liposomes in 1.2 mL buffer (Y in Figure 29). The 100% release

efficacy was determined from PhotoClick liposomes treated with 100  $\mu$ L of 5% v/v Triton X-100 (Z in Figure 29). A background control consisted of PhotoClick liposomes not exposed to ionizing radiation (X in Figure 29). The fluorescence of DOX released from liposomes was determined for all samples and controls approximately six minutes after completing the irradiation. The control background sample (PhotoClick liposomes, no exposure) did not show any substantial release of DOX at rest. In contrast, the exposed PhotoClick liposomes showed a sustained leakage, as indicated by the large fluorescence signal recorded after exposure. Compared with the 100% release efficacy realized by Triton X-100 treatment of the liposomes, around 50 % of the incorporated DOX was released from the PhotoClick liposomes in less than 10 minutes (Figure 29).

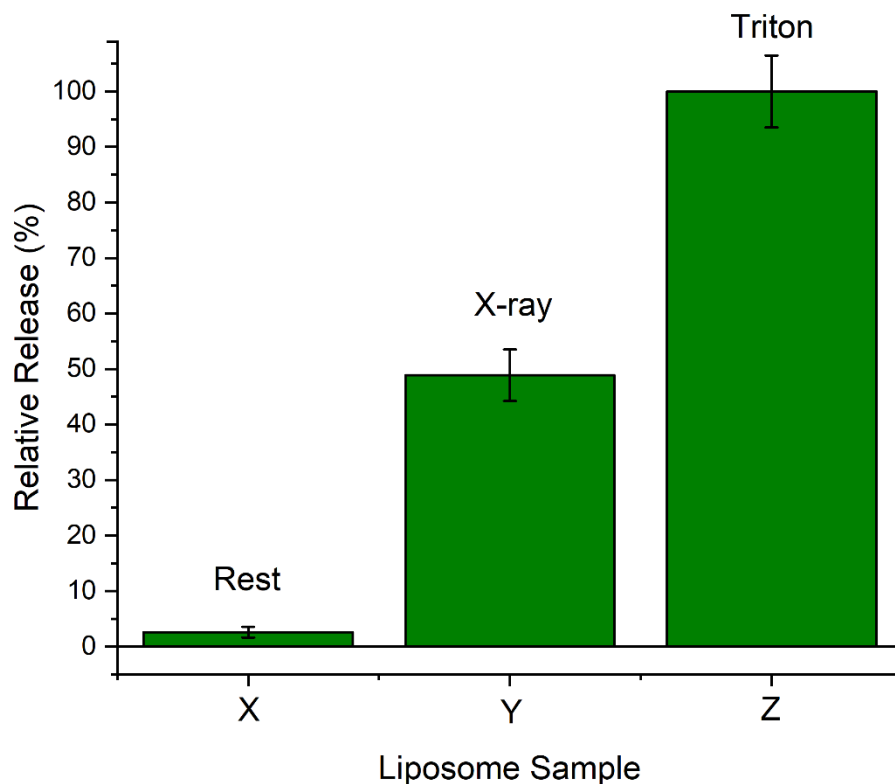


**Figure 14. X-ray induced release of DOX from PhotoClick liposomes. Relative release percent intensity of non-irradiated PhotoClick liposomes loaded with DOX (X), irradiated PhotoClick liposomes loaded with DOX (Y), and PhotoClick liposomes loaded with DOX and treated with Triton X-100 (Z) (100% release).  $p < 0.01$  between Y and X (n = 3).**

#### CIS Release Upon X-ray Exposure

Another frequently used anticancer drug, CIS, was also investigated by using the PhotoClick liposomes. Since CIS does not present fluorescent properties, analysis of CIS release comprised absorbance measurements [59-61]. Prior to analysis of release, a standard curve was created to determine the absorbance behavior of CIS in relation to concentration (Figure 30). The CIS standard curve shows that CIS concentration may be accurately determined with a spectrometer, although it was not utilized to quantify the

release efficacy in an absolute manner since the total inner volume of the liposomes in the samples is not known.

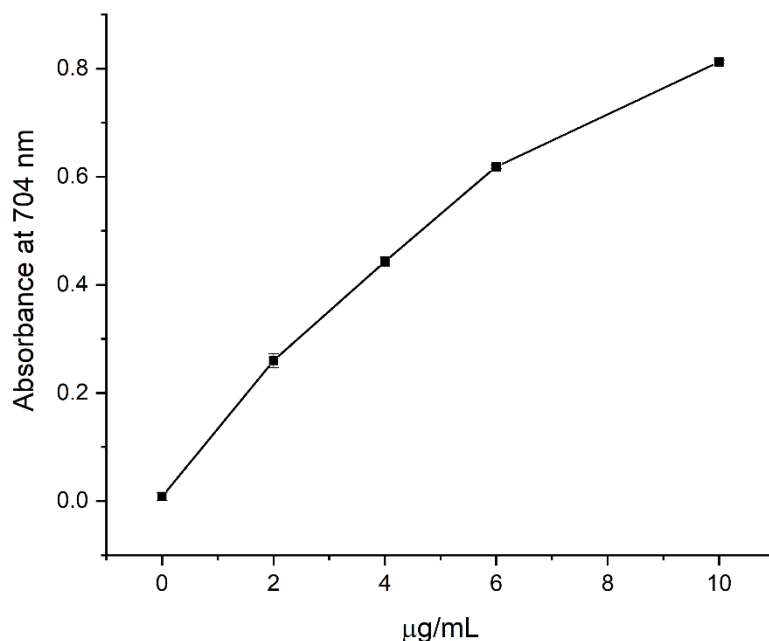


**Figure 15.** A standard curve for CIS is established by measuring the absorbance of the colorimetric product at 704 nm (n = 3).

After the concentration standard curve for CIS was established, an analysis was made regarding the relative release of CIS from PhotoClick liposomes. The comparison was done relative to the absorption data with the maximum release (100%) achieved upon treatment with 50 µL of 5% v/v Triton X-100 of the same PhotoClick liposomes. All samples were prepared by mixing 100 µL of dialysis-purified liposomes loaded with 0.1 mg/mL CIS with 0.9 mL buffered electrolyte (135 mM KCl, 20 mM HEPES, pH 7.2). A non-PhotoClick control and PhotoClick liposomes were irradiated with .125 MeV X-ray. As an additional control, a sample of PhotoClick liposomes was also rested. 140 minutes after treatment, all the liposome mixtures were centrifuged at 4 °C and 20,000

RPM (Labnet Hermle zk36, rotor #19), filtered through 22 nm Whatman filters, and the filtrate was incubated in OPDA/ DMF in sealed vials as described in the Materials and Methods section. After allowing contents to cool to room temperature, absorbance was measured, and the relative release efficacy estimated (Figure 31).

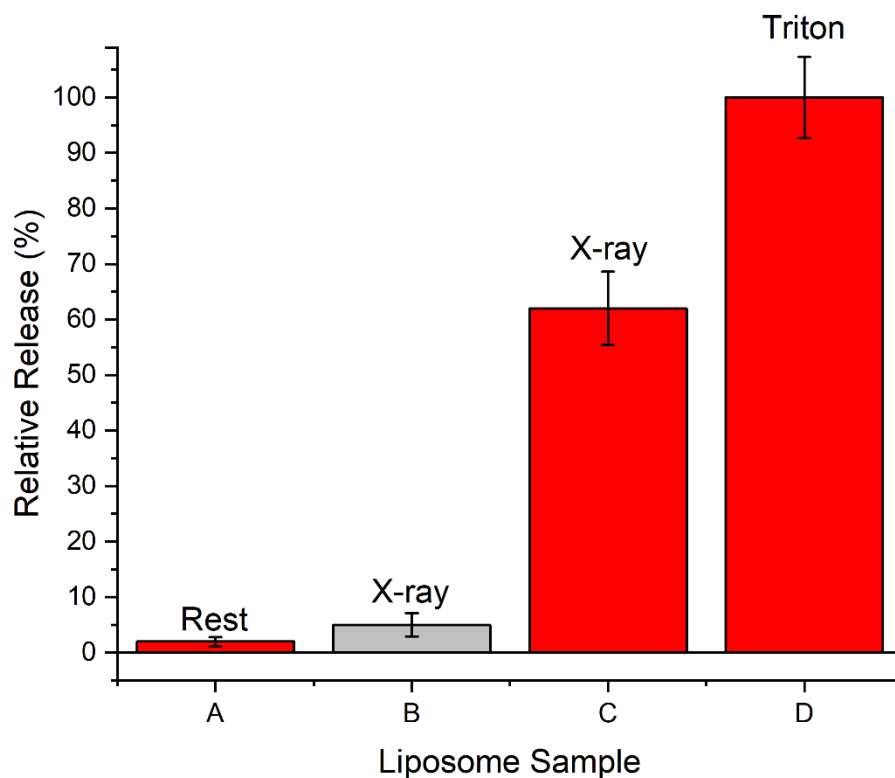


**Figure 16. CIS release upon X-ray exposure of PhotoClick liposomes. PhotoClick liposomes loaded with CIS at rest (A), irradiated control liposomes loaded with CIS (B), irradiated PhotoClick liposomes loaded with CIS (C), and PhotoClick liposomes loaded with CIS and treated with Triton X-100 (D) (100% release).  $p < 0.01$  between C and A as well as C and B ( $n = 3$ ).**

As Figure 31 shows, both controls indicate negligible CIS release; this is indicative of the requirement of X-ray for PhotoClick liposomes to present an increased membrane permeability, as well as stability of non-irradiated PhotoClick liposomes. Within the indicated time frame, approximately 60% of the incorporated CIS was

released from PhotoClick liposomes following irradiation (C) as compared to the same composition liposomes released by Triton X-100 (D). The non-irradiated PhotoClick liposomes (A) showed a great stability, and negligible amounts of the incorporated drug was released at rest. The irradiated control liposomes (containing no PhotoClick components, B) also showed satisfactory stability upon irradiation, with negligible amounts of the drug released within the same time frame, yet slightly more than the rested PhotoClick liposomes. A reasonable explanation of this slightly reduced stability may be provided by considering oxidation and radiolysis processes induced by the exposure to ionizing radiation of this particular composition.

#### Controlled Release From pH-Sensitive Liposomes

pH-sensitive liposomes have long been envisioned as appropriate carriers for delivery of cargo under controlled conditions [19, 38, 71]. As the name suggests, pH-sensitive liposomes undergo modulation of their membrane's permeability as a function of pH. Such changes are readily achievable in vitro, when pH adjustment may be produced by simple addition of proton donors or acceptors to the bulk; in this case, the only stringent requirement is for the target pH not to diminish the chemical reactivity or biological activity of the cargo molecules. However, for the purpose of drug delivery pH modulation in vivo is not an easy task. Since their inception, pH-sensitive liposomes have been considered ideal vehicles for cancer therapy since evidence points towards an acidic pH in the tumor microenvironment. Unfortunately, this varies between large values, it is not predictable, and many times the acidification is very small [72, 73]. Nonetheless, organic halogens provide the opportunity to locally control the pH by utilizing the sustained proton release upon exposure to ionizing irradiation [48, 50, 51]. We exploited

this feature and produced pH-sensitive liposomes, which were further exposed to ionizing radiation (X-ray) to initiate drug delivery.

Based on one of the many recipes presented in literature [38], we produced 400 nm pH-sensitive liposomes composed of DSPC, PE, Chol, OA, and DSPE-PEG at mass ratios of 10:3.3:1.2:0.7:2.1. The liposome sample intended for exposure to X-ray was hydrated with 150 mM bromal hydrate (brought to pH 7.2 with NaOH) and 3 mM CAL. A different compositional mixture, non-pH-sensitive (DSPC: Chol: DSPE-PEG, mass ratio of 10:1.2:2.1) hydrated with 135 mM KCl (pH 7.2) and 3 mM CAL was used as an X-ray exposed control. An additional test sample utilized for testing the drug release upon external exposure to an acidic pH had identical pH-sensitive composition but was hydrated with 135 mM KCl (pH 7.2) and 3 mM CAL. Upon production, all liposome samples were purified by cassette dialysis.

The first test involved investigating the release of dye from the pH sensitive test liposomes upon acidification of the external bulk by HCl addition. When the external pH was changed from 7.2 to 6.44, a sudden increase in the fluorescence signal of CAL was recorded (Figure 32), indicative of CAL leakage from the pH sensitive liposomes. The release of the dye was relatively slow, which is characteristic to pH-sensitive liposomes. Nonetheless, external change of the pH led to the release of approximately 75% of the incorporated dye (based on comparison with Triton X-100 induced release) in less than one hour.

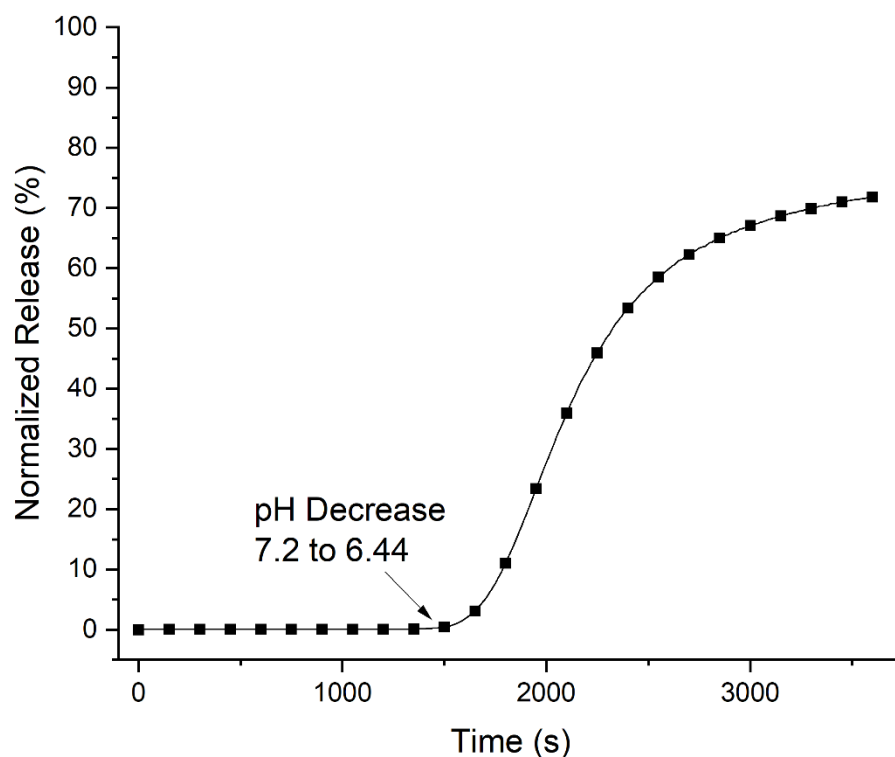


**Figure 17. CAL release from pH sensitive liposomes. External pH was reduced from 7.2 to 6.44 by addition of dilute HCL. Percent release is normalized to an identical liposome sample treated with Triton X-100**

Once our investigations indicated that the dye may be released upon acidification. We exposed the pH-sensitive liposomes filled with BH to X-ray (0.125 MeV); the control (not pH-sensitive) was simultaneously exposed to identical conditions. Another sample with PhotoClick liposomes, not exposed to X-ray, was utilized as leakage indicator at rest; the fluorescence spectra of all samples were recorded after four hours (Figure 33). A non-exposed sample presented a high fluorescent signal after membrane solubilization with 50  $\mu$ L of 5% v/v Triton X-100 (#4, 100% release efficacy); an identical non-exposed sample showed negligible fluorescence in the absence of membrane solubilization (#1). The non-pH sensitive liposomes also showed negligible release upon exposure to X-ray

(#2). However, the pH-sensitive liposomes exposed to X-ray showed over 50% release, indicative of sustained dye leakage (#3).

The only reasonable explanation for the increased release upon X-ray exposure is that irradiation of the BH solution led to a massive release of protons [48-56]. which acidified the intraliposomal space. Upon acidification, the membrane composed of pH-sensitive lipids underwent an increase in permeability; this leakage reduced the dye concentration, which led to the observed increase in fluorescence.

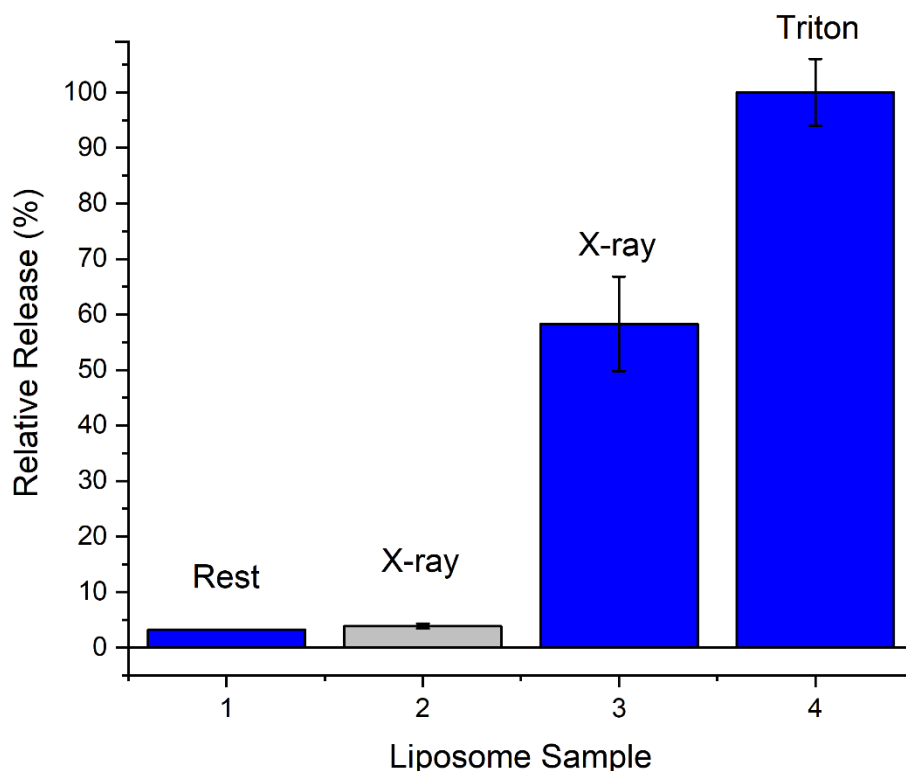


**Figure 33.** Relative release of CAL fluorescence intensity of pH sensitive CAL and BH loaded liposomes. pH sensitive liposomes at rest (1), non-pH sensitive control liposomes loaded with CAL and irradiated with X-ray (2), pH sensitive CAL and BH loaded liposomes irradiated with X-ray (3), pH sensitive CAL and BH loaded liposomes treated with Triton X-100 (4).  $p < 0.01$  between 3 and 1 as well as 3 and 2 ( $n = 3$ ).

## Conclusions

Our investigations led to the conclusion that liposomes may be tailored to release their payload in a controllable fashion and by using ionizing radiation as a triggering mechanism. The two modalities of controlled drug release presented here rely on direct and indirect adjustments of the membrane permeability upon X-ray exposure. For the PhotoClick liposomes, specific components in the membrane undergo covalent bonding, which translates into reduced fluidity and increased permeability. The intimate mechanisms by which such changes occur under exposure to ionizing radiation are still obscure. PhotoClick components are designed to interact directly with UV photons [23, 74] which have a much lower energy than X-ray. Likewise, it has been documented that photopolymerizable lipids also interact with UV light when included into liposome membranes, rendering the vesicular structures responsive to X-ray [30]. However, it is not clear if initiation of polymerization is a consequence of direct interaction with high energy photons or through indirect radiolysis products. Nonetheless, an important conclusion from this prior work relates to the important role presented by lipid separation into domains. Our work exploits this important feature by including components known to segregate into lipid rafts (i.e., SM, and Chol [25, 67]), which apparently promote covalent bonding between neighboring molecules without the need of other transmembrane components. The investigations do not provide any indication if the cargo is either released through the segregated domain or around it; such investigations may be initiated by determining the permeability changes in response to radiation by adjusting the size of the lipid rafts to maximize either their surface area or perimeter while maintaining a satisfactory stability of the liposomes at rest.

As an alternative to PhotoClick liposomes, cargo release from pH sensitive liposomes is well documented in literature, and many compositions responsive to pH changes for a relatively large range of pHs have been reported [47]. However, our investigations focused on controlling the release by adjusting the internal pH via proton release from organic halogen solutions exposed to ionizing radiation [48-56], which provides opportunities for real control over release upon external stimulation. This is not a common feature of other release mechanisms, which rather rely on potential physiological pH variations at the site to achieve drug delivery [18, 71].

Both approaches presented here show that drug release can be initiated by utilizing liposomes specially designed to respond to X-ray and adjust the membrane permeability through direct and indirect interactions with the ionizing radiation. However, technical limitations restricted our investigations to only relatively low X-ray energies. While this may be an option for controlled drug delivery without added radiotoxicity, modern tumor treatment by radiotherapy usually employs much larger energies. We anticipate that a larger energy would accelerate the release of drugs from pH sensitive liposomes filled with organic halogens since the pH changes monotonically follow the energy and dose in the MeV range [53, 56]. Nonetheless, we do not know the behavior of PhotoClick components at large energies. If the covalent bonding is an indirect effect of radiolysis products, we anticipate that higher energies leading to a more sustained radiolysis will accelerate the release rate. However, if the direct hit is chiefly responsible for initiating covalent bonding, insufficient stopping power may prevent covalent bonding and effective membrane permeabilization at high energies; this could

be prevented by radiation fractionation in terms of both energy and dose during treatment.

Finally, we showed that X-ray radiation may be used to trigger drug release from specially designed liposomes by changes in the membrane permeability induced by two different mechanisms. Such approaches pave the way for achieving simultaneous and highly localized chemo and radiotherapy, which is postulated to significantly improve the clinical outcome of cancer therapy by reducing the systemic effects of classical chemotherapy, enabling achievement of higher drug concentrations only at the diseased site, and benefiting from the supra-additive effects of the combined therapy approach.

## References

1. Barenholz, Y., Liposome application: problems and prospects. *Current Opinion in Colloid & Interface Science* **2001**, 6 (1), 66-77.
2. Bozzuto, G.; Molinari, A., Liposomes as nanomedical devices. *International journal of nanomedicine* **2015**, 10, 975-999.
3. Eroğlu, İ.; İbrahim, M., Liposome–ligand conjugates: a review on the current state of art. *Journal of Drug Targeting* **2020**, 28 (3), 225-244.
4. Jensen, G. M.; Hodgson, D. F., Opportunities and challenges in commercial pharmaceutical liposome applications. *Advanced Drug Delivery Reviews* **2020**, 154-155, 2-12.
5. Xing, H.; Hwang, K.; Lu, Y., Recent Developments of Liposomes as Nanocarriers for Theranostic Applications. *Theranostics* **2016**, 6 (9), 1336-1352.
6. Brown, S.; Khan, D. R., The treatment of breast cancer using liposome technology. *Journal of drug delivery* **2012**, 2012, 212965-212965.
7. Mathiyazhakan, M.; Wiraja, C.; Xu, C., A Concise Review of Gold Nanoparticles-Based Photo-Responsive Liposomes for Controlled Drug Delivery. *Nano-Micro Letters* **2017**, 10 (1), 10.
8. Chen, J.; He, C.-q.; Lin, A.-h.; Gu, W.; Chen, Z.-p.; Li, W.; Cai, B.-c., Thermosensitive liposomes with higher phase transition temperature for targeted drug delivery to tumor. *International Journal of Pharmaceutics* **2014**, 475 (1), 408-415.
9. Kono, K.; Nakashima, S.; Kokuryo, D.; Aoki, I.; Shimomoto, H.; Aoshima, S.; Maruyama, K.; Yuba, E.; Kojima, C.; Harada, A.; Ishizaka, Y., Multi-functional liposomes having temperature-triggered release and magnetic resonance imaging for tumor-specific chemotherapy. *Biomaterials* **2011**, 32 (5), 1387-1395.
10. Mueller, A.; Bondurant, B.; O'Brien, D. F., Visible-Light-Stimulated Destabilization of PEG-Liposomes. *Macromolecules* **2000**, 33 (13), 4799-4804.

11. Yavlovich, A.; Singh, A.; Blumenthal, R.; Puri, A., A novel class of photo-triggerable liposomes containing DPPC:DC8,9PC as vehicles for delivery of doxorubicin to cells. *Biochimica et Biophysica Acta (BBA) - Biomembranes* **2011**, *1808* (1), 117-126.
12. Evjen, T. J.; Nilssen, E. A.; Røgnvaldsson, S.; Brandl, M.; Fossheim, S. L., Distearoylphosphatidylethanolamine-based liposomes for ultrasound-mediated drug delivery. *European Journal of Pharmaceutics and Biopharmaceutics* **2010**, *75* (3), 327-333.
13. Schroeder, A.; Honen, R.; Turjeman, K.; Gabizon, A.; Kost, J.; Barenholz, Y., Ultrasound triggered release of cisplatin from liposomes in murine tumors. *Journal of Controlled Release* **2009**, *137* (1), 63-68.
14. Yang, Y.; Yang, X.; Li, H.; Li, C.; Ding, H.; Zhang, M.; Guo, Y.; Sun, M., Near-infrared light triggered liposomes combining photodynamic and chemotherapy for synergistic breast tumor therapy. *Colloids and Surfaces B: Biointerfaces* **2019**, *173*, 564-570.
15. Amstad, E.; Kohlbrecher, J.; Müller, E.; Schweizer, T.; Textor, M.; Reimhult, E., Triggered Release from Liposomes through Magnetic Actuation of Iron Oxide Nanoparticle Containing Membranes. *Nano Letters* **2011**, *11* (4), 1664-1670.
16. Béalle, G.; Di Corato, R.; Kolosnjaj-Tabi, J.; Dupuis, V.; Clément, O.; Gazeau, F.; Wilhelm, C.; Ménager, C., Ultra Magnetic Liposomes for MR Imaging, Targeting, and Hyperthermia. *Langmuir* **2012**, *28* (32), 11834-11842.
17. Vlasova, K. Y.; Piroyan, A.; Le-Deygen, I. M.; Vishwasrao, H. M.; Ramsey, J. D.; Klyachko, N. L.; Golovin, Y. I.; Rudakovskaya, P. G.; Kireev, I. I.; Kabanov, A. V.; Sokolsky-Papkov, M., Magnetic liposome design for drug release systems responsive to super-low frequency alternating current magnetic field (AC MF). *Journal of Colloid and Interface Science* **2019**, *552*, 689-700.
18. Fan, Y.; Chen, C.; Huang, Y.; Zhang, F.; Lin, G., Study of the pH-sensitive mechanism of tumor-targeting liposomes. *Colloids and Surfaces B: Biointerfaces* **2017**, *151*, 19-25.

19. Paliwal, S. R.; Paliwal, R.; Vyas, S. P., A review of mechanistic insight and application of pH-sensitive liposomes in drug delivery. *Drug Delivery* **2015**, *22* (3), 231-242.
20. Wang, J.-Y.; Wu, Q.-F.; Li, J.-P.; Ren, Q.-S.; Wang, Y.-L.; Liu, X.-M., Photo-sensitive liposomes: chemistry and application in drug delivery. *Mini reviews in medicinal chemistry* **2010**, *10* (2), 172-181.
21. Chen, W.; Goldys, E. M.; Deng, W., Light-induced liposomes for cancer therapeutics. *Progress in Lipid Research* **2020**, *79*, 101052.
22. Punnamaraju, S.; You, H.; Steckl, A. J., Triggered release of molecules across droplet interface bilayer lipid membranes using photopolymerizable lipids. *Langmuir* **2012**, *28* (20), 7657-64.
23. Haberkant, P.; Stein, F.; Höglinger, D.; Gerl, M. J.; Brügger, B.; Van Veldhoven, P. P.; Krijgsveld, J.; Gavin, A. C.; Schultz, C., Bifunctional Sphingosine for Cell-Based Analysis of Protein-Sphingolipid Interactions. *ACS Chem Biol* **2016**, *11* (1), 222-30.
24. Gomes, A. F.; Gozzo, F. C., Chemical cross-linking with a diazirine photoactivatable cross-linker investigated by MALDI- and ESI-MS/MS. *J Mass Spectrom* **2010**, *45* (8), 892-9.
25. D'Aprile, C.; Prioni, S.; Mauri, L.; Prinetti, A.; Grassi, S., Lipid rafts as platforms for sphingosine 1-phosphate metabolism and signalling. *Cellular Signalling* **2021**, *80*, 109929.
26. Lingwood, D.; Simons, K., Lipid Rafts As a Membrane-Organizing Principle. *Science* **2010**, *327* (5961), 46.
27. Lawrence, J. C.; Saslowsky, D. E.; Michael Edwardson, J.; Henderson, R. M., Real-Time Analysis of the Effects of Cholesterol on Lipid Raft Behavior Using Atomic Force Microscopy. *Biophysical Journal* **2003**, *84* (3), 1827-1832.

28. Ando, J.; Kinoshita, M.; Cui, J.; Yamakoshi, H.; Dodo, K.; Fujita, K.; Murata, M.; Sodeoka, M., Sphingomyelin distribution in lipid rafts of artificial monolayer membranes visualized by Raman microscopy. *Proceedings of the National Academy of Sciences* **2015**, *112* (15), 4558.
29. Puri, A., Phototriggerable Liposomes: Current Research and Future Perspectives. *Pharmaceutics* **2014**, *6* (1).
30. O'Brien, D.; McGovern, K.; Bondurant, B.; Sutherland, R. Radiation sensitive liposomes. 2002.
31. Lock, M. I.; Hoyer, M.; Bydder, S. A.; Okunieff, P.; Hahn, C. A.; Vichare, A.; Dawson, L. A., An international survey on liver metastases radiotherapy. *Acta Oncol* **2012**, *51* (5), 568-74.
32. Kalogeridi, M.-A.; Zygogianni, A.; Kyrgias, G.; Kouvaris, J.; Chatziioannou, S.; Kelekis, N.; Kouloulis, V., Role of radiotherapy in the management of hepatocellular carcinoma: A systematic review. *World journal of hepatology* **2015**, *7* (1), 101-112.
33. Green, J.; Kirwan J Fau - Tierney, J.; Tierney J Fau - Vale, C.; Vale C Fau - Symonds, P.; Symonds P Fau - Fresco, L.; Fresco L Fau - Williams, C.; Williams C Fau - Collingwood, M.; Collingwood, M., Concomitant chemotherapy and radiation therapy for cancer of the uterine cervix. *Cochrane Database of Systematic Reviews* **2001**, (1469-493X (Electronic)).
34. Lambert, B.; De Ridder, L.; Slegers, G.; De Gelder, V.; Dierckx, R. A.; Thierens, H., Screening for supra-additive effects of cytotoxic drugs and gamma irradiation in an in vitro model for hepatocellular carcinoma. *Can J Physiol Pharmacol* **2004**, *82* (2), 146-52.
35. Seiwert, T. Y.; Salama, J. K.; Vokes, E. E., The concurrent chemoradiation paradigm--general principles. *Nat Clin Pract Oncol* **2007**, *4* (2), 86-100.
36. Eberhardt, W.; Pöttgen, C.; Stuschke, M., Chemoradiation paradigm for the treatment of lung cancer. *Nature Clinical Practice Oncology* **2006**, *3* (4), 188-199.

37. Vokes, E. E.; Kies, M. S.; Haraf, D. J.; Stenson, K.; List, M.; Humerickhouse, R.; Dolan, M. E.; Pelzer, H.; Sulzen, L.; Witt, M. E.; Hsieh, Y.-C.; Mittal, B. B.; Weichselbaum, R. R., Concomitant Chemoradiotherapy as Primary Therapy for Locoregionally Advanced Head and Neck Cancer. *Journal of Clinical Oncology* **2000**, *18* (8), 1652-1661.
38. Hazemoto, N.; Harada, M.; Komatsubara, N.; Haga, M.; Kato, Y., pH-Sensitive Liposomes Composed of Phosphatidylethanolamine and Fatty Acid. *Chem. Pharm. Bull.* **1990**, *38* (3), 748-751.
39. Kitano, H.; Akatsuka, Y.; Ise, N., pH-responsive liposomes which contain amphiphiles prepared by using lipophilic radical initiator. *Macromolecules* **1991**, *24* (1), 42-46.
40. Slepushkin, V. A.; Simoes, S.; Dazin, P.; Newman, M. S.; Guo, L. S.; Pedroso de Lima, M. C.; Duzgunes, N., Sterically Stabilized pH-sensitive Liposomes. *The Journal of Biological Chemistry* **1997**, *272* (4), 2382-2388.
41. Lee, R. L.; Wang, S.; Turk, M. J.; Low, P. S., The Effects of pH and Intraliposomal Buffer Strength on the Rate of Liposome Content Release and Intracellular Drug Delivery. *Bioscience Reports* **1998**, *18* (2), 69-78.
42. Hafez, I. M.; Ansell, S.; Cullis, P. R., Tunable pH-Sensitive Liposomes Composed of Mixtures of Cationic and Anionic Lipids. *Biophysical Journal* **2000**, *79*, 1438-1446.
43. Mohamed, M.; Abu Lila, A. S.; Shimizu, T.; Alaaeldin, E.; Hussein, A.; Sarhan, H. A.; Szebeni, J.; Ishida, T., PEGylated liposomes: immunological responses. *Science and Technology of Advanced Materials* **2019**, *20* (1), 710-724.
44. Immordino, M. L.; Dosio, F.; Cattel, L., Stealth liposomes: review of the basic science, rationale, and clinical applications, existing and potential. *International journal of nanomedicine* **2006**, *1* (3), 297-315.
45. Ngoune, R.; Peters, A.; von Elverfeldt, D.; Winkler, K.; Pütz, G., Accumulating nanoparticles by EPR: A route of no return. *Journal of Controlled Release* **2016**, *238*, 58-70.

46. Maeda, H.; Wu, J.; Sawa, T.; Matsumura, Y.; Hori, K., Tumor vascular permeability and the EPR effect in macromolecular therapeutics: a review. *Journal of Controlled Release* **2000**, *65* (1), 271-284.
47. Hashim, A. I.; Zhang, X.; Wojtkowiak, J. W.; Martinez, G. V.; Gillies, R. J., Imaging pH and metastasis. *NMR in Biomedicine* **2011**, *24* (6), 582-591.
48. Andrews, H. L.; Shore, P. A., X-ray Dose Determinations with Chloral Hydrate. *The Journal of Chemical Physics* **1950**, *18* (9), 1165-1168.
49. Freeman, G. R.; Van Cleave, A. B.; Spinks, J. W., Irradiation of Aqueous Chloral Hydrate Solutions with Co<sup>60</sup> Gamma-Rays. *Canadian Journal of Chemistry* **1953**, *32*, 322-326.
50. Freeman, G. R.; Van Cleave, A. B.; Spinks, J. W., Irradiation of One Molar Aqueous Chloral Hydrate Solution with Co<sup>60</sup>-Gamma-Rays and Betatron X Rays. *Canadian Journal of Chemistry* **1953**, *31*, 1164-1172.
51. Andrews, H. L.; Murphy, R. E.; LeBrun, E., Gel Dosimeter for Depth-Dose Measurements. *The Review of Scientific Instruments* **1957**, *28* (5), 329-332.
52. Woods, R. J.; Spinks, J. W., The Action of Co<sup>60</sup> Gamma Rays and of Fenton Reagent on Aqueous Bromal Hydrate Solutions. *Canadian Journal of Chemistry* **1957**, *35*, 1475-1486.
53. Heusinger, H.; Woods, R. J.; Spinks, J. W., Study of the Radiolysis of Bromal Hydrate Solutions Using C<sup>14</sup>-labelled Bromal. *Canadian Journal of Chemistry* **1959**, *37* (7), 1127-1131.
54. Platford, R. F.; Spinks, J. W., Irradiation of Aqueous Chloral Hydrate With Sr<sup>90</sup>-Yr<sup>90</sup> Beta Rays. *Canadian Journal of Chemistry* **1959**, *37*, 1022-1028.
55. Hilsenrod, A., Irradiation of Chloral Hydrate Solutions. *Journal of Chemical Physics* **1956**, *24*, 917-918.
56. Woods, R. J.; Spinks, J. W., The Radiolysis of Some Organic Halogen Compounds in Aqueous Solution. *Canadian Journal of Chemistry* **1960**, *38*, 77-93.

57. Odeh, F.; Ismail, S. I.; Abu-Dahab, R.; Mahmoud, I. S.; Al Bawab, A., Thymoquinone in liposomes: a study of loading efficiency and biological activity towards breast cancer. *Drug Delivery* **2012**, *19* (8), 371-377.
58. Simonsen, J. B., A liposome-based size calibration method for measuring microvesicles by flow cytometry. *Journal of Thrombosis and Haemostasis* **2016**, *14* (1), 186-190.
59. Olson, F.; Hunt, C. A.; Szoka, F. C.; Vail, W. J.; Papahadjopoulos, D., Preparation of liposomes of defined size distribution by extrusion through polycarbonate membranes. *Biochimica et Biophysica Acta (BBA) - Biomembranes* **1979**, *557* (1), 9-23.
60. Lattin, J. R.; Pitt, W. G.; Belnap, D. M.; Hussein, G. A., Ultrasound-Induced Calcein Release From eLiposomes. *Ultrasound in Medicine & Biology* **2012**, *38* (12), 2163-2173.
61. Anilamert, B.; Yalcin, G.; Ariozz, F.; Dolen, E., THE Spectrophotometric Determination of Cisplatin in Urine, Using o-Phenylenediamine as Derivatizing Agent. *Analytical Letters* **2001**, *34* (1), 113-123.
62. Basotra, M.; Singh, S. K.; Gulati, M., Development and Validation of a Simple and Sensitive Spectrometric Method for Estimation of Cisplatin Hydrochloride in Tablet Dosage Forms: Application to Dissolution Studies. *ISRN Analytical Chemistry* **2013**, *2013*, 8.
63. Raut, I. D.; Doijad, R. C.; Mohite, S. K.; Manjappa, A. S., Preparation and Characterization of Solid Lipid Nanoparticles Loaded with Cisplatin. *Journal of Drug Delivery and Therapeutics (JDDT)* **2018**, *8* (6), 125-131.
64. Özlem Ögün, Ç.; Vasif, H., UV-induced drug release from photoactive REV sensitized by suprofen. *Journal of controlled release* **2004**, *96* (1), 85-96.
65. Hamann, S.; Kiilgaard, J. F.; Litman, T.; Alvarez-Leefmans, F. J.; Winther, B. R.; Zeuthen, T., Measurement of Cell Volume Changes by Fluorescence Self-Quenching. *Journal of Fluorescence* **2002**, *12* (2), 139-145.

66. Jayaraman, S.; Song, Y.; Verkman, A. S., Airway Surface Liquid Osmolality Measured Using Fluorophore-Encapsulated Liposomes. *Journal of General Physiology* **2001**, *117* (5), 423-430.
67. Levental, I., Lipid rafts come of age. *Nature Reviews Molecular Cell Biology* **2020**, *21* (8), 420-420.
68. Yang, L.; Kindt, J. T., Line Tension Assists Membrane Permeation at the Transition Temperature in Mixed-Phase Lipid Bilayers. *Journal of Physical Chemistry B* **2016**, *120* (45), 11740-11750.
69. Cooper, J. S.; Ang, K. K., Concomitant chemotherapy and radiation therapy certainly improves local control. *International journal of radiation oncology, biology, physics* **2005**, *61* (1), 7-9.
70. Chronowski, G. M.; Wilder, R. B.; Tucker, S. L.; Ha, C. S.; Younes, A.; Fayad, L.; Rodriguez, M. A.; Hagemester, F. B.; Barista, I.; Cabanillas, F.; Cox, J. D., Analysis of in-field control and late toxicity for adults with early-stage Hodgkin's disease treated with chemotherapy followed by radiotherapy. *Int J Radiat Oncol Biol Phys* **2003**, *55* (1), 36-43.
71. Abri Aghdam, M.; Bagheri, R.; Mosafer, J.; Baradaran, B.; Hashemzaei, M.; Baghbanzadeh, A.; de la Guardia, M.; Mokhtarzadeh, A., Recent advances on thermosensitive and pH-sensitive liposomes employed in controlled release. *Journal of Controlled Release* **2019**, *315*, 1-22.
72. Estrella, V.; Chen, T.; Lloyd, M.; Wojtkowiak, J.; Cornnell, H. H.; Ibrahim-Hashim, A.; Bailey, K.; Balagurunathan, Y.; Rothberg, J. M.; Sloane, B. F.; Johnson, J.; Gatenby, R. A.; Gillies, R. J., Acidity Generated by the Tumor Microenvironment Drives Local Invasion. *Cancer Research* **2013**, *73* (5), 1524.
73. Boedtkjer, E.; Pedersen, S. F., The Acidic Tumor Microenvironment as a Driver of Cancer. *Annual Review of Physiology* **2020**, *82* (1), 103-126.
74. Hulce, J. J.; Coggnetta, A. B.; Niphakis, M. J.; Tully, S. E.; Cravatt, B. F., Proteome-wide mapping of cholesterol-interacting proteins in mammalian cells. *Nature Methods* **2013**, *10* (3), 259-26

## CHAPTER FIVE: CONCLUSIONS AND PERSPECTIVES

Through the span of the previous chapters, we caught a small glimpse of the vast and intricate world of liposomes. The long-revered concept of spherical bilayers made of phospholipids is relatively simple and straightforward. They found applicability in science, biotechnology, medicine, and other fields. Continuous advancements and progress have been the result of the investigations scientists have made looking into developing novel means for their production, as well as finding scientific or medical applications difficult to achieve by utilizing alternative approaches and practices. In this respect, the focus of this dissertation pertains to better understanding their production and providing potential improvements for their application as drug carriers.

Having been a keen topic of research since their discovery in the 60's, initial interest chiefly resided in their formation and production [1]. The realization that they could be used as drug carriers in the following decades only increased interest in them, ranging from their production, to formation, to composition. The basic requirements for drug carriers include retaining and protecting the drugs, evading the immune system of the host, targeting the desired organ or tissue, and releasing the drug in a controlled manner. Liposomes satisfy many of these needs [2, 3]. The protective membrane encases a water-filled cavity that can be passively or actively loaded with hydrophilic drugs and molecules of interest. In addition, hydrophobic drugs and molecules may be included in the hydrophobic core of the phospholipid membrane, therefore liposomes present a great versatility with respect to their ability to retain and protect various cargos of interest, as

well as transporting them to a desired location within the host. The ability to functionalize their surface by bioconjugation endows liposomes with endless targeting capabilities, which is essential for avoiding a systemic release of the bioactive cargo. This feature is crucial for the release of antineoplastic drugs used for the treatment of solid tumors. In the case of small liposomes (diameters below 200 nm), they self-accumulate into tumors via the EPR effect [4-6]. The added ability to avoid immune detection by PEGylation made liposomes particularly appealing for use as chemotherapeutic carriers [7]. These attributes are essential in making them available on the pharmaceutical market and as an FDA approved treatment option for cancer [8]. Although triggered release methods for liposomal content are being considered and undergoing greater exploration to enhance their usefulness, use in a clinical setting is still in the early stages of clinical research and years from final approval.

Our initial explorations investigated liposome production by hydration, sonication, and extrusion. Early assessment investigated size and distribution using DLS and microscopy, with comparison between liposomes of regular (asolectin and cholesterol) and PEGylated (DSPC, DSPE-PEG, and cholesterol) membrane composition. Furthermore, liposomes were prepared and loaded using both passive and active methods. Finally, we established that containment and release of both actively and passively loaded liposomes could be monitored with the use of fluorescent molecules such as CAL, R6G, AO, and DOX. This relied on the fluorescence self-quenching properties of all the molecules used, allowing us to confirm high loading concentrations by inducing release using a non-ionic detergent to solubilize the liposomal membranes, resulting in a significant fluorescence increase resulting from cargo dilution into the bulk.

Next, we delved into the exploration of new methods for the production and purification of liposomes. Traditional approaches require multiple steps which require lengthy periods of waiting, resulting in a lag between initial demand and availability. Knowing that detergent removal is a proven method of liposome formation, we exploited this feature and significantly sped up the process by utilizing ionic detergents which we later removed by using an electrophoretic force. The electrodialysis-driven depletion (EDD) method not only enabled simultaneous production, loading, and purification of, but was also applicable to obtaining long-circulating liposomes. The potential of this technique was further proven by showing comparable size and distribution characteristics of EDD-produced liposomes to those made by extrusion and sonication. Although the procedure is limited to effectively purifying only charged molecules, it allows the rapid production of loaded and purified liposomes from lipid film in a matter of hours from start to finish. With classic approaches, the entire process can take multiple days. In many instances, EDD could allow for same day preparation and experimentation with liposomes, possibly extending into medical applications. The extraordinary potential of this technique must be further investigated to understand the full scope of its capabilities and possibility for modification [9].

As stated earlier, one of the major standing challenges for drug delivery via liposomes is the release of the cargo in a well-controlled manner. In this respect, we proposed and investigated two novel controlled release methods to deliver liposomal contents at will. The first approach exploits the crosslinking properties of photosensitive PhotoClick components upon UV exposure. Not only were we able to confirm membrane permeabilization in liposomes with PhotoClick components under UV irradiation, but we

also showed that PhotoClick component bearing liposomes are similarly responsive to X-ray. In addition, we utilized known increase of membrane permeability of pH sensitive liposomes in combination with loaded radiation-sensitive bromal hydrate (BH) to achieve controlled release. Upon X-ray exposure, the loaded BH decomposed and induced a pH drop, causing permeabilization of pH sensitive membranes and leading to cargo release. The importance of these studies does not only reside in demonstration of the highly localized and controlled capabilities of X-ray driven cargo release from specially formulated liposomes, but also the potential of X-ray to be used as a concomitant treatment with release of chemotherapeutic. The reduced combined toxicity of simultaneous radiation and chemotherapy application made possible by such liposomes could dramatically improve clinical outcomes of cancers treated in this manner due to the suggested synergistic benefits of concomitant radio-chemotherapy treatment [10, 11]. Beyond increasing the effectiveness of treatment, this combination could also allow for overall smaller doses of both chemotherapy and radiation [12].

### **Outlooks and Perspectives**

There is no doubt that the biomedical applications of liposomes will undergo a continuous expansion in the coming years. Promising results have been already achieved for incorporating into liposomes various anticancer drugs such as cisplatin, paclitaxel, and temozolomide, [13-15], which will enable direct clinical applications to cancer for which systemic chemotherapy is currently the only option. Immunotherapy is one of the newest advances in cancer treatment, and we are confident that liposomes will be soon utilized to improve the clinical outcome of such therapies. The ability to use radiation for simultaneous radiotherapy and localized chemotherapy is anticipated to significantly

improve the local and loco-regional control of tumors. Another expected advancement is providing liposomes with targeting and killing capabilities of circulating cancer cells, with direct clinical applicability to metastasis control and treatment [16].

Biomedical applications for liposomes are also not limited as drug carriers. Their versatility has been shown as having potential applications as both therapeutic and diagnostic tools (theranostics) [17]. Furthermore, liposomes have been proposed as antivirulence factors, serving to compete with host cell membranes to absorb toxins. This has been shown to significantly inhibit the lytic activity of toxins [18], which suggests possible use of specially formulated liposomes to mitigate biological activities of virulence factors and contribute to improving the treatment of infectious diseases.

The ever-developing world of liposomal research shall continue to impress us with newer and better applications. Simple, yet versatile, liposomes will further prove their worth and capabilities with the progression of time. Whether it is for medical treatments, diagnostics, fundamental research of membranes, food sciences, or even agriculture, they enhance the capabilities of much that was previously considered impossible, unlikely, and impractical.

### References

1. Bangham, A. D.; Horne, R. W., Negative staining of phospholipids and their structural modification by surface-active agents as observed in the electron microscope. *Journal of Molecular Biology* **1964**, *8* (5), 660-690.
2. Bozzuto, G.; Molinari, A., Liposomes as nanomedical devices. *International journal of nanomedicine* **2015**, *10*, 975-999.
3. Laouini, A.; Jaafar-Maalej, C.; Limayem-Blouza, I.; Sfar, S.; Charcosset, C.; Fessi, H., Preparation, Characterization and Applications of Liposomes: State of the Art. *Journal of Colloid Science and Biotechnology* **2012**, *1* (2), 147-168.
4. Maeda, H.; Wu, J.; Sawa, T.; Matsumura, Y.; Hori, K., Tumor vascular permeability and the EPR effect in macromolecular therapeutics: a review. *Journal of Controlled Release* **2000**, *65* (1), 271-284.
5. Maruyama, K., Intracellular targeting delivery of liposomal drugs to solid tumors based on EPR effects. *Advanced Drug Delivery Reviews* **2011**, *63* (3), 161-169.
6. Ngoune, R.; Peters, A.; von Elverfeldt, D.; Winkler, K.; Pütz, G., Accumulating nanoparticles by EPR: A route of no return. *Journal of Controlled Release* **2016**, *238*, 58-70.
7. Immordino, M. L.; Dosio, F.; Cattel, L., Stealth liposomes: review of the basic science, rationale, and clinical applications, existing and potential. *International journal of nanomedicine* **2006**, *1* (3), 297-315.
8. Barenholz, Y., Doxil®--the first FDA-approved nano-drug: lessons learned. *J Control Release* **2012**, *160* (2), 117-34.
9. Abatchev, G.; Bogard, A.; Hutchinson, Z.; Ward, J.; Fologea, D., Rapid Production and Purification of Dye-Loaded Liposomes by Electrodialysis-Driven Depletion. *Membranes* **2021**, *11* (6).
10. Cooper, J. S.; Ang, K. K., Concomitant chemotherapy and radiation therapy certainly improves local control. In *Int J Radiat Oncol Biol Phys*, United States, 2005; Vol. 61, pp 7-9.

11. Seiwert, T. Y.; Salama, J. K.; Vokes, E. E., The concurrent chemoradiation paradigm--general principles. *Nat Clin Pract Oncol* **2007**, *4* (2), 86-100.
12. Chronowski, G. M.; Wilder, R. B.; Tucker, S. L.; Ha, C. S.; Younes, A.; Fayad, L.; Rodriguez, M. A.; Hagemester, F. B.; Barista, I.; Cabanillas, F.; Cox, J. D., Analysis of in-field control and late toxicity for adults with early-stage Hodgkin's disease treated with chemotherapy followed by radiotherapy. *Int J Radiat Oncol Biol Phys* **2003**, *55* (1), 36-43.
13. Zahednezhad, F.; Zakeri-Milani, P.; Shahbazi Mojarrad, J.; Valizadeh, H., The latest advances of cisplatin liposomal formulations: essentials for preparation and analysis. *Expert Opinion on Drug Delivery* **2020**, *17* (4), 523-541.
14. Huang, S.-T.; Wang, Y.-P.; Chen, Y.-H.; Lin, C.-T.; Li, W.-S.; Wu, H.-C., Liposomal paclitaxel induces fewer hematopoietic and cardiovascular complications than bioequivalent doses of Taxol. *International journal of oncology* **2018**, *53* (3), 1105-1117.
15. Nordling-David, M. M.; Yaffe, R.; Guez, D.; Meirrow, H.; Last, D.; Grad, E.; Salomon, S.; Sharabi, S.; Levi-Kalisman, Y.; Golomb, G.; Mardor, Y., Liposomal temozolomide drug delivery using convection enhanced delivery. *J Control Release* **2017**, *261*, 138-146.
16. Zhang, Z.; King, M. R., Nanomaterials for the Capture and Therapeutic Targeting of Circulating Tumor Cells. *Cell Mol Bioeng* **2017**, *10* (4), 275-294.
17. Xing, H.; Hwang, K.; Lu, Y., Recent Developments of Liposomes as Nanocarriers for Theranostic Applications. *Theranostics* **2016**, *6* (9), 1336-1352.
18. Ayllon, M.; Abatchev, G.; Bogard, A.; Whiting, R.; Hobdey, S. E.; Fologea, D., Liposomes Prevent In Vitro Hemolysis Induced by Streptolysin O and Lysenin. *Membranes* **2021**, *11* (5).